

# Ph.D. Thesis

This dissertation is submitted for the degree of Doctor of  
Philosophy

## Ph.D. in Science and Technology for Electronic and Telecommunication Engineering Cycle XXXVII (2022-2024)

---

**Study on the use of low-cost low-power microwave  
technologies for the real-time detection of gravity-  
driven natural hazards.**

---

Tutor: Daniele Caviglia

Co-Tutor: Andrea Randazzo

**Assil CHAWRABA**

**In collaboration with:**



UNIVERSITÀ DEGLI STUDI  
DI GENOVA

Techcom



Borsa di dottorato cofinanziata con risorse del  
Programma Operativo Nazionale Ricerca e Innovazione 2014-2020 (CCI 2014IT16M2OP005),  
risorse Fondo Sociale Europeo REACT-EU, Azione I.1 “Dottorati Innovativi con caratterizzazione industriale”,  
Azione IV.4 “Dottorati e contratti di ricerca su tematiche dell’innovazione” e Azione IV.5 “Dottorati su tematiche  
Green”



## Acknowledgments

First and foremost, I would like to express my deepest gratitude to my supervisor, Daniele Caviglia, whose guidance, expertise, and unwavering support have been instrumental in the successful completion of this work. Your patience, encouragement, and belief in my abilities have pushed me to grow both personally and professionally.

To my co-supervisor, Andrea Randazzo, I am incredibly thankful for your valuable insights, constructive criticism, and for always being there to provide a fresh perspective. Your contributions have added immense value to this work.

Thank you for being a mentor in the truest sense, not only offering academic guidance but also instilling in me a sense of perseverance and purpose. I will always be grateful for the opportunity to learn from you.

I would like to extend my heartfelt gratitude to my supervisor in Lebanon, Hussein Chebli. Your ability to provide clarity amidst challenges and your belief in my potential have motivated me to push my limits and achieve more than I thought possible.

I would like to express my profound gratitude to my co-supervisor, Alaa Ghaith, who has been a guide in my academic journey since my third year of university, through my master's studies, and now as my co-supervisor in my PhD.

Your unwavering belief in my abilities has been a constant source of motivation. Your encouragement and trust have reminded me that I am capable of success if I put my heart into it.

Thank you for seeing beyond my doubts and for inspiring me to work harder and aim higher.

I am deeply grateful to my friends, who have been my pillars of support. Whether it was offering a listening ear, a word of encouragement, or simply a distraction when needed, your presence made this journey much more bearable.

To my family, thank you for your unconditional love and for standing by me, even during my most challenging moments. I owe everything to your sacrifices and constant support.

Finally, to the person whose actions have caused me pain thank you. You unknowingly taught me resilience, focus, and the value of surrounding myself with kindness and sincerity. Your negativity became a catalyst for my growth, and for that, I am grateful.



# Abstract

Accurate monitoring and characterization of water dynamics are critical for applications in coastal safety, renewable energy, and environmental management. This thesis explores the potential of Frequency Modulated Continuous Wave radar technology for non-contact monitoring and analysis of sea waves and river flows. By leveraging advanced signal processing techniques, including two-dimensional Fast Fourier Transform (2D-FFT) and Constant False Alarm Rate filtering, this study aims to enhance the precision of wave parameter measurements such as range, velocity, and energy distribution.

Experimental assessments were conducted in real-world coastal and river environments, validating the radar system's effectiveness in providing reliable and detailed water dynamics data. Key contributions include the development of methodologies for resolving range-velocity ambiguities, analyzing wave energy patterns, and optimizing radar performance for real-time applications. The findings demonstrate that low-cost FMCW radar systems can serve as practical tools for water state monitoring, with potential applications in disaster mitigation, renewable energy resource assessment. This work contributes to the advancement of radar-based hydrological sensing technologies, highlighting their importance in modern environmental studies, particularly for monitoring debris flow and its impacts.

Keywords: FMCW Radar, 2D-FFT, CA-CFAR, Sea Waves, Water Flow, Wave Speed, IQ signals, Energy Distribution.



UNIONE EUROPEA  
Fondo Sociale Europeo



Ministero dell'Istruzione,  
dell'Università e della Ricerca



PON  
RICERCA  
E INNOVAZIONE  
2014 - 2020

“Strive not to be a success, but rather to be of value”

By Albert Einstein



UNIONE EUROPEA  
Fondo Sociale Europeo



*Ministero dell'Istruzione,  
dell'Università e della Ricerca*



PON  
RICERCA  
E INNOVAZIONE  
2014 - 2020

# Table of Contents

Abstract.....	3
Table of Contents.....	5
Abbreviations.....	7
List of Figures.....	8
List of Tables.....	9
Publications.....	11
<b>Chapter 1: Introduction.....</b>	<b>12</b>
1.1 State of the art.....	14
1.2 Objectives.....	17
1.3 System Design Overview.....	18
1.4 Structure of the Thesis.....	19
<b>Chapter 2: System Design and Components.....</b>	<b>21</b>
2.1 Introduction.....	21
2.2 FMCW Radar Architecture.....	21
2.3 Working Principle of FMCW radar.....	22
2.3.1 Overview.....	22
2.3.2 Antennas.....	23
2.3.3 Radar System Setup Parameters.....	25
2.3.4 Advantages of FMCW Over Pulsed RADAR.....	28
2.3.5 Applications of FMCW RADAR Systems.....	28
2.3.6 Limitations and Challenges.....	29
2.3.7 Modern Developments and Emerging Trends.....	29
2.3.8 Design and Implementation.....	29
2.4 Conclusion.....	32
<b>Chapter 3: Signal Model and Processing Techniques.....</b>	<b>34</b>
3.1 Introduction.....	34
3.2 Hardware Architecture.....	35
3.3 Software Architecture.....	36
3.4 FMCW Radar Signal Processing.....	37
3.4.1 Range FFT.....	39
3.4.2 Doppler FFT.....	40
3.4.3 2D-FFT and Range-Doppler Map.....	40
3.5 Calibration and Noise Reduction.....	40
3.6 Clutter Reduction Using Frame Subtraction.....	41
3.6.1 Windowing for FFT Optimization.....	42
3.6.2 Purpose of Windowing.....	42
3.6.3 Application of Windowing in FMCW RADAR.....	42



3.7 Principles of CFAR.....	50
3.7.1 Cell-averaging CFAR.....	52
3.7.2 Applying CFAR for Range-Doppler Map Filtering.....	53
3.8 Conclusion.....	60
<b>Chapter 4: Time Domain and Spectral Analysis of FMCW Radar Signals for Sea Wave Characterization.....</b>	<b>62</b>
4.1 Introduction.....	62
4.2 Time-Domain Representation of FMCW Radar Signals.....	63
4.2.1 Overview of Time-Domain Signals.....	63
4.2.2 Sampling and Processing.....	63
4.3 Analysis of I/Q Components.....	64
4.3.1 I/Q Signal Characteristics.....	64
4.3.2 Visualizing I/Q Signals.....	64
4.3.3 Signal Dynamics Across Sea States.....	65
4.3.4 Interpretation of I/Q Signal Dynamics.....	66
4.3.5 Advantages of I/Q Signal Analysis.....	66
4.4 Representation of I/Q Signals.....	66
4.5 Experimental Setup and Data Processing.....	66
4.6 Analysis of Wave Dynamics Using FMCW Radar and Power Spectrum Techniques.....	72
4.6.1 Methodology for Power Spectrum Analysis.....	72
4.6.2 Power Spectrum Analysis.....	73
4.7 Conclusion.....	78
<b>Chapter 5: Tracking and Analysis of Water Flow.....</b>	<b>80</b>
5.1 Introduction.....	80
5.2 Experiments.....	80
5.2.1 Sea Waves Experiment.....	80
5.3 Conclusion.....	90
<b>Chapter 6: Conclusion and Future work.....</b>	<b>92</b>
6.1 Conclusion.....	92
6.2 Future Work.....	93
<b>References.....</b>	<b>94</b>

## Abbreviations

**FMCW:** Frequency Modulated Continuous Wave

**FFT:** Fast Fourier Transform

**2D-FFT:** Two-dimensional Fast Fourier Transform

**CWT:** Continuous Wavelet Transform

**CFAR:** Constant False Alarm Rate

**VCO:** voltage-controlled oscillator

**IF:** Intermediate frequency

**ADC:** Analog-to-digital converter

**MIMO:** Multi-input multi-output

**CUT:** Cell Under Test

**FOV:** Field of View

**TX:** Transmitting antenna

**RX:** Receiving antenna

**RF:** Radio Frequency

**CA-CFAR:** Cell averaging constant false alarm rate

**2D-CA-CFAR:** Two-dimensional cell averaging constant false alarm rate

**PLL:** Phase-Locked Loop.

**SPI:** Serial Peripheral Interface



UNIONE EUROPEA  
Fondo Sociale Europeo



Ministero dell'Istruzione,  
dell'Università e della Ricerca



PON  
RICERCA  
E INNOVAZIONE  
2014 - 2020

## List of Figures

**Figure 2.1. Block Diagram of FMCW Radar.**

**Figure 2.2: Main components and dimensions of the Distance2Go board.**

**Figure 2.3: Simulated 2D and 3D radiation patterns for micro-strip patch antennas.**

**Figure 2.4. Transmitted and Received signal sequences.**

**Figure 3.1. System Block Diagram and Connections.**

**Figure 3.2. Flowchart of the Developed Data Analysis Method.**

**Figure 3.3. Block diagram of the Infineon Distance2Go board.**

**Figure 3.4. Results of Signal Processing for rolling wave: (a) Camera image (b) Range FFT Mapping, (c) Doppler window Mapping, (d) Range-Doppler map.**

**Figure 3.5. Results of Signal Processing for subside wave: (a) Camera image (b) Range FFT Mapping, (c) Doppler window Mapping, (d) Range-Doppler map.**

**Figure 3.6 presents the results: (a) a camera image, (b) the Range-Doppler map, and (c) the range FFT before and after calibration using the frame subtraction algorithm.**

**Figure 3.7. Workflow of signal processing in FMCW Radar for Range-Doppler Map Generation.**

**Figure 3.8. Illustrating the Cell Under Test (CUT), Reference Cells, and Guard Cells.**

**Figure 3.9. Illustration of CFAR Detection with Sliding Window and Thresholding.**

**Figure 3.10. Radar Data Signal Processing Flowchart.**

**Figure 3.11. Visualization of Time-Averaged Velocity Processing.**

**Figure 3.12. showcases Range-Doppler plots before and after post-processing for maritime settings, utilizing 2D-CFAR filtering. Image (a) shows the 2D-FFT without filters, and image (b) shows the results post-filter application.**

**Figure 3.13. Camera Image of sea wave.**

**Figure 3.14. Range-Doppler Map (2D) and 2D CFAR Detection of sea wave.**

**Figure 3.15. Range-Doppler Map (3D) and 2D CFAR Detection (3D) of sea wave.**

**Figure 4.1. Experimental environment for different Sea State.**

**Figure 4.2. Time-Domain Representation of FMCW Radar Signal for Sea state.**

**Figure 4.3. Range-Doppler map.**

**Figure 4.4. Camera Images Depicting Two Different Sea States: (a) Active Waves with High Energy and Strong Water Flow, and (b) Calmer Waves with Gentle Water Flow.**

**Figure 4.5. Normalized Power Spectrum Analysis of Two Sea States: (a) High Sea State with Larger, Lower-Frequency Waves and (b) Calmer Sea State with Lower Overall Power.**

**Figure 4.6. R-D Maps of Two Sea States: (a) High Waves with Strong Water Flow, and (b) Moderate Energy Waves with Less Intense Flow.**

**Figure 5.1. The environment of experiment.**

**Figure 5.2. Camera Image, R-D map and Doppler spectrum at 4 m range for sea wave.**

**Figure 5.3. Tracking Sea wave.**

**Figure 5.4. Tracking calm Sea wave.**

**Figure 5.5. Tracking turbulence Sea wave.**

**Figure 5.6. Camera image and Range Doppler map for sea states.**

**Figure 5.7. Camera image and Range Doppler map for sea states.**

## List of Tables

**Table 2.1. Radar parameters.**

**Table 4.1: Characteristics of Sea State Conditions from FMCW Radar Signal Observations.**



UNIONE EUROPEA  
Fondo Sociale Europeo



*Ministero dell'Istruzione,  
dell'Università e della Ricerca*



PON  
RICERCA  
E INNOVAZIONE  
2014 - 2020

## **Publications:**

### **I. Conference Papers:**

1. A. Chawraba, A. Rizik, A. Randazzo, and D. D. Caviglia, "Real-time sea monitoring using FMCW radar," in *Proc. Int. Conf. Appl. Electron. Pervading Ind., Environ. Soc.*, Cham, Switzerland, Sep. 2023, pp. 468–473.
2. A. Chawraba, A. Randazzo, H. Chebli, and D. D. Caviglia, "Near-shore sea-wave monitoring using FMCW radar," in *Proc. 25th Int. Microw. Radar Conf. (MIKON)*, Jul. 2024, pp. 349–352.
3. A. Chawraba, A. Randazzo, and D. D. Caviglia, "Noncontact measurement of sea wave dynamics and velocity estimation with a low-cost FMCW radar sensor," in *Proc. 7th Int. Conf. Signal Process. Inf. Secur. (ICSPIS)*, 2024.
4. A. Chawraba, A. Randazzo, and D. D. Caviglia, "Characterizing coastal wave energy dynamics using enhanced FMCW radar signal processing techniques," in *Proc. Int. Symp. Electron. Telecommun. (ISETC)*, 2024.
5. A. Chawraba, A. Randazzo, A. A. Ghaith, and D. D. Caviglia "Hydrological sensing via FMCW radar technology of sea waves," in *Proc. Int. Symp. Electron. Telecommun. (ISETC)*, 2024.

### **II. Journal**

1. A. Chawraba, A. Randazzo, A. A. Ghaith, and D. D. Caviglia, "Tracking sea waves and sea conditions based on FMCW radar technology," submitted.

# Chapter 1: Introduction

Traditional sea wave monitoring methods, such as in-situ sensors and buoys, present significant challenges due to their high operational costs, limited spatial coverage, and safety risks during deployment, especially in extreme weather conditions. While radar-based systems offer a promising alternative, their ability to accurately capture complex wave dynamics, such as range, velocity, and energy distribution, is often hindered by technical constraints. Notably, issues such as range-velocity ambiguity, noise interference, and limitations in signal processing reduce the precision and reliability of these systems. Furthermore, many existing radar solutions are either too costly or require extensive calibration, making them less accessible for widespread use. This creates a pressing demand for innovative, cost-effective, and non-contact radar systems that can provide accurate, real-time measurements of sea wave dynamics under diverse conditions. Addressing these challenges is critical to advancing applications in coastal safety, renewable energy assessment, and environmental monitoring.

The monitoring and analysis of sea wave dynamics are of paramount importance across various domains, including coastal safety, maritime navigation, environmental management, and renewable energy assessment. Coastal regions, particularly those prone to extreme weather events, face increasing vulnerabilities such as flooding, erosion, and storm surges. Accurate and real-time monitoring of sea wave characteristics, such as wave height, velocity, and energy, is essential for mitigating these risks and ensuring the sustainable management of coastal resources. Additionally, the global push toward renewable energy has highlighted the untapped potential of wave energy, necessitating advanced methodologies to quantify and harness this resource effectively.

Traditional sea wave monitoring techniques, including in-situ methods like buoys, pressure sensors, and ultrasonic devices, have long been utilized to gather valuable hydrological data. However, these methods are often expensive, operationally complex, and limited in their spatial and temporal coverage. Their deployment in extreme environmental conditions poses significant risks to both equipment and personnel. Furthermore, the inability to monitor large areas simultaneously limits their applicability for comprehensive wave analysis. These limitations have driven the search for alternative technologies capable of overcoming these challenges.

Water flow tracking is a critical component of environmental and engineering studies. Whether analyzing river currents, ocean waves, or debris flows during landslides, understanding these patterns is vital for evaluating their dynamics and the external factors influencing them. This knowledge is indispensable for a range of applications, including flood prediction, coastal management, water resource optimization, landslide risk assessment, and the preservation of aquatic and terrestrial ecosystems. In the case of landslides, tracking debris flow helps identify



high-risk areas, improve early warning systems, and design mitigation measures to reduce damage to infrastructure and communities.

Sea waves and river flows represent two distinct yet interconnected aspects of water movement. Sea waves are primarily generated by wind acting on the ocean's surface, though they are also influenced by factors such as seismic activity (e.g., tsunamis), tides driven by gravitational interactions between the Earth, Moon, and Sun, and local ocean currents. In contrast, river flows are shaped by gravity, which drives water downhill through drainage basins, as well as by precipitation, snowmelt, groundwater contributions, and human interventions such as dams and diversions. This knowledge is critical for addressing challenges such as coastal erosion, riverine flooding, and sustainable water resource management.

RADAR, an acronym for "Radio Detection and Ranging," refers to a system that utilizes electromagnetic waves to identify and locate objects in its operational environment. The origins of RADAR systems date back to World War II, where they were primarily employed to detect enemy aircraft. Over time, these electronic devices have undergone significant advancements, achieving high levels of accuracy and expanding their use from military to civilian applications.

Radar-based systems have emerged as a promising solution for sea wave monitoring, offering non-contact measurement capabilities and real-time data acquisition. Among these, Frequency Modulated Continuous Wave (FMCW) radar technology has gained traction due to its cost-effectiveness, compact design, and ability to measure critical wave parameters such as range, velocity, and energy distribution. FMCW radar operates by emitting a continuous signal whose frequency is modulated over time, allowing the extraction of range and Doppler information from the reflected signals. This capability makes it particularly suitable for short- to medium-range applications in near-shore environments.

Despite the advantages of FMCW radar, several challenges persist. Issues such as range-velocity ambiguity, noise interference, and limitations in signal processing reduce the accuracy and reliability of radar-based measurements. These technical constraints must be addressed to unlock the full potential of FMCW radar for sea wave monitoring. Furthermore, there is a need to develop methodologies that are both cost-effective and scalable, enabling broader adoption of radar technology in various applications.

This research focuses on the application of FMCW radar technology for non-contact sea wave monitoring in near-shore environments. It also addresses the development and optimization of signal processing algorithms aimed at enhancing radar performance. Furthermore, experimental validation campaigns were conducted in coastal regions, including Genoa, Italy, to demonstrate the system's effectiveness under varying sea conditions.



This thesis focuses on leveraging FMCW radar technology to develop an advanced system for the non-contact monitoring and analysis of sea wave dynamics. By integrating innovative signal processing techniques based on two-dimensional Fast Fourier Transform and Constant False Alarm Rate filtering, the research aims to enhance the precision, reliability, and robustness of radar-based measurements. Experimental campaigns conducted in real-world coastal environments, such as Genoa, Italy, validate the system's effectiveness and demonstrate its potential for practical applications.

The contributions of this work extend beyond traditional wave monitoring, encompassing renewable energy resource assessment, disaster mitigation, and coastal infrastructure protection. By addressing the limitations of existing methods and advancing radar-based sensing technologies, this research aims to provide a significant step forward in the field of hydrological monitoring and environmental studies. The following sections will review the state of the art in sea wave monitoring and radar technologies, providing a foundation for the methodologies and experiments presented in this thesis.

## 1.1 State of the art

The state-of-the-art in sea wave monitoring and radar-based hydrological sensing reveals significant advancements across multiple research domains. Efforts to address the lack of high-resolution experimental data for validating geophysical flow models have led to the development of sophisticated radar instruments capable of capturing 3D images of flows such as snow avalanches and pyroclastic flows [1]. Similarly, experimental radar studies, such as those in the Yellow Sea of China, have contributed to sea clutter modeling and prediction, showcasing improved accuracy in deriving parameters based on radar data and sea states [2]. Acoustic sensor-based monitoring, particularly using Fast Fourier Transform (FFT) and Continuous Wavelet Transform (CWT), has classified wave types in coastal areas, offering insights into the tidal patterns and mixed tide behaviors of specific regions [3]. Furthermore, innovative methods like weighted multidirectional gradient measures have enhanced the detection of small maritime targets amidst heavy waves, improving search and rescue capabilities in challenging conditions [4].

FMCW radar technology continues to demonstrate its versatility, with studies utilizing X-band radar backscatter for wave parameter estimation in near-shore environments, tank level measurement, and sea-keeping applications [5]. Advanced techniques such as orthogonal projection have been employed to suppress first-order sea clutter in high-frequency surface wave radar systems, enhancing target detection accuracy in cluttered maritime settings [6]. Small target detection using FMCW radar has also seen advancements, with extensive testing refining signal processing approaches to classify small vessels effectively in varying sea conditions [7]. Hydrological applications of FMCW radar, including river surface velocity and water level



measurements, have achieved high accuracy rates using iterative adaptive approaches and frequency-modulated chirps [8].

The influence of nonlinearity on radar observations has been analyzed through the dispersion relationship of finite amplitude ocean wave theory, emphasizing the need for accurate wave amplitude and water depth measurements to improve radar-based ocean state analysis [9] [10]. Doppler polarimetry has been explored for distinguishing low-RCS targets in littoral environments, offering potential enhancements in target detection amidst sea clutter. Continuous wave radar systems such as Riverscat have demonstrated the ability to monitor river surface currents effectively, leveraging the Bragg scattering phenomenon to estimate surface velocity [11]. Additionally, phase-feature detectors for small target detection in sea clutter have addressed challenges related to low signal-to-clutter ratios, improving detection performance in cluttered maritime environments [12].

Cable-based wave monitoring systems and chirp sequence radar systems have been utilized for real-time wave height observation [13] and river flow behavior characterization, respectively, demonstrating practical applications in hydrological monitoring [14]. Deep neural network (DNN) models have further advanced sea clutter characterization by correlating environmental factors with radar clutter properties, enabling accurate parameter inversion and prediction [15]. Coherent X-band radar systems have been employed for surface velocity mapping and hydrodynamic process analysis, highlighting dynamic features such as sand waves and current shears [16]. Unmanned surface craft with integrated radar systems have demonstrated capabilities in sea-state sensing and navigation safety, utilizing both long- and short-range radar for enhanced obstacle detection [17].

Finally, comprehensive reviews of sea wave monitoring techniques have emphasized the importance of integrating technologies such as buoys, satellite observation, coastal radars, and microseism analysis to improve overall accuracy and efficiency in sea wave monitoring [18]. Spectrum estimation methods, including Welch and Thomson approaches, have been compared for their effectiveness in assessing sea state parameters, providing recommendations for optimizing spectrum reconstruction [19]. These advancements collectively highlight the rapid evolution of radar technology and signal processing techniques, laying a strong foundation for future innovations in sea wave monitoring and hydrological sensing.

Non-contact measurement systems provide significant advantages over traditional contact-based methods, particularly in challenging environments where maintenance and installation efforts are cumbersome. These systems enable early intervention by supporting flood early warning frameworks that promptly detect potential flooding risks and deliver critical information in real-time. Radar-based non-contact technologies are particularly notable for their reliability and efficiency compared to conventional systems, such as mechanical devices (e.g., propeller-based current meters) [20][21] or ultrasonic sensors requiring direct interaction with the measured

medium [22][23]. These radar systems enhance flood early warning capabilities by delivering vital data rapidly and dependably at critical monitoring sites [20].

A key parameter for monitoring both natural river flows and man-made channels is the volume flow rate, or discharge. However, direct measurement of discharge using sensors is impractical. Instead, it can be estimated by combining information on river bathymetry, water surface levels, and velocity. While bathymetry in artificial channels is often predefined, estimating it for natural rivers presents challenges due to irregular and dynamic riverbed conditions. Various methods for addressing natural river bathymetry estimation have been proposed in previous research [25][26]. Radar sensors provide a robust alternative by directly measuring water surface levels and surface velocity. Doppler radar, widely used across multiple domains, is employed for measuring water surface velocities, flow monitoring, and river profiling. These systems, operating across UHF frequencies up to 24 GHz [27][28][29], are capable of detecting water surface velocities and determining water levels with high precision [30][31]. However, surface velocity in natural rivers varies significantly due to complex hydrological processes, ranging from zero at the riverbed to a maximum velocity just below the surface [32][33]. Approaches such as entropy-based models enable the estimation of mean velocity from observed maximum values, a methodology validated using 24 GHz Doppler radar systems in prior studies [34][35][36].

Frequency-Modulated Continuous-Wave (FMCW) radar offers additional advantages over Doppler radar in flood warning systems. Beyond detecting surface velocity, FMCW radar provides precise measurements of water surface levels by delivering accurate distance information, accounting for observation geometry. This makes FMCW radar a valuable tool for stationary-mounted sensors in river and ocean monitoring applications [37].

The interaction between electromagnetic waves and water surfaces, such as rivers or oceans, is often explained using Bragg scattering [38][39]. However, recent studies have demonstrated that backscattering involves multiple effects, including Fresnel reflections, multipath propagation, and multibounce scattering, rather than Bragg scattering alone [40]. Research further indicates that Fresnel-Kirchhoff diffraction serves as a suitable approximation for radar backscattering, depending on surface roughness and radar frequency [40]. For rough water surfaces, such as those found in rivers, a statistical approach to Fresnel backscattering proves effective. Unlike scenarios with periodic surface components, where the Fresnel model may be less applicable, the stochastic nature of rough river surfaces makes statistical modeling more versatile and accurate for radar-based hydrological sensing [40].

Monitoring and analyzing water flow and wave energy are essential across various domains, including river management, coastal safety, and oceanographic studies. The growing emphasis on disaster mitigation, coastal region protection, and renewable energy utilization from oceans has underscored the necessity for precise and reliable data on sea parameters, particularly wave dynamics [41]. Accurate tracking of these parameters is vital for predicting sea-state conditions, contributing to environmental conservation, and optimizing resource management. To address

these demands, advancements in technology have focused on real-time, high-resolution monitoring systems capable of delivering detailed insights into water flow and wave energy.

Microwave radar instruments have become indispensable tools in remote sensing, significantly advancing oceanographic and atmospheric research [42]. The growing demand for rapid, accurate, and comprehensive sea-state assessments has propelled the development of radar systems operating in high-frequency and microwave domains [43]. Microwave sensors are particularly valued for their versatility and adaptability to diverse deployment platforms, including aircraft and satellites. Their affordability and low power consumption make them ideal for integration into small-scale space platforms, enhancing their accessibility for research and operational purposes [44].

The ability to perform real-time monitoring of sea-state conditions and ocean surface behavior has become increasingly important, driven by the need to ensure safe maritime navigation and to advance scientific understanding of air-sea interactions and global climate phenomena. Real-time observations of ocean dynamics are indispensable for capturing the transient and evolving nature of the sea, offering valuable data for maritime operations, disaster preparedness, and climate studies. Advanced remote sensing technologies now provide continuous measurements of wave energy, a critical factor in improving predictive models for weather forecasting and contributing to more accurate climate research [45].

## 1.2. Research Objectifs:

The goal of the water flow monitoring system using FMCW radar, Raspberry Pi, and a camera is to create an efficient and precise method for measuring the range and speed of water flow.

1. Range Measurement: Use a 24 GHz FMCW radar to measure the distance to the water flow. Develop algorithms to process the radar signals and determine the range, allowing for accurate monitoring of water flow positions and changes.
2. Doppler Analysis: Analyze the Doppler shift in radar signals caused by water movement. Develop algorithms to extract the Doppler frequency shift and interpret it as the speed of the water. This will provide insights into water flow behavior, such as propagation and energy.
3. Integrated System: Combine radar measurements, camera data, and environmental information into a unified system. Utilizing software algorithms for data processing and analysis to enable real-time monitoring of water flow behavior. This system will provide valuable information about water characteristics and dynamics, aiding in accurate range and speed analysis.

4. Real-Time Monitoring: Enable continuous, real-time monitoring of water flow to detect and respond to changes promptly. This will help in identifying potential issues such as floods or changes in water dynamics, facilitating immediate action and prevention measures.

5. Environmental Data Integration: Incorporate relevant environmental data, such as conditions and water quality, to enhance the accuracy and reliability of the monitoring system. This comprehensive approach will provide a more detailed understanding of water flow and its influencing factors, supporting better decision-making and management.

The system's performance was tested and validated in two different environments, showing excellent results in detecting targets passing through the radar's field of view. These results will be discussed in detail in the following chapters.

This thesis provides the following contributions:

1. A Comprehensive Methodology for FMCW Radar-Based Sea Wave Monitoring: The research details an innovative approach for employing Frequency Modulated Continuous Wave (FMCW) radar to accurately monitor and analyze sea wave dynamics in near-shore environments. This methodology includes the design and implementation of radar systems tailored for hydrological applications, with a focus on capturing detailed wave parameters.

2. Advanced Signal Processing Techniques: The study introduces enhanced signal processing techniques to address challenges inherent in radar-based hydrological sensing. These techniques include the application of two-dimensional Fast Fourier Transform (2D-FFT) for signal analysis, and Constant False Alarm Rate (CFAR) filtering to improve detection accuracy. These advancements significantly enhance the precision and reliability of radar measurements for range, velocity, and energy distribution of sea waves.

3. Experimental Validation and Practicality: Through rigorous experimental campaigns conducted in real-world coastal and river environments, the proposed FMCW radar system is validated for its effectiveness. The experiments demonstrate the system's ability to provide reliable and detailed data on water dynamics, thus proving its practicality for non-contact monitoring of sea waves and river flows. The robustness of the radar system is also assessed under various environmental conditions.

### 1.3 System Design Overview

In this framework, we introduce an innovative short-range monitoring technique leveraging low-cost FMCW radar technology to address common challenges such as limited resolution, slow acquisition speed, and signal ambiguity often encountered with this hardware. This novel approach



includes a custom-designed processing chain specifically developed to detect and monitor a single target, such as water flow, ensuring accurate and efficient measurement.

The system comprises a Distance2Go radar board from Infineon Technologies, a Raspberry Pi 3B+ mini-PC, and a portable PC running MATLAB software [46]. The radar board functions by continuously transmitting radar signals and receiving the echo signals reflected from the water flow. These echo signals are then collected by the Raspberry Pi and transmitted to the portable PC for advanced processing.

A key component of the proposed system is the initial clutter and leakage mitigation stage, achieved through a background subtraction (BS) technique tailored for radar signal processing applications [47], [48]. This approach enables the isolation of dynamic water flow signals from static background clutter and spurious reflections, significantly improving the accuracy and reliability of the measurements. The integration of these components and techniques creates a robust and cost-effective solution for water flow monitoring, capable of handling complex environments. This system not only improves the quality of data acquired but also ensures faster processing and clearer results, making it a valuable tool for precise water flow measurement.

Subsequently, a stretch processing technique is employed to compute the range-Doppler maps for each collected data frame.

The proposed system was tested in two different environments, specifically a river and the sea. The total cost of the measurement setup, as outlined in this paper, is approximately 300 €. This cost breakdown includes around 200 € for the radar board, 50 € for the Raspberry Pi 3B+, an optional camera costing about 10 €, and an additional 50 € for a power bank, casing, and other expenses. The system's affordability is one of its key features.

## 1.4 Structure of the Thesis

This thesis is organized as follows:

- Chapter 2 reviews existing methods for sea wave monitoring and the principles of FMCW RADAR technology.
- Chapter 3 presents signal processing techniques, and the application of Constant False Alarm Rate detection for accurate target identification.
- Chapter 4 explores FFT-based spectral analysis and power distribution methods to extract wave parameters.
- Chapter 5 Discusses real-time wave tracking, flow dynamics, and applications in coastal hazard monitoring
- Chapter 6 concludes the study with key findings for future research.



# Chapter 2



UNIONE EUROPEA  
Fondo Sociale Europeo



*Ministero dell'Istruzione,  
dell'Università e della Ricerca*



# Chapter 2: System Design and Components

## 2.1 Introduction:

This chapter provides a comprehensive overview of the hardware and software architectures of the developed water flow monitoring system. It starts by detailing the hardware components, including sensors and radar equipment, and explains how they are interconnected to measure water flow. Following this, the chapter describes the software's operating logic, focusing on the different processing blocks designed to analyze the data collected from the hardware. This includes data acquisition, signal processing, and flow velocity calculation. The chapter aims to give a clear understanding of how the system is designed to accurately monitor and analyze water flow.

## 2.2 FMCW Radar Architecture:

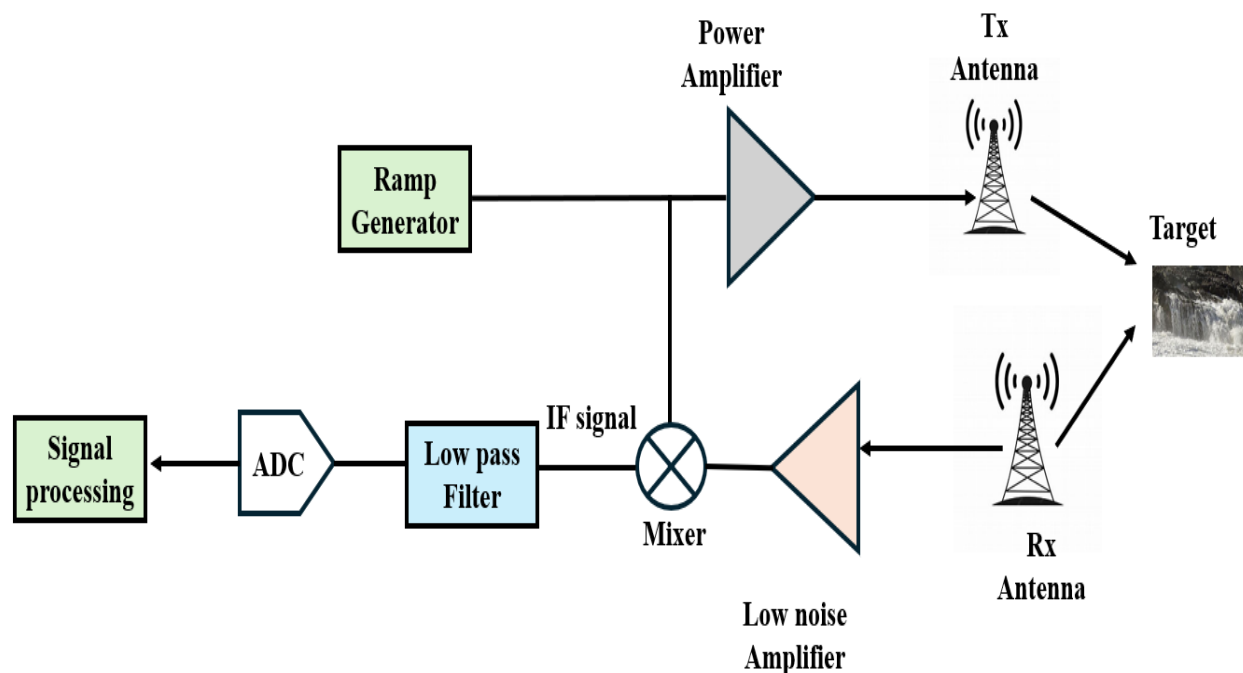


Figure 2.1. Block Diagram of FMCW Radar.

Figure 2.1 illustrates the architecture of a Frequency Modulated Continuous Wave radar system, highlighting its key components and their roles in transmitting, receiving, and processing radar signals. The system begins with a frequency synthesizer that controls a voltage-controlled oscillator to generate a chirp signal a frequency-modulated waveform crucial for precise measurements of distance and velocity. The VCO produces the chirp signal by varying its output frequency over time, enabling accurate frequency modulation. The signal is then amplified by a power amplifier before being transmitted via the Tx antenna toward the target, such as sea waves. The reflected signal, containing information about the target, is received by the Rx antenna and amplified by a low-noise amplifier to preserve its integrity. The received signal is then mixed with a portion of the transmitted signal in the mixer, generating an intermediate frequency signal that encodes the frequency difference between the transmitted and reflected signals. This IF signal undergoes further processing, including high-pass and low-pass filtering to remove noise and unwanted components, as well as amplification to improve signal clarity. Finally, the refined analog signal is converted to a digital format using an analog-to-digital converter. The digital signal is then analyzed to extract target characteristics such as range, velocity, and surface dynamics. This system architecture enables the FMCW radar to operate effectively in applications like sea wave monitoring, providing accurate and reliable measurements in real time.

## 2.3 Working Principle of FMCW radar:

### 2.3.1 Overview:

The Distance2Go module consists of two main components: the radar main board and a detachable debugger board, as shown in Figure 2.2 The radar main board has four key sections:

1. RF Part: This section includes the Infineon 24 GHz radar MMIC BGT24MTR11 and microstrip patch antennas for transmitting TX and receiving RX signals.
2. Analog Amplifier Part: It interfaces between the RF and digital sections of the board.
3. Frequency Control Part: This contains a low-noise fractional-N PLL.
4. Digital Part: This features the XMC4200, a 32-bit Arm® Cortex®-M4 microcontroller from Infineon, which samples and processes analog data from the radar front end and configures the BGT24MTR11 and PLL via an SPI.

The board showcases the capabilities of the BGT24MTR11 RF front-end chip, providing a complete “plug and play” radar solution. It allows users to easily collect sampled radar data, which can be used to develop radar signal processing algorithms on a PC or to implement target detection algorithms directly on the microcontroller.

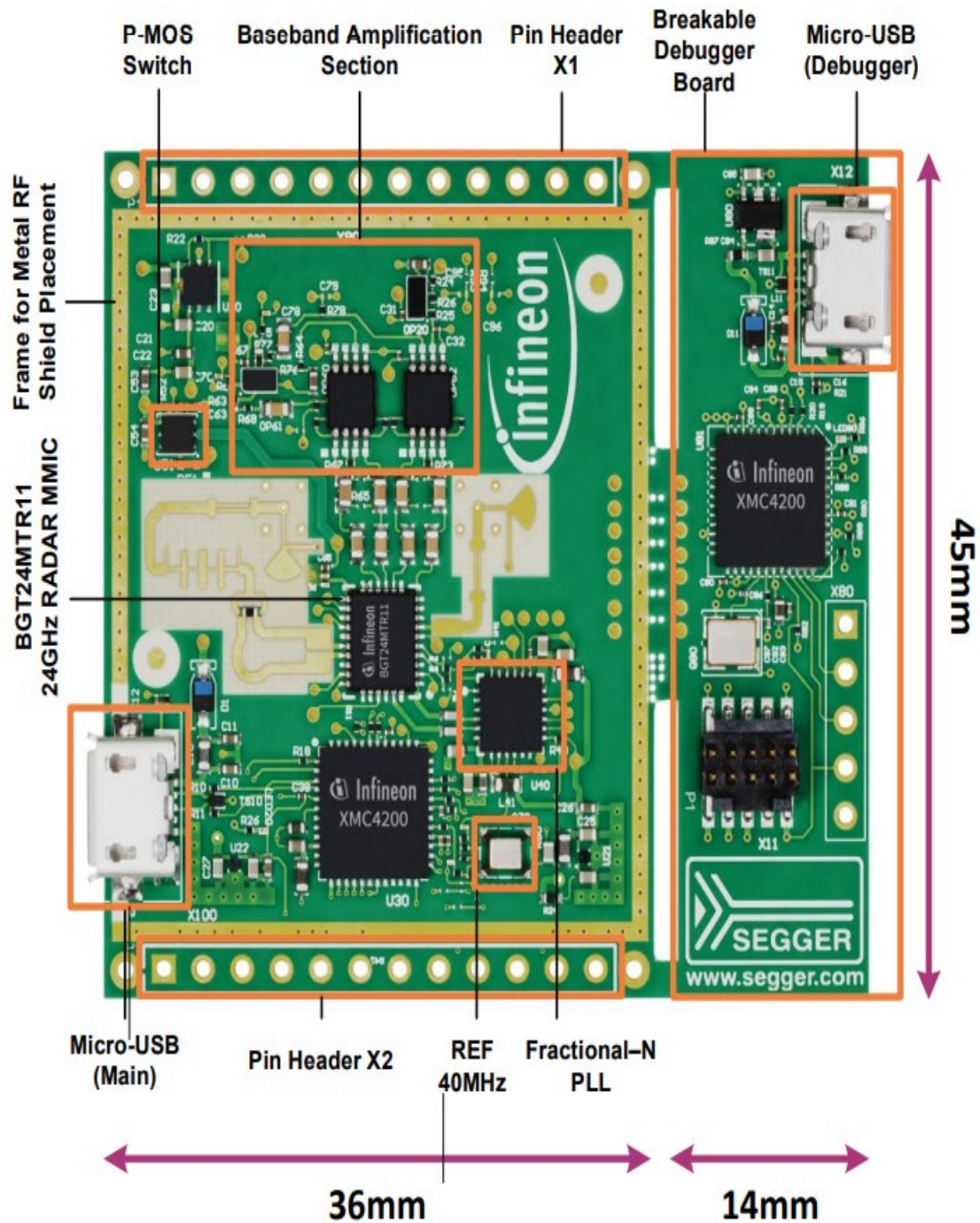


Figure 2.2: Main components and dimensions of the Distance2Go board [46].

### 2.3.2 Antennas:

The Distance2Go board is equipped with  $2 \times 4$  micro-strip patch antennas, with one array dedicated entirely to transmission TX and the other to reception RX. These antennas have a

simulated gain of approximately 12 dBi and an opening angle of 20 x 42 degrees, with the simulation accounting for via losses. Figure 2.3 illustrates the simulated 2D and 3D radiation patterns.

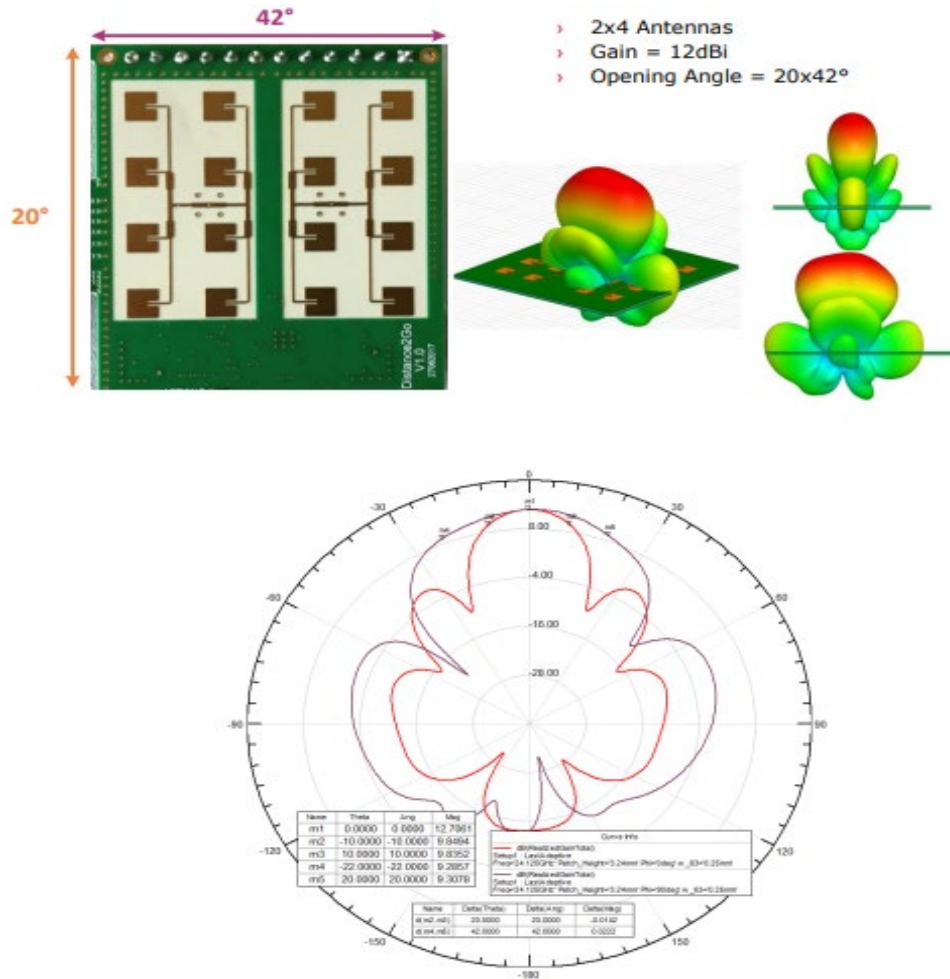


Figure 2.3: Simulated 2D and 3D radiation patterns for micro-strip patch antennas [46].

The  $20 \times 42$ -degree values represent the 3 dB Half Power Beamwidth, meaning the antenna's gain decreases by 3 dB at these angles from the maximum gain at 0 degrees. In practical situations, targets with a large Radar Cross Section can still be detected even with reduced gain outside these angles. Additionally, weaker targets with low RCS near the radar can also be detected outside the main beamwidth. Therefore, it's important to carefully consider both the distance of the target from the radar and the target's RCS when determining the radar's detection zone.

The sensor was tested in an anechoic chamber to determine its Effective Isotropic Radiated Power and opening angle. Figure 2.3 displays the measured radiation characteristics within the ISM band.

During these measurements, the sensor operated in continuous-wave mode with the duty cycle turned off, leading to a PCB temperature of approximately 80°C. This elevated operating temperature reduced the output power of the BGT24MTR11 MMIC by about 1 dB [46].

### Antenna Beamwidth Considerations:

The radar uses microstrip patch antennas with a beamwidth of about  $20^\circ \times 42^\circ$ . This wide beam is useful because it covers a large area of the sea surface, allowing the radar to observe several wave crests at the same time. However, the wide beam also reduces the radar's angular resolution. Signals arriving from different directions within the beam are combined together, which can make it harder to separate returns from nearby waves or other scatterers. As a result, the radar can show that a wave is present, but it cannot always identify exactly where within the beam the wave occurred. In this work, signal processing methods such as range-Doppler analysis and clutter suppression were used to reduce the impact of this limitation.

### 2.3.3 Radar System Setup Parameters:

The manufacturer has preset the following radar module parameters, which cannot be altered unless there are changes to the XMC firmware or modifications to the board's circuitry.

$$T_{rd} = 200 \mu\text{s} \quad (2.1)$$

$$T_{pll} = 400 \mu\text{s} \quad (2.2)$$

$$P_{out} = 10 \text{ dBm} \quad (2.3)$$

In this context,  $T_{rd}$  represents the down-chirp time following the transmitted up-chirp. Avoiding an abrupt transition from the maximum frequency of the up-chirp to the minimum frequency of the next up-chirp is crucial, as it can lead to various issues, including the generation of spurious signals. The parameter  $T_{pll}$  denotes the recovery time (steady-state time) required by the phase-locked loop (PLL) before it can generate the next up-chirp. Additionally,  $P_{out}$  refers to the maximum transmitted power. It is important to note that no samples are collected during the  $T_{rd}$  and  $T_{pll}$  periods.

In contrast to the parameters mentioned earlier, the following settings can be modified via commands sent to the board through the serial interface. However, adjusting these settings away

from the manufacturer's specified optimal values can result in significant discrepancies in the digitized signal compared to theoretical expectations for FMCW radar performance.

$$T_c = 1.5 \mu\text{s} \quad (2.4)$$

$$B = 200 \text{ MHz} \quad (2.5)$$

In this context,  $T_c$  refers to the duration of the chirp, while  $B$  denotes the bandwidth. The frequency modulation specifically covers the range from  $F_c$  to  $F_c + B$ , where  $F_c$  is set at 24 GHz.

Furthermore, to ensure a maximum unambiguous detection distance of 25 meters ( $R_{max} = 25\text{m}$ ), it is necessary to choose an appropriate number of time-equally spaced samples ( $N_s$ ) for digitizing the radar echo. This selection should be based on the following formula:

$$N_s \geq \frac{4BR_{max}}{c} = 67 \quad (2.6)$$

To optimize the execution of FFTs needed for processing the received signal, a sample size of ( $N_s=64$ ). This size offers a good trade-off between computational efficiency and frequency resolution, enabling reliable detection of target range and velocity while maintaining real-time processing capabilities on embedded hardware. This choice ensures efficient computation while accepting a minor reduction in the maximum detectable distance. Choosing the next power of two, ( $N_s = 128$ ), was not feasible due to the limited memory capacity of the XMC microcontroller, which would result in a significant reduction in the number of chirps per frame ( $N_c$ ) from 24 to 12, thus degrading the Doppler spectrum resolution. Additionally, using ( $N_s = 128$ ) would lead to an unnecessarily large instrumental range, far exceeding the radar's actual maximum detectable distance, considering the transmitted and reflected power levels.

It is important to note that the above values meet the following critical condition:

$$T_c \geq \frac{2R_{max}}{c} \quad (2.7)$$

This requires that the duration of the up-chirp be longer than the maximum round-trip time, which is the time taken for the electromagnetic wave to travel to a target at the maximum distance and back to the antenna. This prevents ambiguity in interpreting the demodulated signal. Additionally, the following points are important to consider:

- The maximum round-trip time is significantly shorter than the recovery time, which is the sum of ( $T_{rd}$  and  $T_{pll}$ )

$$\frac{2R_{max}}{c} = 166 \text{ ns} \ll T_{rd} + T_{pll} = 600 \text{ } \mu\text{s} \quad (2.8)$$

This means that the received chirp does not overlap with the next transmitted chirp, preventing the generation of spurious beat frequencies in the receiving mixer.

- The maximum round-trip time is significantly shorter than the sampling time is

$$\frac{2R_{max}}{c} = 166 \text{ ns} \ll T_s = \frac{T_c}{N_s} = 23.4 \text{ } \mu\text{s} \quad (2.9)$$

The ADC timer starts counting as soon as the transceiver initiates the chirp transmission, and the first sample is taken after a delay of ( $T_s$ ). This timing ensures that the first sample is captured when the demodulated signal is already present at the ADC input. As a result, the effective observation window for the echo is ( $T_c$ ), meaning the actual bandwidth utilized for modulation is ( $B$ ).

Because of the microcontroller's limited memory, only 24 chirps can be transmitted and collected per frame ( $N_c = 24$ ). In the initial setup, interface issues between the Raspberry Pi mini-PC and the control PC reduced this number to 21 ( $N_c = 21$ ). This reduction affects the system's capacity to detect radial velocities from the Doppler shift in the radar signal, leading to the following outcomes:

$$v_{max} = \frac{\lambda}{4T_{PRT}} \quad (2.10)$$

$$\Delta R = \frac{c}{2B} \quad (2.11)$$

$$\Delta v = \frac{\lambda}{2T_{CPI}} \quad (2.12)$$

In this context,  $v_{max}$  is the maximum detectable radial speed, and  $T_{PRT} = T_c + T_{rd} + T_{pl}$  represents the Pulse Repetition Time. The wavelength in vacuum,  $\lambda$ , corresponds to the frequency  $F_c = F_0 + B/2$ . The resolution of the radial speed measurement is denoted as  $\Delta v$ . The duration of the frame, also known as the Coherent Processing Interval, is  $T_{CPI} = N_c T_{PRT}$ . However, due to the radar's duty cycle, this interval is shorter than the total frame duration, i.e.,  $T_{CPI} < T_f$ .

Given the bounded value of  $v_{max}$  relative to the radial speeds of objects that can pass through the monitored gate, careful selection of the algorithms in the processing chain for target classification is crucial. Each frame lasts  $T_{CPI} = N_c T_{PRT} = 0.05$  seconds, and the time between the start of one frame and the next is  $T_f = 0.2$  seconds.

The FMCW RADAR operates by transmitting a continuous wave signal with a frequency that varies linearly over time. When the signal reflects off a target, the received signal is delayed based on the distance to the target, creating a frequency difference between the transmitted and received signals. The frequency difference, known as the beat frequency, is proportional to the range of the target and is calculated by processing the intermediate frequency (IF) signal. In FMCW radar systems such as the Distance2Go, the estimation of radial velocity is not performed using the beat frequency shift. Instead, the system employs the spatial Doppler method, which relies on detecting phase shifts between successive received chirps. This phase progression across chirps allows the extraction of the target's radial velocity with high accuracy[53].

### 2.3.4 Advantages of FMCW Over Pulsed RADAR

FMCW RADAR systems offer several advantages over traditional pulsed RADAR. The continuous wave operation eliminates the need for high-power transmitters, making FMCW systems more energy efficient. FMCW radar can achieve high accuracy, especially in applications requiring precise distance and velocity measurements. Its ability to process frequency-modulated signals enables superior resolution, making it effective for detecting both stationary and moving objects. Additionally, FMCW radar is less prone to interference from external sources, which makes it particularly well-suited for environments with high signal congestion. These features have made FMCW RADAR a preferred choice for applications where precision and low power consumption are critical.

### 2.3.5 Applications of FMCW RADAR Systems

FMCW RADAR systems are extensively utilized in a variety of applications due to their precision and versatility. In water-related fields, they are used for sea wave analysis, water flow measurement, and monitoring of ocean surface conditions, aiding in navigation safety, marine

research, and offshore engineering. These systems are also employed in hydrology to track river discharge, measure water levels in reservoirs, and monitor flood patterns for early warning systems. Beyond water-focused uses, they play a critical role in environmental monitoring by assessing weather conditions, such as rainfall intensity and snowpack levels. Their adaptability also extends to detecting subsurface water, mapping underwater structures, and contributing to coastal erosion studies, showcasing their broad applicability across diverse domains.

### **2.3.6 Limitations and Challenges**

FMCW RADAR systems, while offering numerous advantages, face certain limitations and challenges that impact their performance in real-world applications. The complex signal processing required to extract accurate data increases computational demands and complicates system design, making implementation more intricate. Environmental factors such as heavy rain, fog, and snow further degrade signal strength, limiting the effective range and reliability. Addressing these challenges through advanced algorithms, robust hardware, and adaptive interference mitigation techniques is essential to enhance the performance and dependability of FMCW RADAR systems across various fields.

### **2.3.7 Modern Developments and Emerging Trends**

Modern advancements in FMCW RADAR technology, particularly in the 24 GHz frequency band, have greatly enhanced its precision and adaptability for various applications. The integration of machine learning and artificial intelligence has enabled sophisticated signal processing, allowing for improved detection accuracy and target classification within this frequency range. The 24 GHz band strikes a balance between range and resolution, making it ideal for applications like water flow analysis, sea wave monitoring, and short-range environmental sensing. Additionally, emerging trends such as multi-input multi-output systems have improved coverage and accuracy by leveraging multiple antennas, even at this frequency. These developments highlight the ongoing innovation in 24 GHz FMCW RADAR systems, expanding their utility while maintaining efficient and cost-effective designs.

### **2.3.8 Design and Implementation**

The design and implementation of an FMCW RADAR system involves several key considerations. The hardware design must balance performance and cost, selecting components such as antennas, mixers, and amplifiers that meet system requirements. Signal processing techniques play a critical role in analyzing the received signals, requiring robust algorithms to extract range and velocity information. Proper calibration and testing are essential to ensure that the system operates as intended, with validation performed through simulations and experimental setups. This process ensures that the final design meets the specific needs of the intended application.



The complete set of radar sensor parameters is shown in Table 2.1.

**Table 2.1.** Radar parameters.

Parameters	Description	Value
$F_0$	Center Frequency	24 GHz
$F_s$	Sampling Frequency	42667 Hz
$B$	Bandwidth	200 MHz
$R_{max}$	Maximum Range	25 m
$V_{max}$	Maximum Velocity	5.4 km/h
$\Delta R$	Range Resolution	0.75 m
$\Delta v$	Velocity Resolution	0.4 km/h
$N_s$	Number of samples/Chirp	64
$N_c$	Number of Chirps/Frame	21
$D$	Duty Cycle	25%

Figure 2.4 illustrates the basic operation of FMCW radar, focusing on the transmitted and received signals, as well as their relationship over time.

1. Transmitted Signal:

- It is a linear frequency modulation (or "chirp"), where the frequency of the transmitted signal increases linearly with time. The bandwidth of the chirp is denoted by  $B$ , and the period of one chirp is represented as  $T$ .

2. Received Signal:

- It is the reflected version of the transmitted signal after bouncing off a target. The time delay between the transmitted and received signals is denoted as  $\tau$  (tau). This delay corresponds to the time it takes for the signal to travel to the target and back to the radar receiver.

### 3. Beat Frequency ( $f_b$ ):

- This frequency difference arises because of the time delay  $\tau$  between the transmission and reception of the signal. The beat frequency carries information about the distance of the target from the radar.

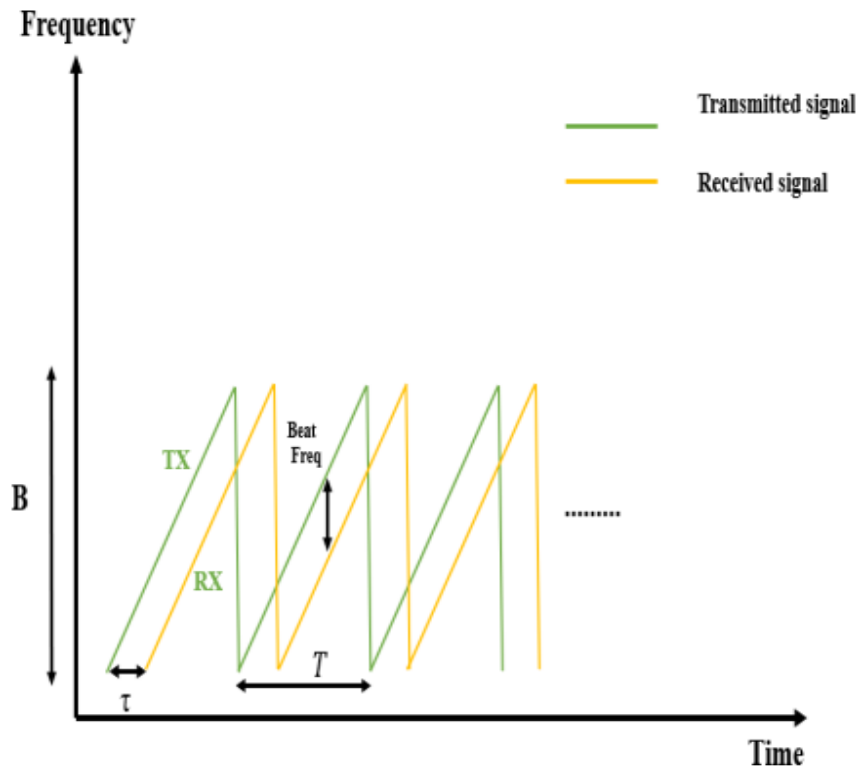


**Figure 2.4.** Illustration of transmitted and received chirp sequences with recovery intervals between chirps.

### 4. Time Delay ( $\tau$ ):

- This delay is proportional to the range (distance) of the target, and by measuring this delay, the radar can calculate how far the target is from the radar system.

### 5. Slope of the Chirp ( $B/T$ ):

- The slope of the transmitted and received signals reflects the rate at which the frequency increases with time. This slope is important for calculating the beat frequency and therefore determining the range.

By measuring the beat frequency, the radar system can compute the range to the target. The higher the beat frequency, the greater the time delay, which corresponds to a further distance between the radar and the target.

## 2.4 Conclusion:

This chapter has reviewed the fundamentals of FMCW radar technology, outlining its operating principles, advantages in terms of cost-effectiveness and precision, and relevance for various sensing applications. While the focus has not been specifically on sea wave monitoring, the insights provided lay the groundwork for understanding how FMCW radar can be applied in such contexts. The next chapter will present the methodology adopted in this thesis, detailing the radar setup, signal processing techniques, and experimental design employed to achieve accurate and reliable sea wave monitoring.



UNIONE EUROPEA  
Fondo Sociale Europeo



*Ministero dell'Istruzione,  
dell'Università e della Ricerca*



PON  
RICERCA  
E INNOVAZIONE  
2014 - 2020

# Chapter 3



UNIONE EUROPEA  
Fondo Sociale Europeo



*Ministero dell'Istruzione,  
dell'Università e della Ricerca*



PON  
RICERCA  
E INNOVAZIONE  
2014 - 2020

# Chapter 3: Signal Model and Processing Techniques

## 3.1 Introduction:

In the field of marine and water flow monitoring, FMCW radars at 24 GHz frequency are integral tools due to their high precision and real-time data processing capabilities. These radars enable continuous monitoring of crucial parameters like water levels, wave height, and flow velocities. However, one of the main challenges in such systems is the presence of environmental clutter, which can significantly hinder the accuracy of measurements. Clutter arises when radar waves reflect off static objects such as bridge structures, boats, or even vegetation near the water. These unwanted reflections create noise that can mask the actual target signals, complicating the task of detecting and tracking dynamic water surfaces or flow patterns.

For these reasons, the radar's data processing includes pre-processing steps aimed at minimizing the impact of environmental clutter. A key aspect of this is the calibration phase, where extraneous noise and reflections are filtered out. This ensures that the Range-Doppler map, which is used to visualize the movement of water waves and flows, only contains relevant information. The core of this process lies in the FMCW technique, which involves transmitting a frequency-modulated signal and analyzing the return signal's frequency shift to determine both the distance and velocity of the detected targets.

To further enhance target detection, a CFAR filter is employed. The most commonly used CFAR method is Cell Averaging CA-CFAR, which averages the signal values in surrounding cells to determine the noise level and set an adaptive detection threshold. In addition to CA-CFAR, other variations like Ordered Statistics OS-CFAR may be used depending on the specific characteristics of the radar data.

Once clutter and noise are sufficiently reduced, the radar system can reliably track and measure water flows with high precision. The processed data provide insights into flow speed, wave dynamics, and changes in water levels, which are essential for applications like flood forecasting, bridge stability assessment, and maritime navigation. By continuously improving noise floor estimation and target detection algorithms, modern FMCW radar systems are becoming even more reliable and accurate in these critical environmental monitoring applications.

The chapter also examines the computational efficiency of the proposed pre-processing algorithms when implemented in real-world scenarios. MATLAB simulations are used to validate the effectiveness of these techniques, with results indicating that the radar system can adapt to various environmental conditions while maintaining high detection accuracy.

### 3.2 Hardware Architecture:

The system primarily comprises three main components, which are visually represented in Figure 1 as the prototype and in Figure 1 through a schematic of their connections. These components are the radar board, the Raspberry Pi 3B+ embedded PC, and the control PC.

In the system, a camera sensor, as shown in Figure 3.1, is also included, primarily used during the data acquisition phase to capture images of the target. In addition to the radar board and processing units, a low-cost camera was included in the experimental setup. The purpose of the camera was not to perform quantitative measurements, but to act as a validation tool for the radar observations. Visual recordings provided a reference for identifying the timing and characteristics of wave crests and surface disturbances, particularly during field experiments in dynamic sea states. This cross-check allowed us to verify that features detected in the Range-Doppler maps corresponded to actual wave events, thereby increasing confidence in the interpretation of radar data. Furthermore, the camera facilitated the qualitative labeling of datasets used in this study, ensuring that events of interest were correctly distinguished from background clutter.

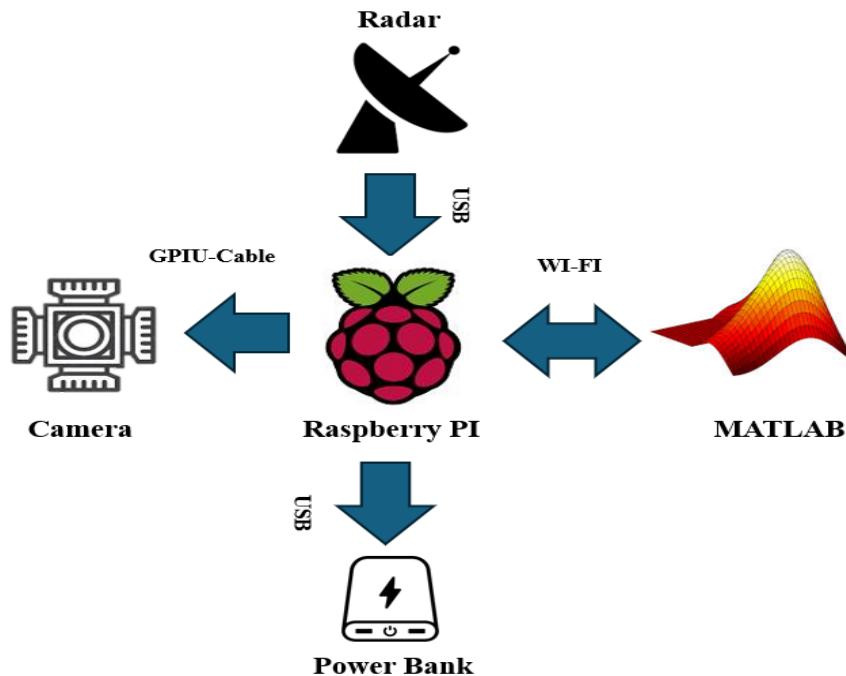


Figure 3.1. System Block Diagram and Connections.

The radar device utilized is based on the Distance2Go demo board from Infineon [52], which is compact, roughly the size of a credit card. This device consists of two main parts: the radar main board and the debugger board.

The communication between the control PC and the radar board is established through serial communication via a USB port. This setup allows for efficient data transfer and control signals between the two devices.

The second major component of the system is the Raspberry Pi 3B+ embedded PC. This device acts as an intermediary between the control PC and the radar board, providing a crucial link for data transmission and system control. The Raspberry Pi is directly connected to the Distance2Go radar board via a USB port and communicates with the control PC wirelessly through a Wi-Fi network. This wireless setup allows for remote control and data collection from the radar system without the need for physical wiring, enhancing the system's flexibility and ease of deployment.

Power for both the Distance2Go radar board and the Raspberry Pi can be supplied using a power bank or an external power supply with a USB output, providing versatility in different operational environments. The Raspberry Pi collects data from the radar board and transmits it to the main PC over the Wi-Fi network, ensuring a seamless data flow for further analysis.

The final component of the system is a PC running MATLAB, which is responsible for controlling the radar board via the Raspberry Pi. This is facilitated by the Raspberry Pi toolbox, which helps establish a virtual port for accessing the USB ports on the Raspberry Pi. The control PC receives the measured radar signals, performs the necessary data processing. This comprehensive setup allows for the efficient management and processing of radar data, making it well-suited for applications in water flow monitoring and other related fields.

### 3.3 Software Architecture:

Figure 3.2 illustrates the radar data processing workflow. The process begins by acquiring raw radar data and cleaning it to remove background noise and clutter, which prepares the data for further analysis. The next step involves using FMCW processing, which enhances the clarity and detail of the signal.

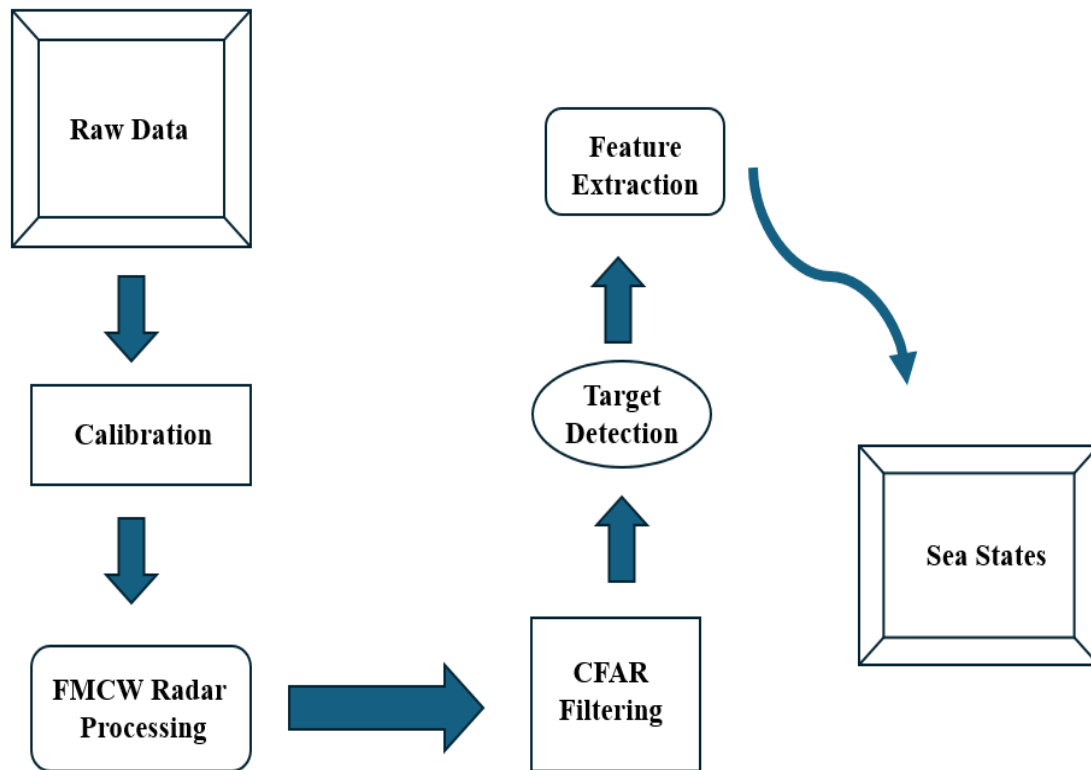


**Figure 3.2.** Flowchart of the Developed Data Analysis Method.

Following FMCW processing, we apply CFAR (Constant False Alarm Rate) filtering to the Range-Doppler matrix obtained from the previous step. This filtering process allows us to isolate and focus on the significant components of the signal, distinguishing them from irrelevant data.

After filtering, we categorize the detected signals into specific groups, ensuring that the signals correspond to actual targets, such as sea waves, rather than random noise or false echoes. This classification step is critical for accurately interpreting the radar data, as it helps eliminate false alarms and confirms the presence of real targets. By implementing this comprehensive data processing approach, we enhance the accuracy and reliability of radar-based object detection and tracking.

### **3.4 FMCW Radar Signal Processing:**

The Distance2Go development kit is a versatile and compact radar system designed for easy integration and testing of radar applications. It includes essential components such as the radar board, antennas, and a debugger, providing a comprehensive solution for developing and evaluating radar signal processing algorithms. The kit's high level of integration and ease of use

make it an ideal choice for both beginners and experienced developers working on radar-based projects.

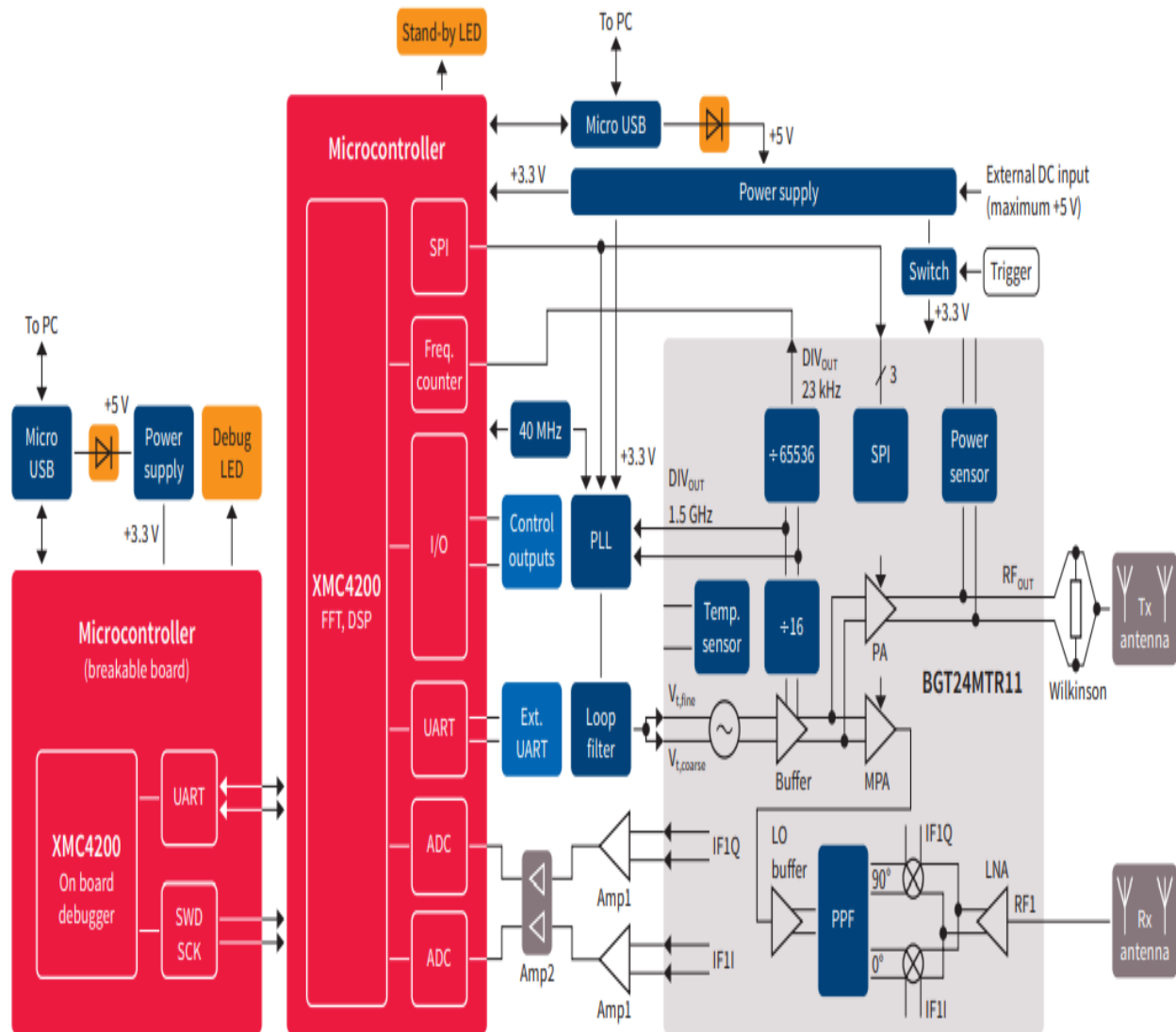


**Figure 3.3.** Block diagram of the Infineon Distance2Go board [46].

The Monolithic Microwave Integrated Circuit (MMIC) used in radar signal processing is highly integrated, combining several essential functions into one chip.

It includes a VCO for frequency control, a transmitter chain with amplifiers for both TX and LO outputs, and a complete receiver section with a Low-Noise Amplifier (LNA) and mixer. The VCO

is a free-running oscillator with two tuning inputs: one for coarse adjustment and one for fine-tuning.

The VCO section features two prescalers: one with a 1.5 GHz output for feeding an RF PLL and another with a 23 kHz square-wave output for a microcontroller-based software loop [67],[68]. The transmitter (TX) section contains a power amplifier with a differential output, typically delivering +11 dBm, adjustable down to 2 dBm in eight steps. Part of the TX signal is used as the LO signal for the on-chip mixer.

The receiver section offers a single-sideband noise figure (NF) of 12 dB and a voltage conversion gain of 26 dB. The LNA gain can be reduced in 5 dB steps. The integrated quadrature down-conversion mixer converts the RF signal directly to zero-IF.

Additionally, the chip includes power sensors for both TX and LO outputs, and a temperature sensor to support a software-based loop for VCO control. All internal settings can be adjusted via an SPI interface.

The fundamental concept of FMCW signals involves generating a linear frequency ramp [54], commonly known as a "chirp" [55]. The signal transmitted during one ramp, characterized by a sweep bandwidth (B) and a duration (T), can be expressed as:

$$S(t) = A \cos \left( 2\pi F_c t + \pi \frac{B}{T} t^2 + \varphi_0 \right) \quad (3.2)$$

In this context, (A) represents the signal's amplitude, ( $F_c$ ) denotes the carrier frequency, and ( $\varphi_0$ ) indicates the signal's initial phase.

The Fast Fourier Transform is a critical step in the processing chain of FMCW RADAR systems, enabling the extraction of both range and velocity information from the received signals. In sea wave monitoring, the FFT plays a dual role: it helps determine the distance of wave features from the RADAR system (range) and their movement characteristics (velocity).

### 3.4.1 Range FFT

The first FFT, commonly referred to as the Range FFT, is applied to the intermediate frequency (IF) signal derived from the RADAR system. This step converts the time-domain signal into the frequency domain, allowing the identification of beat frequencies. Each beat frequency corresponds to a unique range bin, representing the distance to a specific target (e.g., Sea wave). The resolution of the range FFT depends on the sweep bandwidth B and is given by:

$$\Delta R = \frac{c}{2B} \quad (3.3)$$

where,  
c is the speed of light, and B is the sweep bandwidth.

### 3.4.2 Doppler FFT

The second FFT, known as the Doppler FFT, is applied across multiple chirps to estimate the radial velocity of detected targets. In FMCW radar systems such as D2G, this process does not rely on the classical Doppler frequency shift. Instead, it leverages spatial Doppler, which refers to the phase shifts observed between successive chirps. These phase variations encode the target's motion, and the Doppler FFT extracts this information to estimate velocity. The Doppler frequency  $f_d$  is directly proportional to the velocity  $v$  of the target, as given by:

$$v = \frac{\lambda f_d}{2} \quad (3.4)$$

where  $\lambda$  is the wavelength of the transmitted signal. By performing the Doppler FFT, the RADAR system can calculate the velocity of moving wave patterns, such as their propagation speed.

### 3.4.3 2D-FFT and Range-Doppler Map

The 2D-FFT is a key technique in FMCW RADAR systems, enabling the creation of a Range-Doppler map a powerful two-dimensional representation of targets in terms of their range and velocity. The two axes of the Range-Doppler map correspond to distinct physical parameters: one axis represents range bins, which quantify the distance of objects from the RADAR, while the other axis represents Doppler frequencies, which are directly related to the relative velocity of the targets.

In the context of sea wave monitoring, the Range-Doppler map becomes an essential tool for visualizing and analyzing wave dynamics, this capability is crucial for real-time monitoring of sea states.

## 3.5 Calibration and Noise Reduction

In radar-based sea wave monitoring, calibration and noise suppression are critical for ensuring reliable measurements. In our system, calibration was primarily addressed in a relative sense, by compensating for leakage, static clutter, and environmental noise that otherwise dominate the received signal.

### **System Calibration:**

The FMCW radar chain introduces fixed delays and strong self-leakage components due to direct coupling between the transmitter and receiver. These appear as stationary peaks in the range spectrum that can mask true wave signals. To mitigate this effect, we applied a modified background subtraction technique. Each acquired frame was compared, allowing stationary contributions to be removed. This acts as a dynamic calibration step, continuously adapting to the environment and effectively reducing static clutter.

### **Noise Reduction:**

To further refine the signal, windowing functions (such as the Kaiser window) were applied before the FFT operations. Windowing reduces spectral leakage and improves the accuracy of both range and Doppler estimation, especially in cluttered maritime conditions. This step ensured that weak but relevant wave reflections were not hidden by sidelobes of stronger signals.

## **3.6 Clutter Reduction Using Frame Subtraction:**

To address RX-TX leakage and suppress clutter from static objects, a Moving Target Indication (MTI) filtering technique is initially applied. This approach enhances the detection of moving targets by attenuating stationary components in the received signal. In the context of FMCW radar systems, MTI is typically implemented using digital techniques that operate across multiple chirps to isolate dynamic targets. Such methods have been well-established in radar signal processing literature [49][50]. In our developed system, each radar data frame is represented as an  $(N_s * N_c)$  data matrix, akin to a digital image. The BS method detects the foreground by calculating the difference between a newly recorded image and a reference image, often referred to as the “Background model” or “reference model” [50].

Traditional BS methods, which are commonly implemented in commercial radars, use a fixed reference background. To improve this, we devised a modified BS algorithm specifically for calibration and moving object detection.

Our modified BS algorithm differentiates itself by not relying on a fixed reference frame. Since the electromagnetic scattering response of the environment can change over time (e.g., due to shifts in static objects), we employ a dynamic and adaptive background reference model.

This adaptive approach enhances the effectiveness of background removal and improves the detection of moving targets [50].

The calibration process involves fine-tuning the radar system to enhance target detection amidst background clutter, using a technique known as Background Subtraction (BS). Initially, raw data

frames represented as matrices of radar returns undergo signal processing, including Fast Fourier Transform (FFT) operations, to extract range and Doppler information. After this initial processing, our improved BS algorithm is applied. Unlike conventional methods that rely on a static background reference, the proposed algorithm dynamically updates the background model over time to adapt to environmental changes. This adaptive strategy improves the suppression of static clutter and enhances the detection of moving targets. The output from the BS stage is then passed to subsequent stages, such as windowing and further spectral analysis, to refine target characterization.

## **Windowing for FFT Optimization**

Windowing functions play a critical role in FMCW RADAR signal processing, particularly in improving the accuracy and resolution of the Fast Fourier Transform (FFT) operations. By applying windowing functions to the time-domain signal before performing FFTs, spectral leakage a phenomenon where signal energy spreads to adjacent frequencies is minimized. This enhancement is crucial for precise range and velocity measurements, as it ensures that the FFT outputs reflect the true signal characteristics without distortion from adjacent frequency components.

### **3.6.1 Purpose of Windowing**

When the FFT is applied to a finite-length signal, discontinuities at the edges of the signal can cause spurious frequency components to appear in the spectrum, a problem known as spectral leakage. Windowing functions smooth these edges, reducing the impact of such discontinuities and improving the overall spectral representation. This smoothing process is essential in RADAR applications, where accurate detection of target range and velocity is dependent on minimizing interference from unwanted spectral components.

### **3.6.2 Application of the Kaiser Window Function**

Various windowing functions are available, each offering different trade-offs between main-lobe width (resolution) and side-lobe suppression (leakage reduction). In FMCW RADAR systems, the Kaiser window is frequently used because of its flexibility and effectiveness. The Kaiser window is controlled by a parameter known as the "beta value," which can be adjusted to balance between resolution and leakage suppression based on the RADAR's operational requirements.

### **3.6.3 Application of Windowing in FMCW RADAR**

Windowing functions are applied at different stages of the FFT process to optimize specific aspects of signal analysis:

#### **a) FastTime\_Window for Range FFT:**

The FastTime\_Window is applied during the Range FFT, where the goal is to convert the time-domain signal into the frequency domain and determine the distances of targets. The windowing function minimizes spectral leakage, ensuring that the beat frequencies corresponding to different targets are accurately resolved.

The choice of window parameters impacts the range resolution, which is defined as the ability to distinguish between two closely spaced targets in range.

#### **b) SlowTime\_Window for Doppler FFT:**

The SlowTime\_Window is applied during the Doppler FFT, which analyzes the Spatial Doppler caused by the relative motion of targets. This step is important for determining the velocity of moving targets, such as sea waves or objects.

The SlowTime\_Window reduces spectral leakage in the Doppler domain, improving the accuracy of velocity estimation. It ensures that Doppler frequencies corresponding to different velocities are distinctly separated, even for targets with similar speeds.

#### **c) Impact on the Range-Doppler Map:**

The combination of windowing in both the Range FFT and Doppler FFT directly affects the quality of the Range-Doppler map, which represents the relationship between target range and velocity. By reducing spectral leakage:

During calibration, the radar applies Kaiser windows to these data frames, referred to as "FastTime\_Window" and "SlowTime\_Window," each with specific parameters. These windows optimize the FFT processing, improving resolution and accuracy in identifying targets.

The clarity of the map improves, making it easier to identify and track individual targets.

Unwanted artifacts in the map are minimized, allowing for more reliable detection in cluttered or noisy environments.

The overall resolution of the map is enhanced, ensuring that closely spaced targets in range and velocity domains can be distinguished.

#### **d) Tuning Window Parameters:**

The effectiveness of windowing functions depends on the chosen parameters, particularly the beta value in the Kaiser window. Higher beta values result in stronger side-lobe suppression but at the cost of wider main lobes, which may reduce resolution. Conversely, lower beta values prioritize

resolution but may allow more spectral leakage. In RADAR applications, these parameters are fine-tuned based on the specific operational environment:

In environments with high clutter or noise, higher beta values are preferred to suppress interference.

To enhance the accuracy of Doppler frequency estimation in radar-based sea wave monitoring, appropriate windowing functions are applied prior to performing the FFT on slow-time data. This step reduces spectral leakage and improves frequency resolution, allowing for more precise identification of wave motion characteristics. The resulting Range-Doppler Maps offer refined insights into the velocity and spatial distribution of sea waves, supporting more accurate sea state analysis.

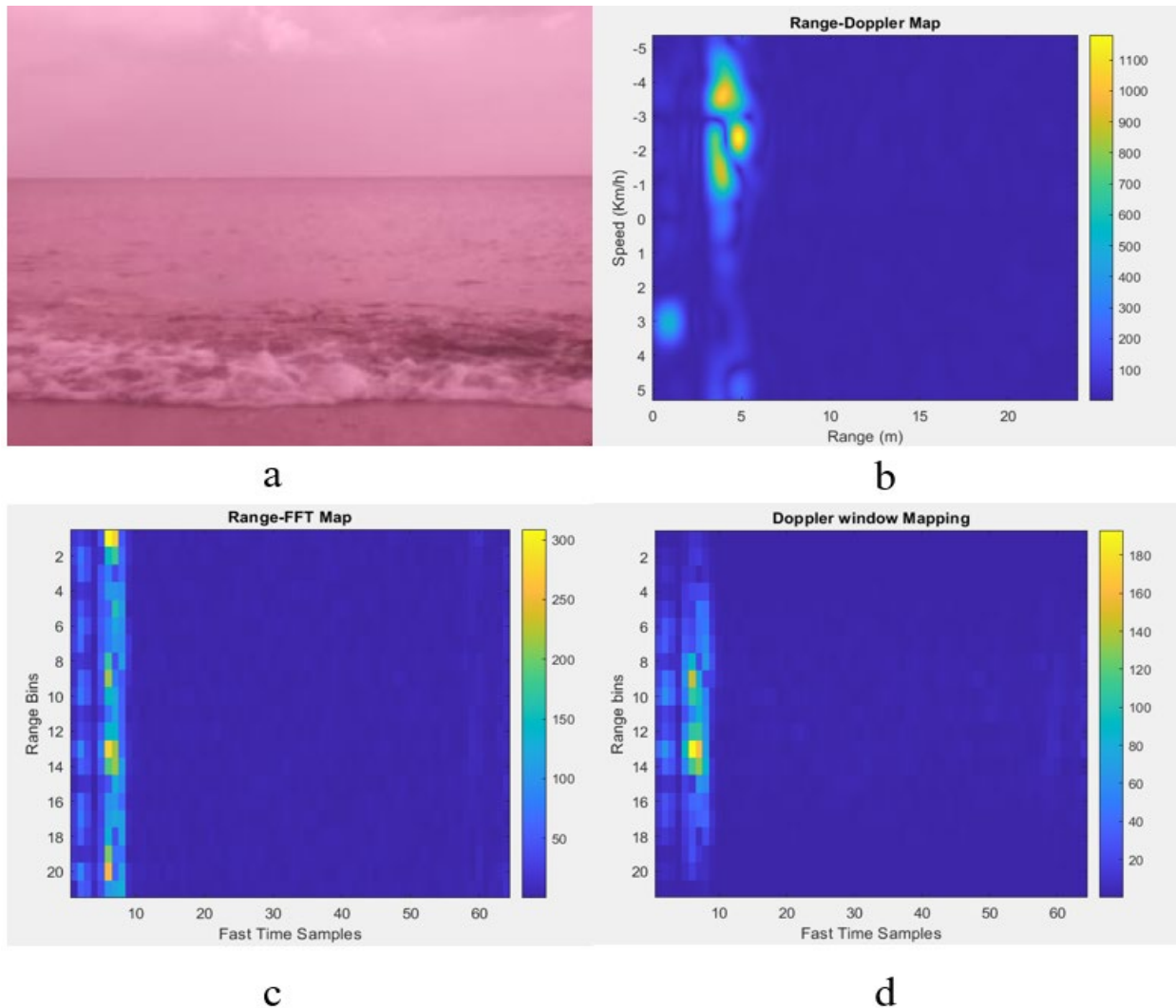


**Figure 3.4.** Results of Signal Processing for rolling wave: (a) Camera image (b) Range-Doppler map, (c) Range FFT Mapping, (d) Doppler window Mapping.

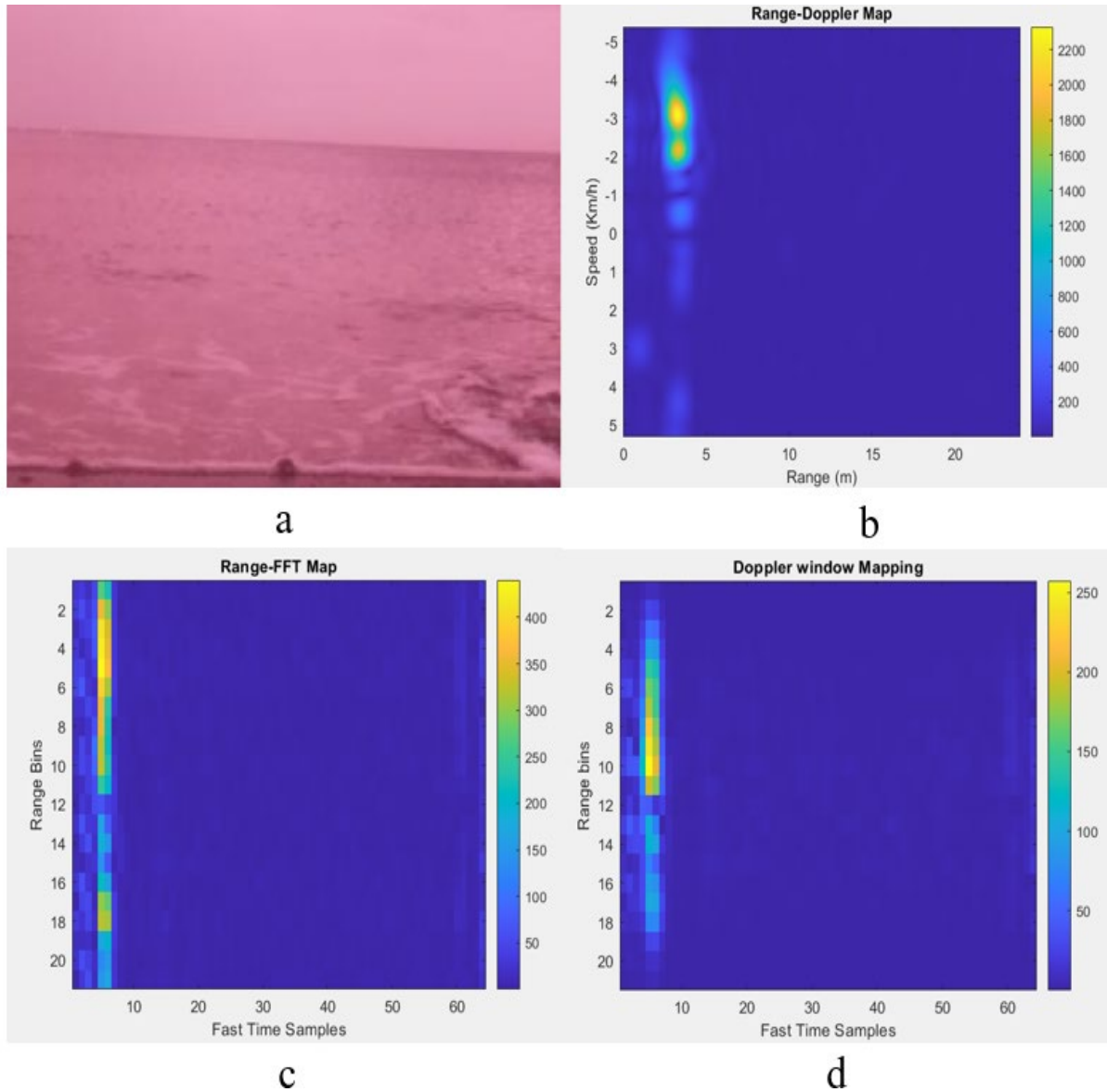


**Figure 3.5.** Results of Signal Processing for subsidence wave: (a) Camera image (b) Range-Doppler map, (c) Range FFT Mapping, (d) Doppler window Mapping.

Figure (a) shows a camera image of the scene, while Figure (b) presents the result of the Range-Doppler (RD) map, representing the spatial distribution of reflected signal energy. Figure (c) demonstrates the range FFT, and Figure (d) depicts the effect of windowing functions on the frequency content prior to FFT, which combines both range and velocity information of the detected targets using color-coded intensity.

In radar-based sea wave analysis, the RD map serves as the primary tool, encapsulating the outcomes of both the range and Doppler FFTs. It provides a comprehensive view of the wave patterns, simultaneously revealing their distance from the radar and their motion characteristics. While the range FFT alone is a subset of the RD map, it can be useful for examining signal behavior along the fast time axis independently, especially during system calibration or windowing assessment.

Windowing techniques, applied before FFT operations, help mitigate spectral leakage an artifact where energy from one frequency bin spills into adjacent bins, reducing frequency resolution. Although the so-called "FFT window map" does not represent a separate radar product, it serves as a visualization of how different windowing functions impact signal shaping and leakage suppression. However, the concept should not be misinterpreted as providing information beyond what is already contained in the RD map. In rolling sea waves depicted in Figure 3.4, the analysis of the map's intensity reveals crucial wave characteristics. Enhanced by camera imagery, this R-D map aids in comprehending sea behavior, highlighting areas of high velocity (-4 km/h) that gradually decrease near the beach, as shown in the subsequent image for subsiding waves in Figure 3.5. Conversely, in subsiding sea waves, the R-D map indicates velocities of -3 km/h, signifying varying wave speeds and directions. FFT range mapping displays broader patterns, indicating increased wave turbulence. The fluctuating fast sample times with range bins for sea waves reveal rapid changes in wave behavior over short time intervals. This reflects the dynamic nature of sea waves, influenced by factors like wind and currents. It emphasizes the importance of meticulous data interpretation to understand sea wave dynamics accurately.

In scenarios requiring high precision, such as distinguishing closely spaced wave patterns, lower beta values may be chosen to enhance resolution.

The "FastTime\_Window" parameter, set to a Kaiser window value of 8, controls the FFT operation for range processing. Similarly, the "SlowTime\_Window," configured with a Kaiser window value of 20, manages the FFT operation for Doppler processing.

This calibration process significantly improves the overall performance of the system, leading to more reliable and accurate results for target identification and tracking.

In this approach, each radar frame is compared with its immediate predecessor to detect changes over time, as described by the following expression:

$$W(K) = Z(K) - Z(K - 1) \quad (3.1)$$

Simply put, we compare the data captured in two consecutive frames:  $Z(k)$  and  $Z(k - 1)$ .

- $Z(k)$  represents the radar data at time step  $k$ .
- $Z(k-1)$  represents the radar data at the previous time step  $k-1$ .
- $W(k)$  represents the result of the differencing operation, which highlights variations between consecutive frames.

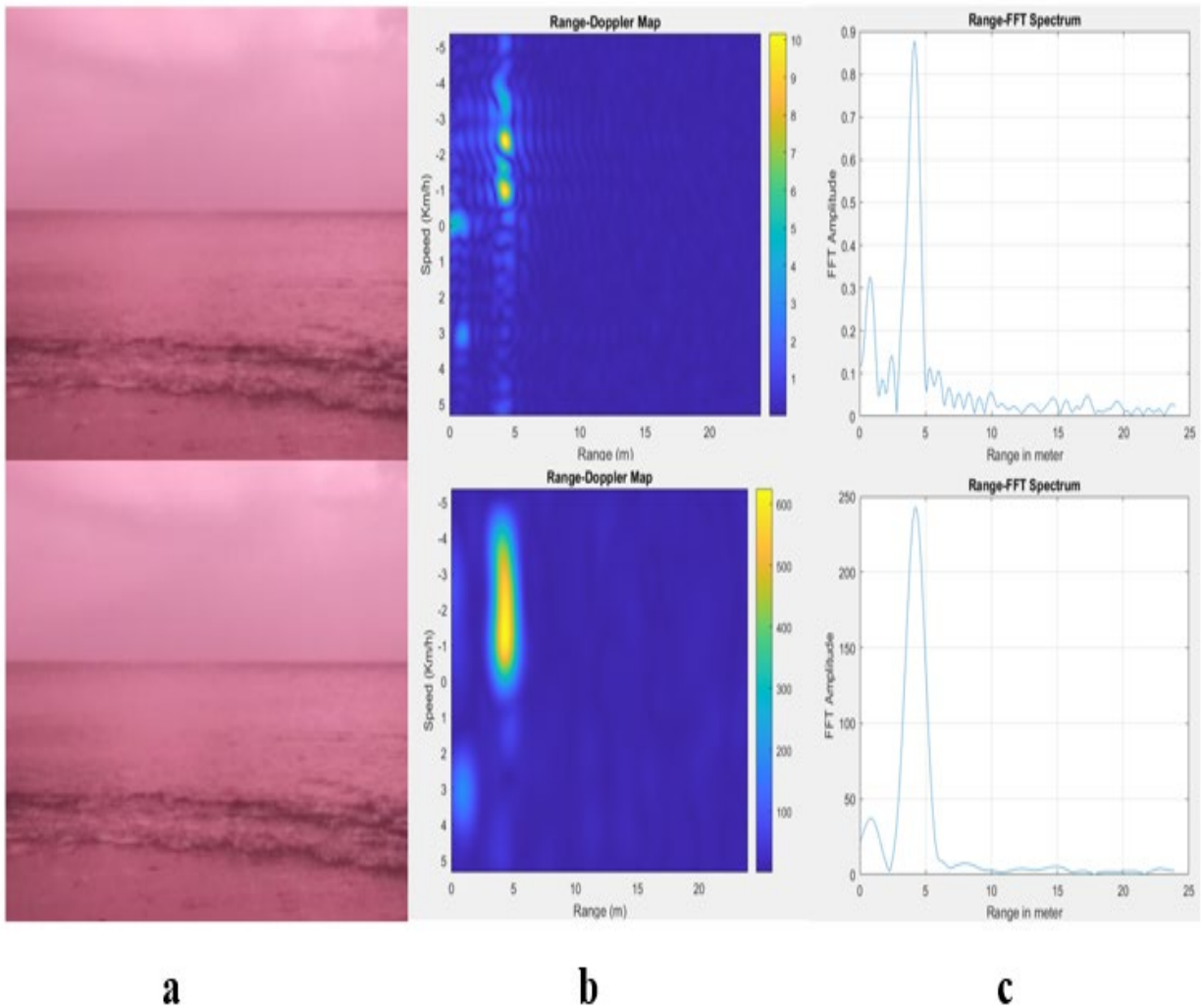
These frames represent radar data recorded at different times. By subtracting the data from the previous frame  $Z(k - 1)$  from the current frame  $Z(k)$ , we can detect any changes that occurred between the two moments.

The raw data matrix used before 2D FFT processing is directly provided by the radar board and serves as the input data for the processing chain. However, it's worth noting that Background Subtraction (BS) can also be effectively performed after FFT computation, yielding comparable results. Although this technique may appear similar to background subtraction, it is more accurately characterized as a two-pulse canceller or single delay line canceller, a method commonly employed in radar signal processing to suppress stationary clutter [51], [52]. In contrast, classical background subtraction involves acquiring a static calibration frame when no targets are present in the monitored area and subtracting it from subsequent frames. This calibration is typically performed once or at predefined intervals, rather than continuously between successive frames.

In our approach, the subtraction is applied to the complex-valued data from the I/Q receiver. This method captures changes in the target's response from frame to frame, allowing peaks to sum constructively or destructively. As a result, the resulting peak may not necessarily have a lower amplitude. However, the static response typically remains consistent, enabling the removal of stationary clutters.

By using frame subtraction, we significantly reduce stationary clutter in the radar image while preserving the scattering response of moving targets. Although the target's amplitude may vary, the crucial information required for tracking is retained. If a target temporarily stops in the monitored area, its response is canceled by BS. Nonetheless, the tracking algorithm maintains a lock on the target, recovering its response when it starts moving again.

In Fig. 3.6, we illustrate the effectiveness of our clutter removal method using a moving target positioned 4 meters from the radar. Initially, in Fig. 3.6(b), the Range-Doppler map is cluttered with significant interference, making it difficult to discern the target. However, after applying our calibration process, the map clarity improves dramatically, revealing the moving target with distinct intensity patterns and minimal clutter interference.



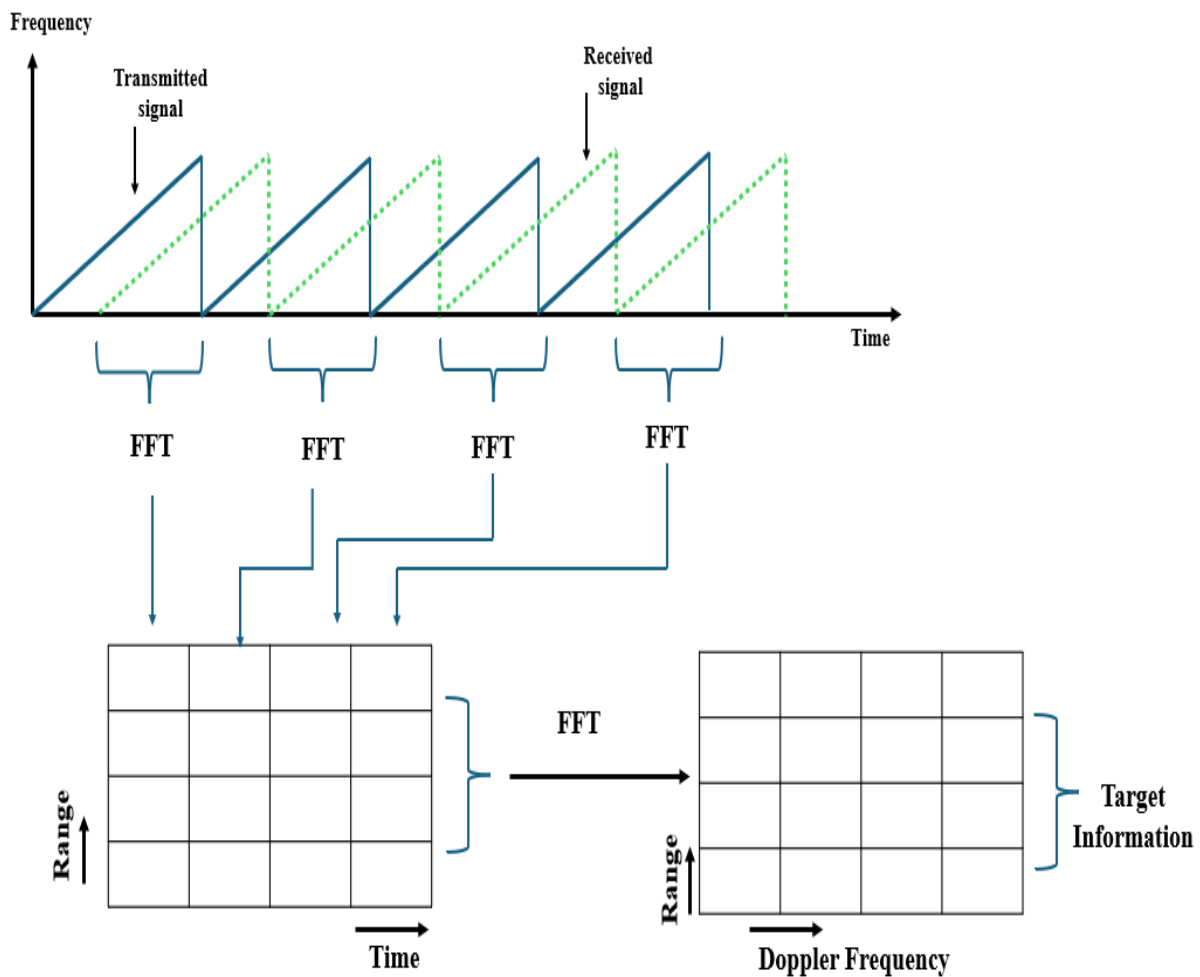
**Figure 3.6** presents the results: (a) a camera image, (b) the Range-Doppler map, and (c) the range FFT before and after calibration using the frame subtraction algorithm.

Fig. 3.6 (c) further demonstrates the impact of our frame subtraction technique by showing the range FFT magnitude before and after its application. Initially, clutter causes multiple minor peaks, including a prominent peak near zero due to antenna leakage. After applying the frame subtraction technique, the clutter is significantly reduced, and a clear, prominent peak appears at 4 meters, accurately representing the moving target. This clear distinction highlights the effectiveness of our method in enhancing target detection amidst clutter interference.

Figure 3.7 illustrates the detailed signal processing workflow within an FMCW radar system, emphasizing the extraction of range and Doppler information from detected targets. At the top, the transmitted signal is shown as a series of linear frequency modulations, known as chirps, which

steadily increase over time. The received signal, depicted as dashed lines, represents the echoes of these transmitted chirps after they reflect off targets. The time delay between the transmitted and received signals is directly proportional to the target's distance from the radar.

Figure 3.7 illustrates the sequence of signal processing steps for FMCW radar, focusing on range and velocity extraction. However, it's important to note that the figure omits the mixing process the crucial step where the transmitted and received signals are combined to generate the intermediate frequency (IF) signal. This IF signal encodes both range and velocity information based on the phase or frequency difference. The IF signal is then processed with a Fast Fourier Transform (FFT) across fast time (within a chirp) to extract range, and a second FFT is applied across slow time (across chirps) to reveal velocity through phase evolution, leading to the construction of the Range-Doppler map.



**Figure 3.7.** Workflow of signal processing in FMCW Radar for Range-Doppler Map Generation.

To determine the range, the radar applies a Fast Fourier Transform (FFT) to each chirp. These bins are then organized into a two-dimensional matrix, with one axis representing range and the other representing time, showing how the target's distance changes over the sequence of chirps.

Next, the radar applies a second FFT along the time axis for each range bin to extract the Doppler frequency, which provides information about the target's velocity. This map contains detailed target information, revealing both the distance and velocity of the detected targets. The Range-Doppler map is essential for accurately tracking multiple targets, making it a critical component in applications like automotive radar systems, surveillance, and environmental monitoring.

### 3.7 Principles of CFAR

The constant false alarm rate (CFAR) circuitry is responsible for setting a power threshold to distinguish probable target signals from spurious sources. A low threshold increases the likelihood of detecting real targets but also raises the occurrence of false alarms. Conversely, a high threshold reduces false alarms but may result in fewer detected targets. Most radar systems set this threshold to achieve a specific false alarm probability or rate, ensuring consistent performance.

In environments where the background noise is constant over time and space, a fixed threshold can be applied to achieve the desired false alarm probability. This threshold depends on the noise's probability density function, typically assumed to follow a Gaussian distribution. In such cases, the detection probability depends on the target's signal-to-noise ratio. However, in practical scenarios with varying clutter and interference, the noise level fluctuates both spatially and temporally. To address this, CFAR detection adjusts the threshold dynamically, maintaining a constant probability of false alarm by raising or lowering the threshold as needed.

Based on this estimated noise power, the detection threshold, represented as ( $T_h$ ), is calculated as follows:

$$T_h = \alpha p_n \quad (3.4)$$

Where ( $p_n$ ) represents the estimated noise power, and ( $\alpha$ ) is a scaling factor referred to as the threshold factor. This equation shows that the threshold adapts based on the data. By choosing an appropriate value for the threshold factor ( $\alpha$ ), the probability of false alarms can be kept constant, which is the core concept behind CFAR.

In radar systems, particularly during CFAR processing, accurately estimating the noise power level is critical for ensuring robust target detection.

The average noise power level can be expressed as follows:

$$p_n = \frac{1}{N} \sum_{i=1}^N x_i \quad (3.5)$$

Where ,

- $p_n$  is the noise power at the cell with indices (i).
- N is the total number of reference cells.

Fig 3.8 illustrates the structure of a CFAR window used in radar signal processing. The Cell Under Test (CUT) represents the target cell being evaluated for detection. Surrounding the CUT are the Reference Cells, which are used to estimate the local noise level and calculate the detection threshold. To avoid contamination of the noise estimate by the target signal, Guard Cells are placed immediately adjacent to the CUT and excluded from the noise calculation.

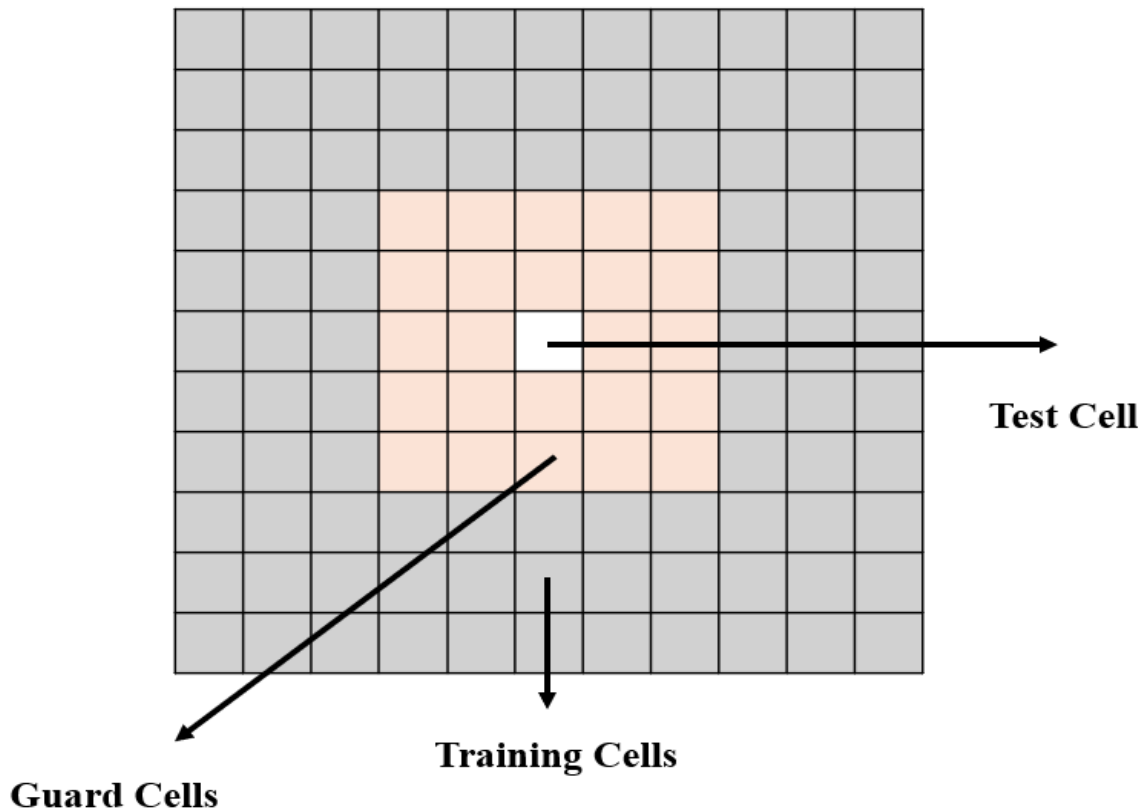


**Figure 3.8.** Illustrating the Cell Under Test (CUT), Reference Cells, and Guard Cells.

### 3.7.1 Cell-averaging CFAR

Detection in radar systems occurs when the signal power in the cell under test exceeds a predefined threshold. In basic CFAR detection methods, this threshold is determined by estimating the noise floor around the CUT. This estimation involves taking a block of surrounding cells and calculating their average power level. A target is considered present in the CUT if its power exceeds both the power levels of all adjacent cells and the estimated local average power level. In some cases, the local power estimate may be slightly adjusted upward to account for the limited number of sampled cells. This straightforward method is known as cell-averaging CFAR .

Alternative CFAR approaches improve performance in certain conditions. For instance, some methods calculate separate averages for the cells on either side of the CUT and then use either the greater or the lesser of these two values to define the local power level. These techniques are referred to as greatest-of CFAR (GO-CFAR) and least-of CFAR (LO-CFAR), respectively. GO-CFAR is particularly effective in detecting targets near areas of clutter, while LO-CFAR can enhance detection in environments with uneven noise distributions.

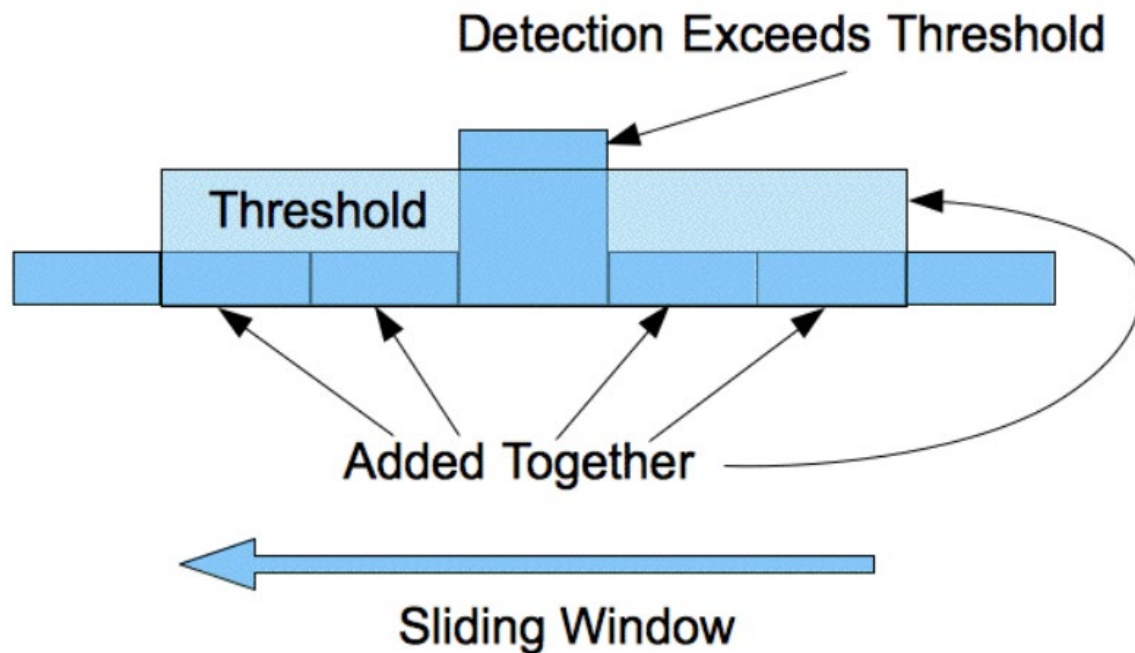


**Figure 3.9.** Illustration of CFAR Detection with Sliding Window and Thresholding [53].

This figure illustrates the Constant False Alarm Rate (CFAR) detection process. The cell under test (CUT) is the central cell whose signal power is being evaluated for target detection.

The sum of the reference cells' power is then multiplied by a scaling constant to account for noise and environmental conditions, resulting in a dynamic threshold value. Detection occurs when the signal power of the CUT exceeds this threshold, indicating the presence of a potential target. This process is applied repeatedly as the sliding window moves across the data, ensuring that each cell is evaluated in turn while maintaining a consistent probability of false alarms.

More advanced CFAR algorithms can adaptively determine the threshold level by thoroughly analyzing the statistical properties of the background in which targets are being detected. This approach is especially valuable in maritime radar applications, where the background, often dominated by sea clutter, exhibits highly spiky characteristics that are not well represented by additive white Gaussian noise. This presents a challenging detection scenario, as it becomes difficult to distinguish between spikes caused by sea surface reflections and those resulting from valid targets, such as submarine periscopes.

### **3.7.2 Applying CFAR for Range-Doppler Map Filtering:**

In radar systems, the primary goal is to detect targets by evaluating the received signal against a predetermined level, known as a threshold. Setting this threshold accurately is critical, as it determines the radar's ability to distinguish between genuine targets and false detections. An optimal threshold ensures that the radar system can reliably identify true targets while minimizing the occurrence of false alarms.

In real-world applications like sea wave analysis, the environmental conditions are constantly changing, making it difficult to rely on fixed, theoretical thresholds for detecting waves. The CFAR detector, particularly the Cell Averaging CFAR, provides a more adaptive and reliable approach by dynamically adjusting the detection threshold based on the surrounding noise. This ensures better performance in environments with fluctuating noise levels, such as the ocean, where reflections from waves and other moving objects create a challenging scenario. Additionally, by implementing the CFAR algorithm in the Phased Array System Toolbox, the process becomes more efficient, enabling real-time analysis of sea wave dynamics. This adaptive nature makes CFAR detectors especially valuable for monitoring maritime environments with high accuracy [54].

A threshold that is too low can result in numerous false alarms, overwhelming the system with incorrect detections and potentially leading to significant operational inefficiencies and costs. Conversely, a threshold set too high might cause the radar to miss genuine targets, compromising the system's effectiveness and reliability.

By implementing CFAR filtering, radar systems can maintain a consistent false alarm rate while improving the detection probability of real targets. This adaptive approach not only enhances the

radar's performance but also optimizes its operational efficiency, ensuring reliable target detection in a wide range of scenarios.

The effectiveness of CFAR filtering is evident in its application to Range-Doppler maps, where it helps in filtering out clutter and isolating significant target signals. By continuously adjusting the threshold, CFAR ensures that the radar system remains sensitive to genuine targets without being overwhelmed by false alarms, thus maintaining a high level of accuracy and reliability in target detection.

Fig 3.10 illustrates our method for analyzing sea waves using radar. The process begins with collecting radar data frame by frame. We then applied a 2D Cell Averaging Constant False Alarm Rate (2D-CA-CFAR) filter to the range-Doppler map. This filtering technique helps to eliminate noise and focus on genuine water movements. The CFAR filter determines a threshold based on the average signal from the surrounding area, thereby highlighting only the significant signals.

The radar data signal processing flowchart demonstrates the extraction of velocity after applying a 2D-FFT to each frame. Following this, a two-dimensional cell averaging constant false alarm rate (2D-CA-CFAR) filter is applied to the range-Doppler map of each frame to eliminate background noise around detected water movements [55].

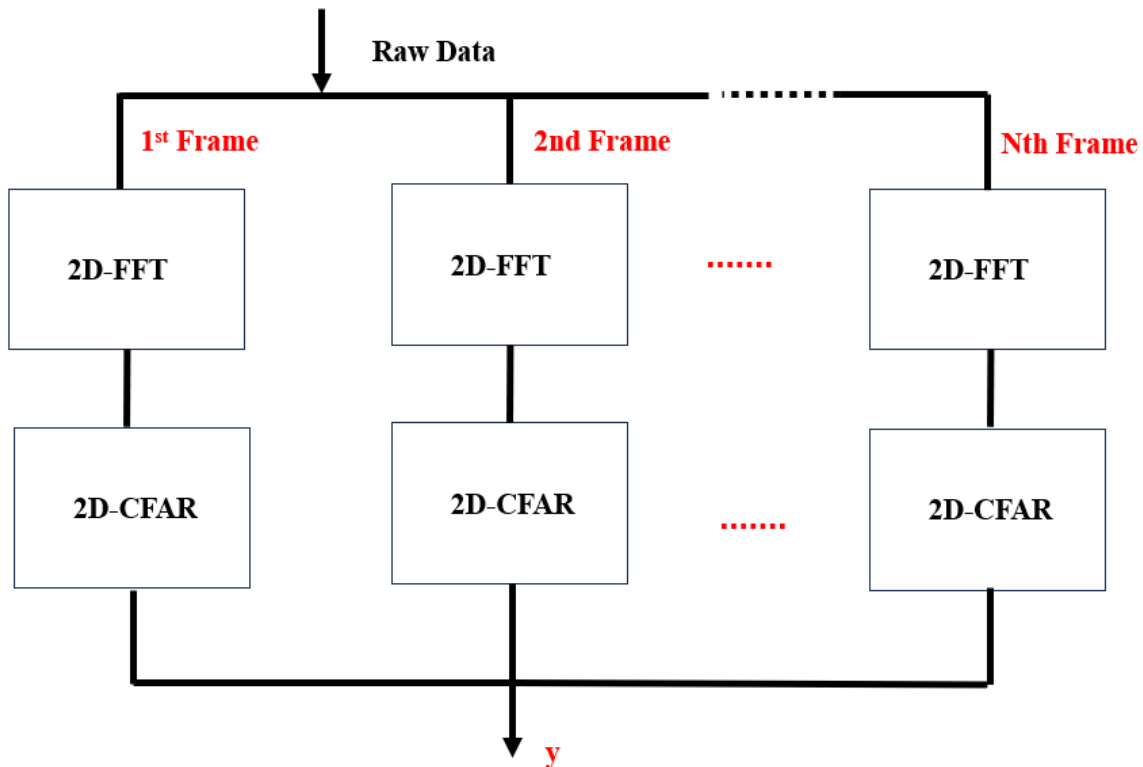


**Figure 3.10.** Radar Data Signal Processing Flowchart.

Alternative CFAR methods, such as ordered statistic CFAR, could also be utilized; however, they are not elaborated upon in this article. For more detailed information on various CFAR techniques, readers can refer to [56] and other sources.

To differentiate between stationary and moving objects, signals near zero Doppler speed, specifically within  $\pm 0.1$  km/h, are excluded. This exclusion is crucial as it helps to avoid confusion between stationary and dynamic targets. By filtering out these signals, the radar data is refined, significantly enhancing the clarity and accuracy of the detected sea wave patterns.

After applying the 2D-CA-CFAR filter, the radar system focuses on significant movements indicative of sea wave dynamics, ensuring precise identification and tracking of these features. This method ensures that the radar system effectively distinguishes between static objects and moving sea wave patterns, providing reliable data for further analysis.

The meticulous approach of filtering out signals near zero Doppler speed enables a clear visualization of sea wave movements. The resulting radar data is more accurate and provides a comprehensive representation of the dynamic sea wave features. As illustrated in the map in Fig. 3.11, this technique allows for a detailed and reliable analysis of sea wave dynamics, ensuring that the radar system captures significant movements without the interference of stationary objects. This enhanced clarity in data presentation is critical for accurate interpretation and further research into sea wave behavior.

By implementing the CA-CFAR method, the radar system remains adaptable to various sea states, making it a robust solution for continuous monitoring. Moreover, the ability to dynamically adjust thresholds based on the surrounding noise level ensures that the radar system performs optimally even in environments with varying clutter levels. The enhanced precision in tracking sea wave dynamics offers a deeper insight into oceanographic studies and maritime operations, where understanding wave patterns is critical for vessel navigation and offshore structure safety.

In Constant False Alarm Rate (CFAR) processing, when detecting signals in a specific cell, known as the Cell Under Test (CUT), the noise power is usually estimated from the surrounding cells.

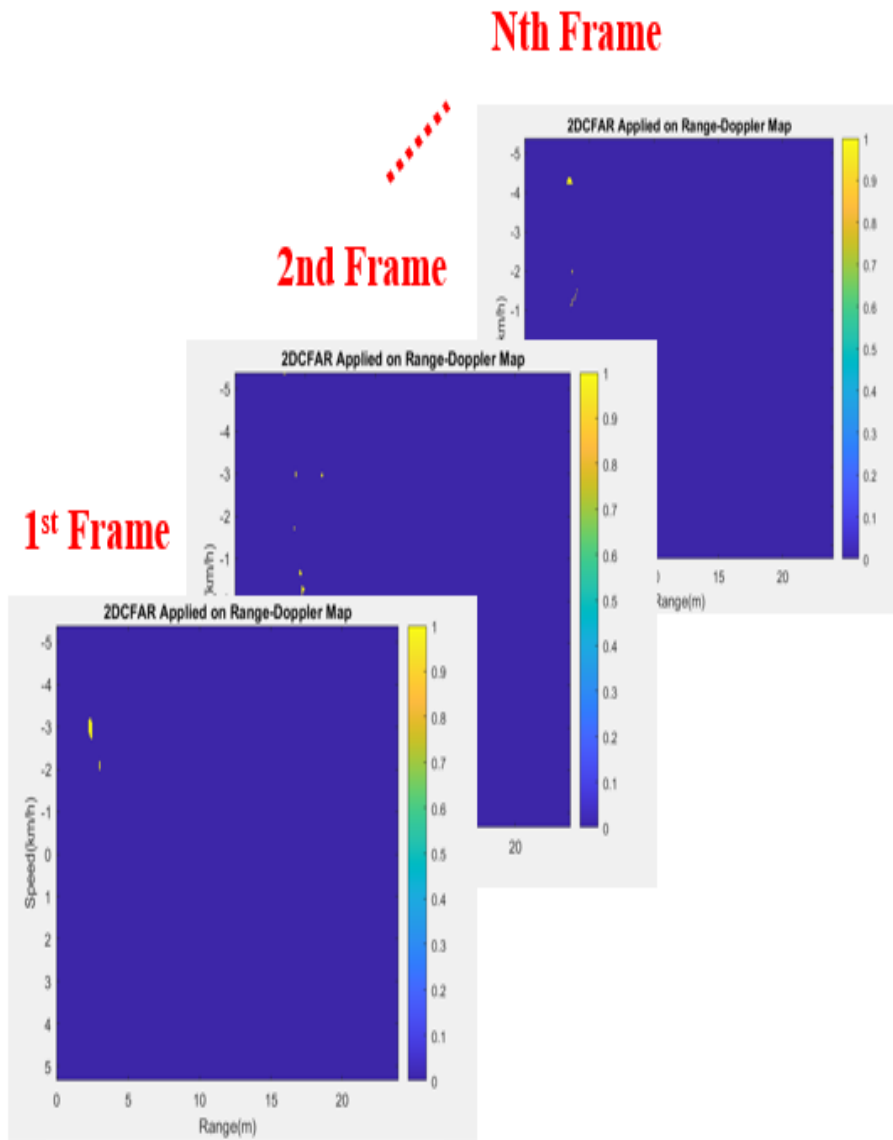


**Figure 3.11.** Visualization of Time-Averaged Velocity Processing.

In Figure 3.12, we discussed the fundamental concepts of CFAR detectors, emphasizing their application in sea wave analysis. We demonstrated how to implement cell averaging CFAR detection on range-Doppler images using the Phased Array System Toolbox. When comparing this approach to one that uses a theoretically calculated threshold, it becomes evident that the CFAR detector is more practical for real-world sea wave analysis.

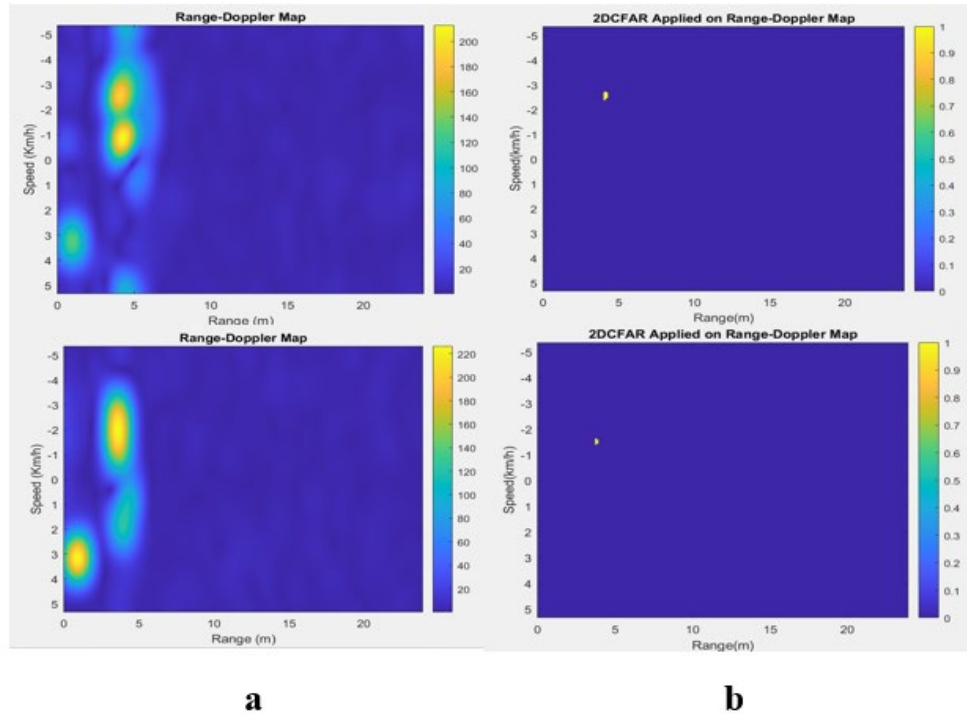
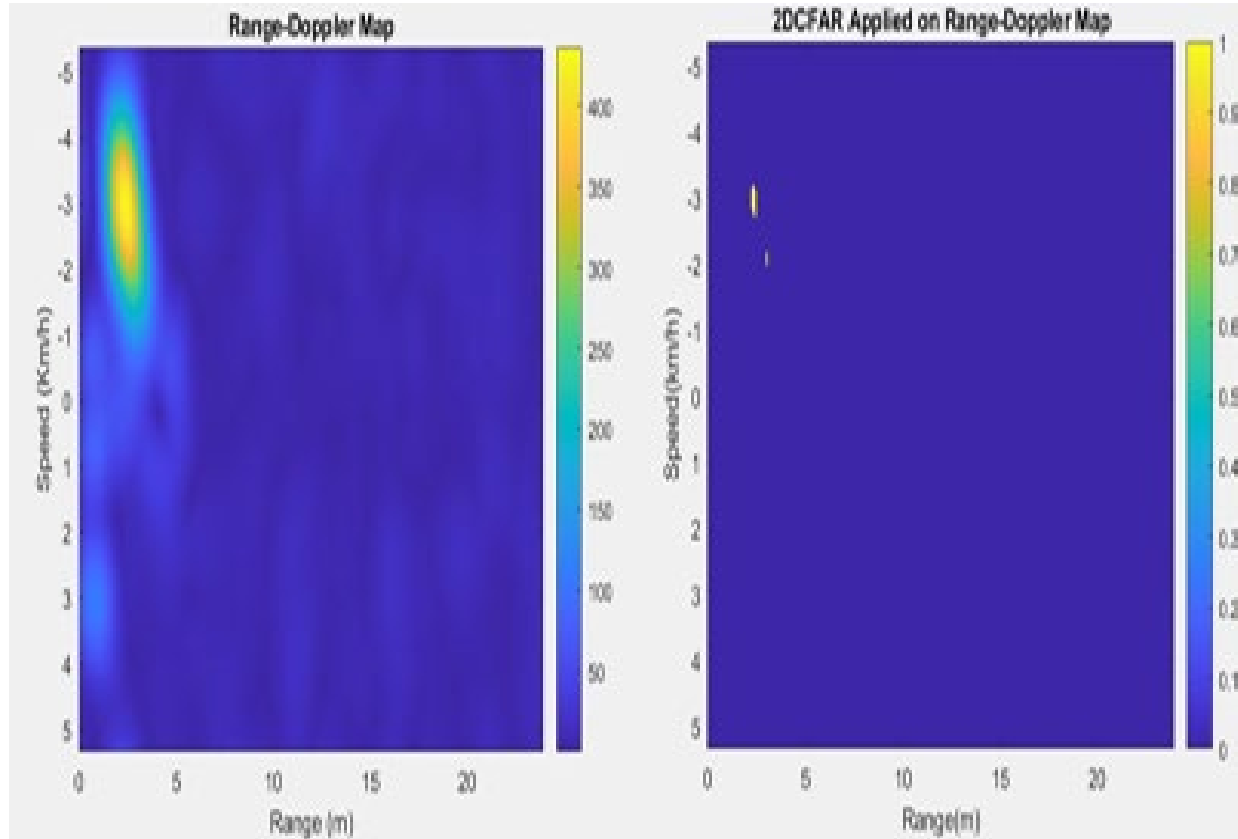


**Figure 3.12.** showcases Range-Doppler plots before and after post-processing for maritime settings, utilizing 2D-CFAR filtering. Image (a) shows the 2D-FFT without filters, and image (b) shows the results post-filter application.



**Figure 3.13.** Camera Image of sea wave.

Figure 3.13 presents a camera image of the sea wave, offering a visual context for the observed phenomena. This image serves as a reference for validating radar data interpretation.



3.14. Range-Doppler Map (2D) and 2D CFAR Detection of sea wave.

Figure 3.14 presents the Range-Doppler map alongside the result of applying a 2D Cell-Averaging CFAR filter. In the left panel, the 2D Range-Doppler map reveals the intensity of received radar signals through a color-coded scale. A distinct bright region at a specific range and Doppler frequency signifies the presence of a strong sea wave. The intensity and concentration of this region suggest a high-energy wavefront, indicating both significant motion and reflectivity.

The right panel, showing the output after applying the 2D CFAR algorithm, retains only the high-energy detections that exceed the adaptive threshold. In this case, the strong wave leads to a clearer and more prominent detection, standing out sharply against the suppressed background. This

demonstrates that stronger wave activity not only increases the radar return signal but also improves the robustness of detection after CFAR processing.

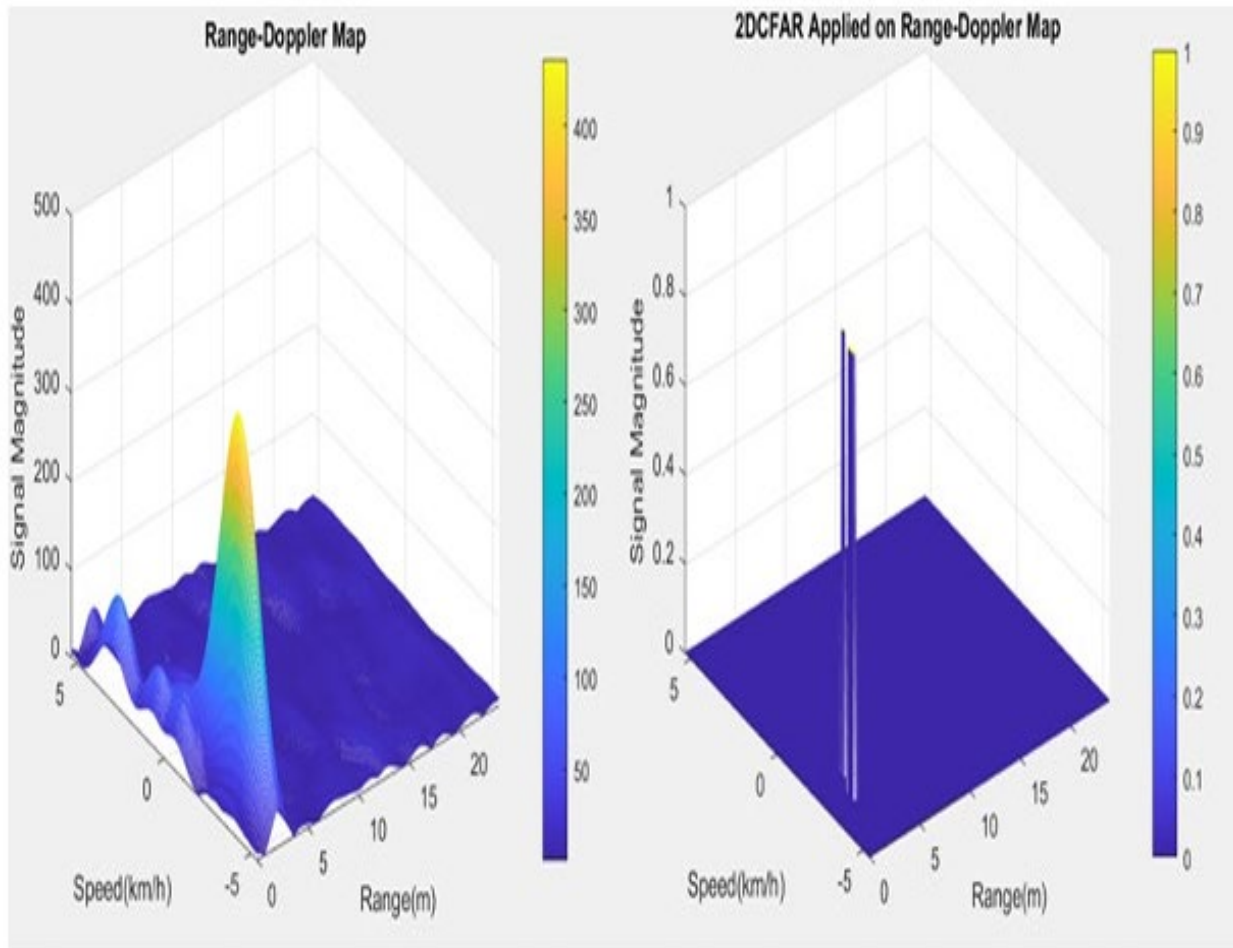


**Figure 3.15.** Range-Doppler Map (3D) and 2D CFAR Detection (3D) of sea wave.

These maps serve as essential tools in radar analysis, providing a visual representation of target range and velocity in two dimensions. On these maps, the vertical axis signifies the target's distance, determined by the time delay of the reflected signal, while the horizontal axis depicts the target's velocity, inferred from the Doppler frequency shift. The color intensity on these maps denotes the strength of the returned signal, with brighter colors indicating stronger reflections, particularly concerning water flow.

### 3.8 Conclusion

In this chapter, the role and performance of Constant False Alarm Rate (CFAR) algorithms in sea wave monitoring and maritime applications were thoroughly evaluated. CFAR techniques, particularly CA-CFAR, were demonstrated to be essential for dynamic thresholding, enabling accurate detection of wave patterns amidst fluctuating environmental noise.

The MATLAB simulations confirmed the robustness of these algorithms, with CA-CFAR offering a balanced performance in terms of detection accuracy, false alarm rate, and computational efficiency for real-time applications. The results emphasized the need for tailoring CFAR parameters, such as reference window size and scaling factors, to specific environmental conditions to maximize performance.

In conclusion, CFAR algorithms represent a powerful tool for improving the precision and reliability of FMCW radar systems in sea wave monitoring and other maritime applications. Their adaptability to complex and dynamic environments underscores their significance, making them a cornerstone for ongoing developments in radar-based environmental monitoring systems.

# Chapter 4



UNIONE EUROPEA  
Fondo Sociale Europeo



*Ministero dell'Istruzione,  
dell'Università e della Ricerca*



# Chapter 4: Time-Domain and Spectral Analysis of FMCW Radar Signals for Sea Wave Characterization

## 4.1 Introduction

In-phase (I) and quadrature (Q) signal processing is a fundamental technique in handling bandpass signals, particularly in radio transceivers and radar systems [56]. In-phase (I) and quadrature (Q) signal processing is a fundamental technique used in modern communication and radar systems to efficiently analyze and manipulate signals. By separating a signal into two components one in-phase with a reference and the other 90 degrees out of phase this method allows for precise modulation, demodulation, and interference reduction. I/Q signal processing plays a crucial role in applications such as wireless communications, radar imaging, and software-defined radio, offering improved signal clarity and enhanced data transmission capabilities [57].

FMCW radar systems, widely used for water flow monitoring, rely on both frequency-domain and time-domain analyses to characterize water dynamics. While frequency-domain analysis provides an overview of the spectral distribution of energy, time-domain analysis focuses on the evolution of the radar signal over time, offering detailed insights into wave motion and hydrodynamic behavior. This chapter integrates these two analytical approaches to achieve a comprehensive understanding of sea wave dynamics.

FMCW radars transmit chirp signals that interact with the sea surface, reflecting back to the receiver as complex data comprising I and Q components. These components represent the real and imaginary parts of the signal, encapsulating its amplitude and phase information. Time-domain analysis interprets these variations in the I and Q components to capture the interaction between the transmitted signal and the dynamic sea surface. This approach reveals temporal changes in wave patterns, amplitudes, and intensities, which are critical for accurate characterization of sea waves and their energy profiles.

In addition to time-domain analysis, the power spectrum derived through frequency-domain methods plays a role in understanding wave dynamics. The power spectrum reveals the distribution of signal energy across different frequencies, enabling the identification of dominant wave frequencies, energy bands, and overall wave energy. This spectral information complements time-

domain analysis by providing a broader perspective on the energy content and periodic behavior of sea waves.

This chapter begins by explaining the principles of I/Q signal processing and its role in radar systems. It then explores the significance of time-domain analysis in sea wave monitoring, emphasizing the insights gained from observing temporal variations in the I and Q components. The chapter also discusses the application of power spectral analysis to identify wave frequencies and energy distributions. By combining time-domain and frequency-domain perspectives, this research enhances the capabilities of FMCW radar systems for real-time monitoring and hydrodynamic studies.

## 4.2 Time-Domain Representation of FMCW Radar Signals

### 4.2.1 Overview of Time-Domain Signals

In Frequency Modulated Continuous Wave (FMCW) radar systems, the received signal is decomposed into two fundamental components: the In-Phase (I) and Quadrature (Q) signals. In Frequency Modulated Continuous Wave (FMCW) radar systems, the received signal is decomposed into two fundamental components: the In-Phase (I) and Quadrature (Q) signals. These time-domain components represent the real and imaginary parts of the analytic signal, encoding both amplitude and phase information together. The I component does not exclusively represent magnitude, nor does the Q component exclusively represent phase rather, they work collectively to describe the full signal structure. This decomposition is essential for analyzing Doppler effects and extracting detailed motion characteristics from radar reflections [58].

The representation of radar signals in the time domain is essential for several reasons. First, it allows for the direct observation of temporal variations in the radar return signal, capturing dynamic behaviors such as wave oscillations, energy fluctuations, and transient events. Second, time-domain signals serve as the foundation for higher-level analyses, including frequency-domain transformations and velocity estimations. By preserving the complete signal information in the I/Q representation, the radar system ensures that no detail is lost during subsequent signal processing steps [59].

### 4.2.2 Sampling and Processing

The radar system operates by continuously transmitting frequency-modulated chirps and receiving their reflections from the sea surface. The received analog signals are digitized to enable further processing and analysis. The conversion from analog to digital signals is a crucial step, as it determines the resolution and accuracy of the radar measurements. Each chirp is sampled at regular intervals, creating a discrete representation of the signal that can be stored, analyzed, and visualized in the time domain.



In this study, the radar generated data frames consisting of 21 chirps per frame. Each chirp had a duration of 1.5 milliseconds, and 64 samples were collected per chirp. This configuration was carefully chosen to balance the trade-off between resolution and hardware constraints. By using 64 samples per chirp, the radar achieved sufficient granularity to capture wave dynamics without overwhelming the system's computational and storage capacities.

The time-domain representation of these I/Q samples provides a detailed snapshot of the radar's interaction with the sea surface. Each frame contains a sequence of amplitude and phase variations corresponding to the reflections from dynamic wave patterns. These variations are directly linked to the physical characteristics of the sea waves, such as their velocity, and energy distribution.

### 4.3 Analysis of I/Q Components

The analysis of In-Phase (I) and Quadrature (Q) components in the time domain provides a detailed understanding of the dynamic behavior of sea waves as captured by the FMCW radar system. These components form the foundation of radar signal representation, encapsulating critical information about amplitude and phase variations that directly correlate with wave characteristics such as height, velocity, and energy .

#### 4.3.1 Representation of I/Q Signals

##### 1. Fundamentals of I/Q Signals:

The In-phase (I) and Quadrature (Q) components are the real and imaginary parts of the analytic radar signal, jointly encoding both amplitude and phase information. The I component primarily reflects amplitude variations, capturing changes in target reflectivity and motion dynamics. Meanwhile, the Q component encodes phase information, which is essential for velocity estimation using the Doppler effect. Neither component exclusively represents magnitude or phase; rather, they work together to describe the full signal structure, ensuring accurate radar signal processing and target characterization.

**2. Mathematical Representation:** The received signal  $S(t)$  can be expressed as:

$$S(t) = I(t) + jQ(t) \quad (4.1)$$

Where,

$I(t)$  is the in-phase component, given by:

$$I(t) = A(t)\cos(\phi(t)) \quad (4.2)$$

Q(t) is the quadrature component, given by:

$$Q(t) = A(t)\sin(\phi(t)) \quad (4.3)$$

- A(t) represents the signal's amplitude, which depends on how well the target reflects the radar waves. It provides information about the strength of the returned signal.
- $\phi(t)$  represents the signal's phase, which is related to the Doppler shift. It helps reveal the motion of the target, including its speed and direction.

### 4.3.2 Signal Dynamics Across Sea States

The behavior of the I/Q components varies significantly across different sea states, reflecting the dynamic nature of wave activity. The following observations were made for three representative sea states:

#### 1. High-Waves:

- Characteristics:
  - The I/Q signals displayed sharp and frequent amplitude variations, with dense oscillatory patterns.
  - These variations indicate high reflectivity and significant Doppler shifts caused by active wave motion.
- Implications:
  - High waves are typically driven by strong winds or tidal forces, resulting in powerful radar reflections.
  - The dense oscillations reflect the rapid and energetic motion of the wave surface.

#### 2. Moderate Waves:

- Characteristics:
  - The I and Q signals exhibited smoother oscillations with moderately spaced peaks and troughs.
  - Amplitudes were lower compared to high-energy waves, indicating reduced reflectivity and motion intensity.
- Implications:
  - Moderate waves represent calmer sea states, where wave energy is distributed more evenly.
  - These signals are indicative of slower and more stable wave movements.

### 4.3.4 Interpretation of I/Q Signal Dynamics

The dynamics observed in the I/Q signals provide crucial information for characterizing sea states:

- Amplitude: The magnitude of the I signal serves as a proxy for wave energy and height, enabling the classification of sea conditions into high-energy, moderate, and low-energy states.
- Oscillation Frequency: The frequency of oscillations in the I and Q components reflects the temporal evolution of wave motion, correlating with the wave period and speed.
- Phase Relationship: The interplay between I and Q components reveals Doppler shifts, which are critical for estimating wave velocity and direction.

By analyzing these dynamics, the radar system can extract detailed and real-time information about wave behavior, supporting applications such as renewable energy assessment and coastal safety monitoring.

### 4.3.5 Advantages of I/Q Signal Analysis

The time-domain analysis of I/Q signals offers several benefits:

1. Real-Time Insights: Time-domain visualization enables the immediate identification of wave patterns and energy fluctuations.
2. Granular Detail: The preservation of amplitude and phase information provides a complete representation of wave dynamics, supporting detailed characterization.
3. Broad Applicability: The insights derived from I/Q analysis are relevant for diverse applications, including disaster mitigation, marine navigation, and environmental studies.

## 4.5 Experimental Setup and Data Processing

The experimental setup for analyzing sea wave dynamics was carried out, using a 24 GHz FMCW radar system. This system was designed to capture and monitor wave behavior in real-time. These chirps formed the foundation of the data collection process, enabling the radar to detect and analyze the complex motion of sea waves.

A Raspberry Pi 3B+ was employed as the primary processing unit, interfaced with MATLAB to handle the raw radar data. This compact and efficient setup allowed the seamless integration of hardware and software for signal processing. The following steps outline the data acquisition and processing workflow:

This experimental setup and processing pipeline were designed to capture high-quality data while maintaining efficiency in real-time operations. The integration of the 24 GHz FMCW radar with

the Raspberry Pi and MATLAB ensured that both data acquisition and analysis could be performed effectively.

Understanding sea wave behavior is crucial for applications like coastal safety, environmental monitoring, and maritime navigation. In this study, we used a comprehensive approach to analyze different sea states by combining various data sources and analytical techniques. High-resolution camera images were used to visually capture the different sea conditions, providing a clear reference for the observed wave states. We also generated Range-Doppler maps using FMCW radar to represent the distance and velocity of waves. These maps help identify wave patterns and movement directions. Additionally, we analyzed time domain representations of FMCW radar signals to capture the real-time evolution of waves and understand their behavior under different conditions. This combined approach offers a thorough understanding of sea wave dynamics for effective coastal monitoring and analysis. Figure 4.1 illustrates the experimental environment for different Sea State.

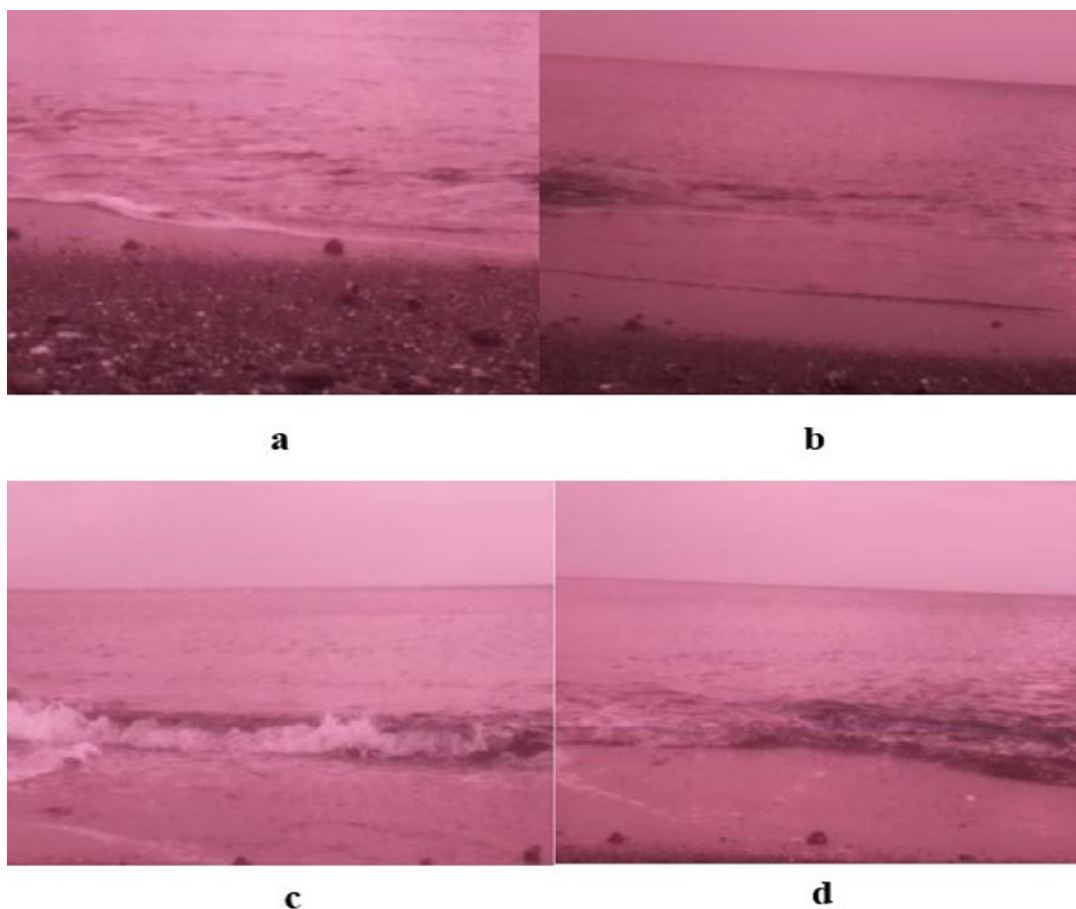


**Figure 4.1.** Experimental environment for different Sea State.

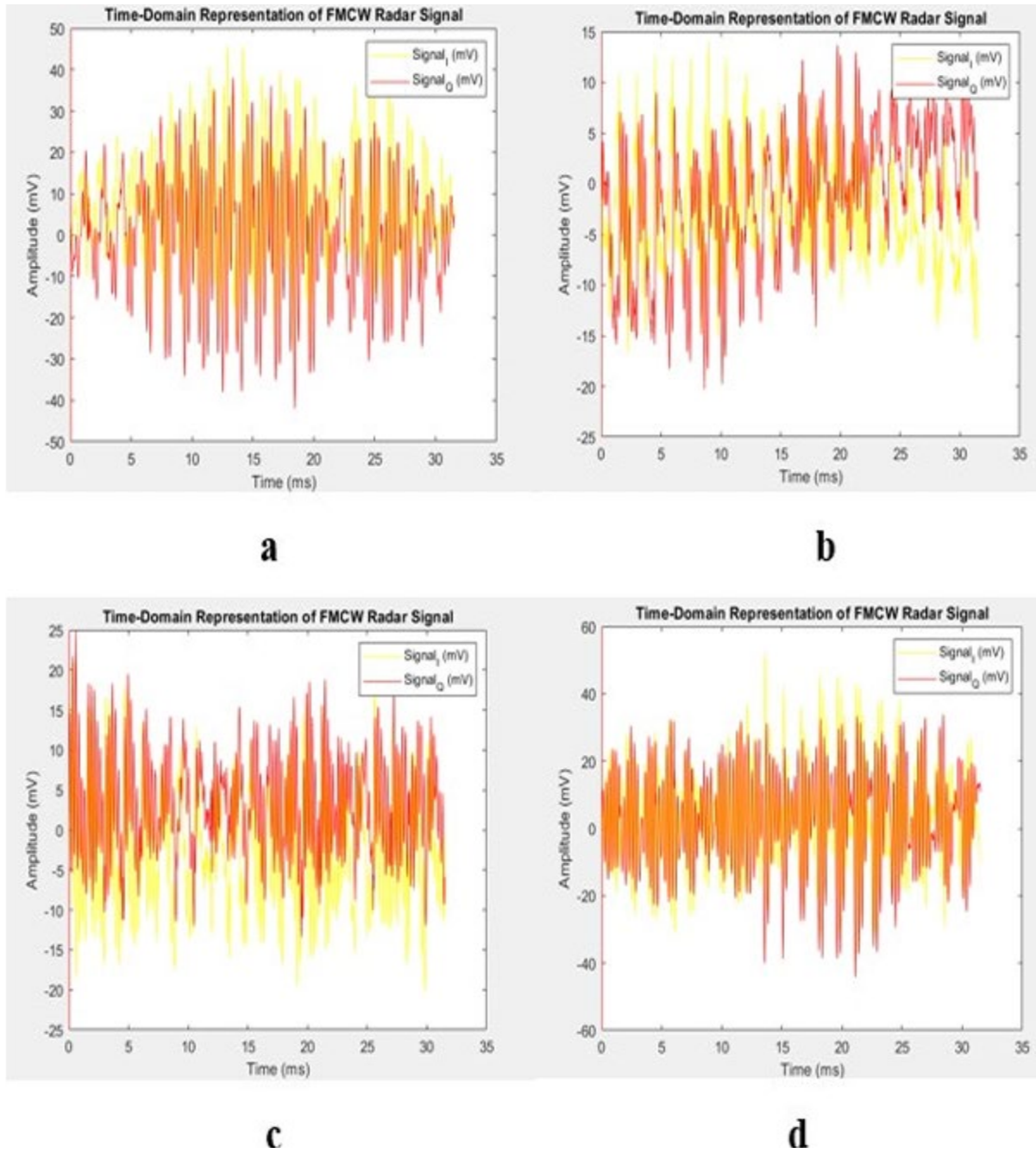


**Figure 4.2.** Time-Domain Representation of FMCW Radar Signal for Sea state.

Fig.4.2 illustrates the time-domain representation of the FMCW radar signal for Sea State. The Fig shows the amplitude (in mV) over time (in ms). Fig (a) significant amplitude variations and densely packed oscillations indicate active and high-energy waves, with consistent wave patterns likely influenced by steady wind or tidal forces. Figure (b) shows the time-domain representation for Sea State (b). The amplitude variations are noticeable but less pronounced compared to Sea State (a),

indicating moderate wave activity. The more spread-out oscillations suggest less frequent wave interactions, representing a calmer sea state with lower energy waves. Figure (c) presents the time-domain representation for Sea State (c). The amplitude variations are like those in Sea State (a), showing significant wave activity. The dense and frequent oscillations indicate active and high-energy wave dynamics, with regular wave patterns suggesting consistent environmental influences. Figure (d) depicts the time-domain representation for Sea State (d). The amplitude variations are moderate, indicating average wave activity. The balanced pattern of oscillations suggests moderate wave dynamics, providing a middle ground between the highly active conditions in Sea States (a) and (c) and the calmer conditions in Sea State (b).

The analysis of FMCW radar signal observations, as summarized in Table 4.1, indicates a strong correlation between wave height variations and changes in sea state conditions, demonstrating the radar's effectiveness in capturing sea surface dynamics.

<b>Figure</b>	<b>Amplitude Range (mV)</b>	<b>Oscillation Frequency (per 10 ms)</b>	<b>Sea State Condition</b>
<b>(a)</b>	-50 to 50	12-15	active waves
<b>(b)</b>	-20 to 15	8-10	Moderate, calmer sea state
<b>(c)</b>	-25 to 25	12-14	Regular waves
<b>(d)</b>	-40 to 40	10-12	Moderate, balanced wave state

**Table 4.1:** Characteristics of Sea State Conditions from FMCW Radar Signal Observations.



UNIONE EUROPEA  
Fondo Sociale Europeo



The Range-Doppler maps in Figure 4.3 (a), (b), (c), and (d) offer a comprehensive analysis of sea wave dynamics by depicting the distance and velocity of waves as detected by the radar system. In figure (a), significant wave activity is observed within the 1 to 5 meters range, with velocities between -1 to -3 km/h, indicating strong wave reflections. Figure (b) shows a target signature around 5 meters range with a velocity close to 1.5 km/h, suggesting less intense wave activity. Figure (c) displays wave dynamics like figure (a), with noticeable activity within the 5 to 10 meters range and velocities from 0 to -2.5 km/h, reflecting significant wave movements. Figure (d) presents moderate wave activity around 5 meters range, with velocities varying from -2 to 1 km/h. Overall, these maps demonstrate that the most substantial wave reflections occur within the 5 to 10 meters range, with velocities predominantly near 0 km/h. This analysis provides crucial insights into the varying sea states and their impact on coastal environments, underscoring the effectiveness of the radar system in monitoring and analyzing wave dynamics.



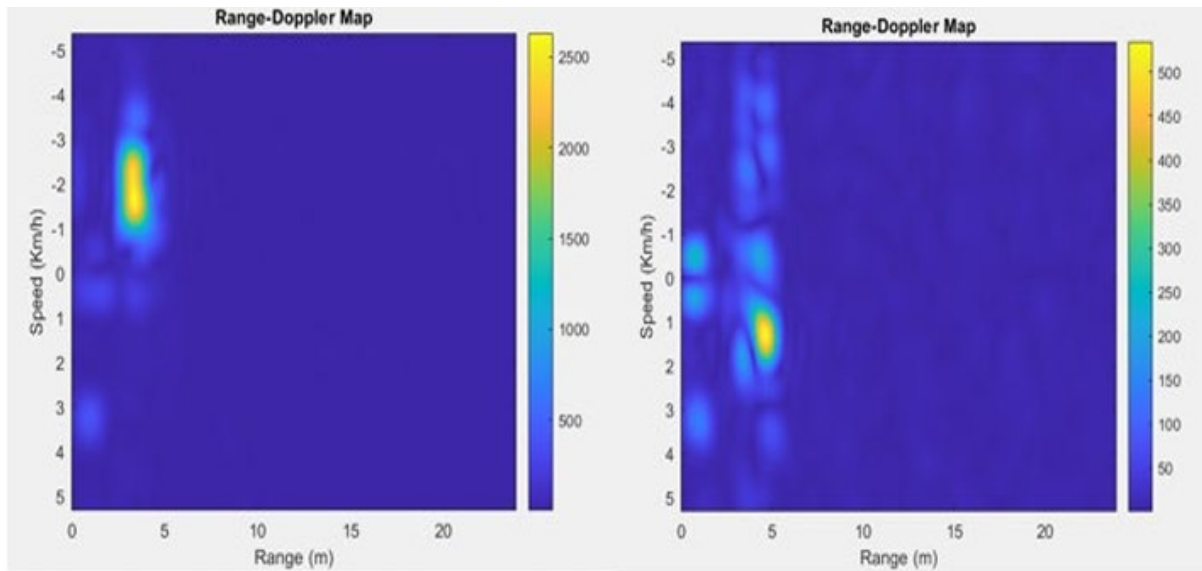
UNIONE EUROPEA  
Fondo Sociale Europeo



*Ministero dell'Istruzione,  
dell'Università e della Ricerca*

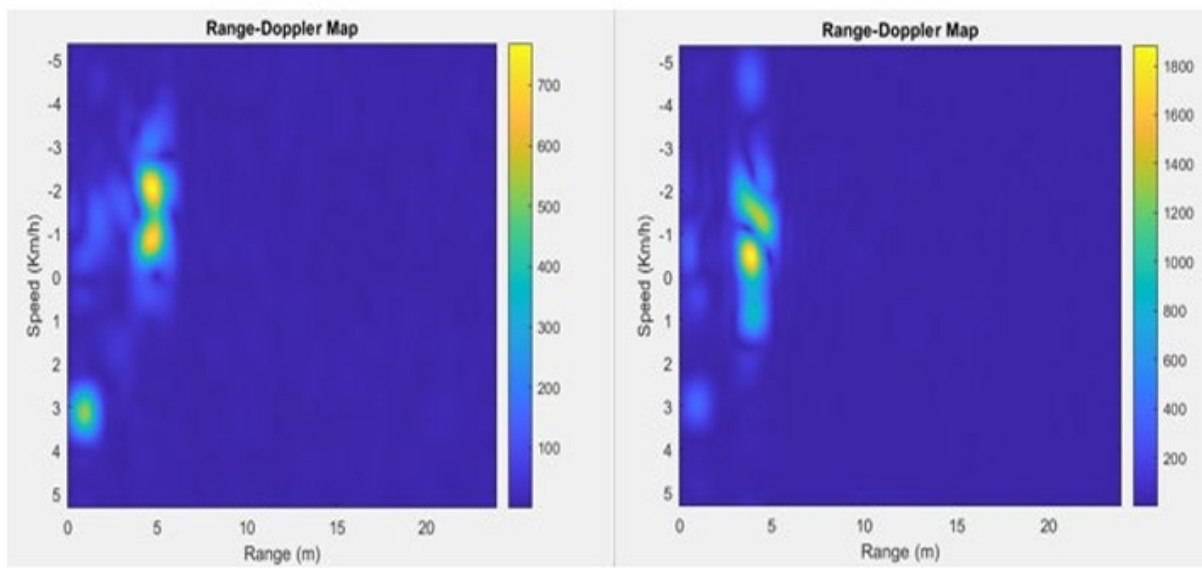


PON  
RICERCA  
E INNOVAZIONE  
2014 - 2020



**a**

**b**



**c**

**d**

Figure 4.3. Range-Doppler map.



UNIONE EUROPEA  
Fondo Sociale Europeo



## 4.6 Analysis of Wave Dynamics Using FMCW Radar and Power Spectrum Techniques

The characterization and analysis of wave dynamics are critical for a wide range of applications, including coastal safety, environmental monitoring, and marine navigation. Understanding how energy is distributed across various sea states and frequencies provides information into the behavior of coastal environments.

The use of radar technologies, particularly FMCW radar, has proven to be a reliable and efficient method for monitoring wave behavior in nearshore environments. FMCW radar systems offer real-time, high-resolution measurements, allowing us to analyze parameters such as frequency, direction, and energy distribution. Unlike traditional methods, radar systems provide a non-contact solution, reducing operational risks while maintaining accuracy.

A key analytical tool in these studies is the power spectrum, which represents the energy distribution of waves across various frequencies. By examining the normalized power spectrum, we can identify dominant wave patterns and assess the energy content of different sea states. This is particularly valuable for distinguishing between calm and turbulent conditions, as well as for quantifying wave energy for renewable energy projects.

This section explores the principles and methodologies used to analyze wave dynamics using FMCW radar technology. It focuses on the processing and interpretation of radar data, particularly the power spectrum, to understand wave behavior under varying environmental conditions.

### 4.6.1 Methodology for Power Spectrum Analysis

The analysis of wave and flow dynamics in this study utilized the power spectrum as a central tool for understanding the distribution of energy across different frequencies. The raw I/Q signals (In-phase and Quadrature components) collected by the FMCW radar system provided detailed information about the amplitude and phase of the returning echoes from the water's surface. These signals were processed using the Fast Fourier Transform (FFT), which converts time-domain data into the frequency domain, allowing for the extraction of the power spectrum. This transformation is critical as it reveals the energy content at various frequencies, offering information into the characteristics of the flow or wave dynamics.

The power spectrum was normalized to ensure that energy levels were accurately represented, regardless of variations in environmental or experimental conditions. Through this analysis, the low-frequency components of the spectrum were identified as indicative of steady flow or slow-moving water, commonly associated with calm sea conditions or large, low-energy waves in coastal regions. Conversely, the high-frequency components highlighted areas of turbulence, rapid fluctuations, or localized disturbances, such as debris movement or breaking waves, which are

characteristic of more dynamic and high-energy conditions. By examining the distribution of energy within the power spectrum, the study was able to distinguish between calm and turbulent flow behaviors and provide detailed insights into the interaction of water flow with its surroundings. This methodology proved to be particularly effective in characterizing dynamic flow patterns, offering a robust framework for analyzing environmental and engineering phenomena. The ability to quantify and interpret these energy distributions has practical applications in fields such as wave monitoring where understanding water movement is critical for developing sustainable and adaptive strategies. Overall, the use of radar-based power spectrum analysis demonstrates its value in advancing our understanding of wave and flow dynamics in complex and diverse environments.

#### 4.6.2 Power Spectrum Analysis

Power spectrum analysis is a fundamental technique used in this experiment to understand the energy distribution of water flow dynamics across different frequencies. By applying the Fast Fourier Transform to the radar's time-domain signals, the power spectrum was derived, revealing how flow energy varies with frequency. This analysis allowed us to identify key patterns in sea behavior, including the detection of flow. Low-frequency components in the power spectrum corresponded to calm flow conditions, while high-frequency components indicated strong flow.

In the context of analyzing sea waves and wave energy, it is crucial to accurately quantify the power distribution across different frequencies, as this provides insights into the dynamics of wave movement. The following equation allows us to calculate the power spectrum, considering the signal's sampling frequency, which is essential for understanding the energy characteristics of the waves [60]:

$$S[m] = \frac{|X[m]|^2}{f_s} \quad (4.5)$$

Where,  $S[m]$  is the power spectrum at the  $m$ -th frequency bin,  $X[m]$  is the FFT output at the  $m$ -th frequency bin,  $|X[m]|^2$  is the magnitude squared of the FFT output, representing the power at that frequency, and  $f_s$  is the sampling frequency of the signal. This equation normalizes the power spectrum by the sampling frequency, which is particularly insightful when analyzing signals at different sampling rates, ensuring an accurate representation of wave.

This preliminary acquisition campaign was designed to test the effectiveness of the radar setup in capturing wave dynamics, ensuring that the radar could accurately monitor and analyze sea conditions in real time. The data collected during this campaign provided information about the behavior of sea waves under different conditions, offering insights into both high-energy and moderate sea states. The results demonstrated the radar's capability to detect and distinguish key wave parameters, such as amplitude variations, wave frequency, and directional movement, even

in complex marine environments. The collected data formed the basis for generating detailed power spectra and Range-Doppler (R-D) maps, both of which provided a clear representation of wave energy distribution and motion. These results validate the radar system's ability to reliably capture dynamic wave behaviors and set the foundation for further in-depth analysis of coastal wave dynamics.



**a**

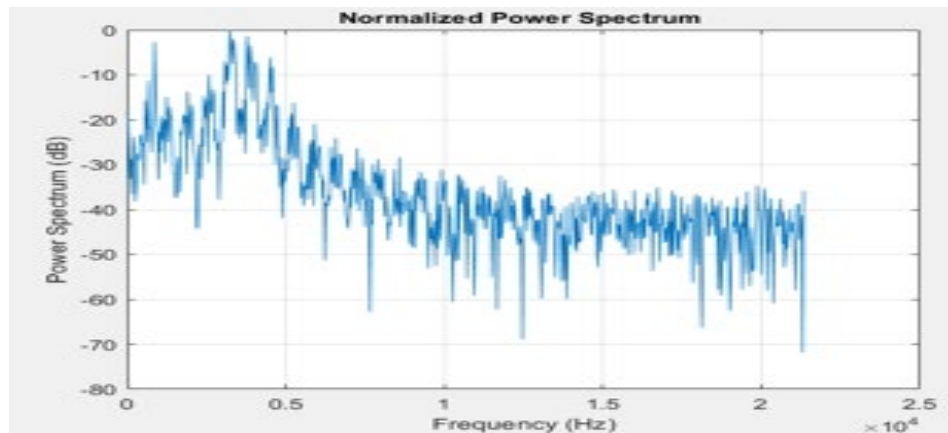


**b**

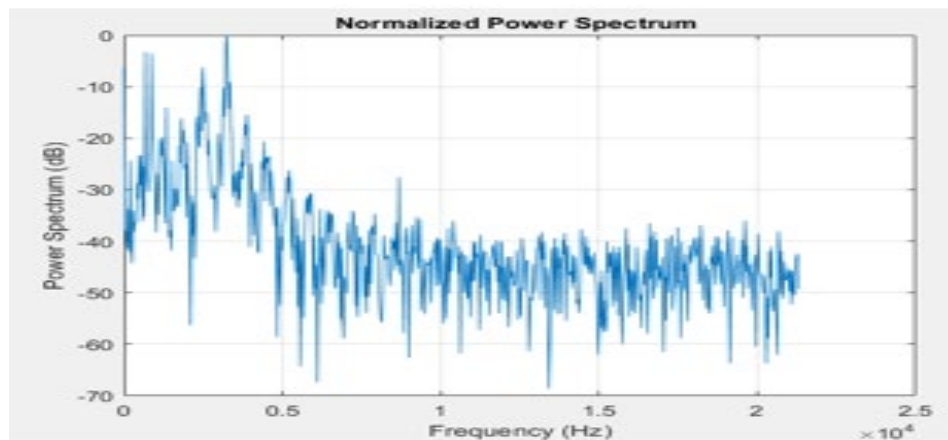
**Figure 4.4.** Camera Images Depicting Two Different Sea States: (a) Active Waves with High and Strong Water Flow, and (b) Calmer Waves with Gentle Water Flow.

Figure 4.4 presents camera images capturing two distinct types of sea waves, labeled as (a) and (b). In fig (a), the waves appear more active, with noticeable whitecaps and churning at the shore, indicating a higher state. This suggests a strong water flow towards the coast, likely driven by wind

or tidal forces, resulting in more pronounced wave crests and faster water movement. In contrast, Fig (b) shows a much calmer sea state, with smoother water surfaces and minimal wave activity. The water flow in this scenario appears to be gentle, with less energy and slower movement, as indicated by the lack of visible turbulence and the flatter wave profiles. These two images illustrate the varying conditions of water flow in coastal environments, where wave activity can shift from dynamic and energetic in Fig (a) to serene and steady in Fig (b), depending on environmental factors such as wind speed, direction, and tidal forces.



**a**



**b**

**Figure 4.5.** Normalized Power Spectrum Analysis of Two Sea States: (a) High Sea State with Larger, Lower-Frequency Waves and (b) Calmer Sea State with Lower Overall Power.



UNIONE EUROPEA  
Fondo Sociale Europeo



In Figure 4.5 (a), the power spectrum reveals a higher concentration of energy in the lower frequency range, particularly around  $0.2 \times 10^4$  Hz, where the power level reaches approximately -10 dB. This peak indicates the presence of high-energy, lower-frequency waves, which typically correspond to larger, more powerful waves. As the frequency increases, the power gradually decreases, falling to around -30 dB at  $0.5 \times 10^4$  Hz and further diminishing to approximately -70 dB as the frequency approaches  $2 \times 10^4$  Hz. The sharp decline in power with increasing frequency suggests that the sea state in Fig 4.5(a) is dominated by slower, larger waves, which carry more energy and are characteristic of a more turbulent or active sea state. Figure 4.5(b), while similar in shape to Fig 4.5(a), shows a slightly lower overall power level, particularly in the lower frequencies. The peak power around  $0.2 \times 10^4$  Hz reaches just below -10 dB, indicating that the waves in this scenario are slightly less energetic than those in Fig 4.5(a). The power spectrum also shows a more gradual decline, with power levels around -40 dB at  $0.5 \times 10^4$  Hz and approaching -70 dB towards  $2 \times 10^4$  Hz. This distribution suggests that the sea state in Fig 4.5(b) is somewhat calmer, with less powerful waves, as reflected by the slightly lower power levels across the spectrum.



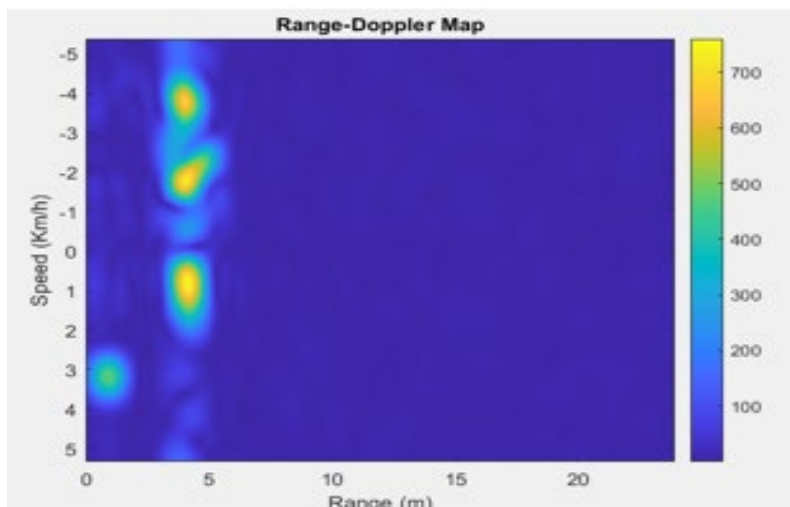
UNIONE EUROPEA  
Fondo Sociale Europeo



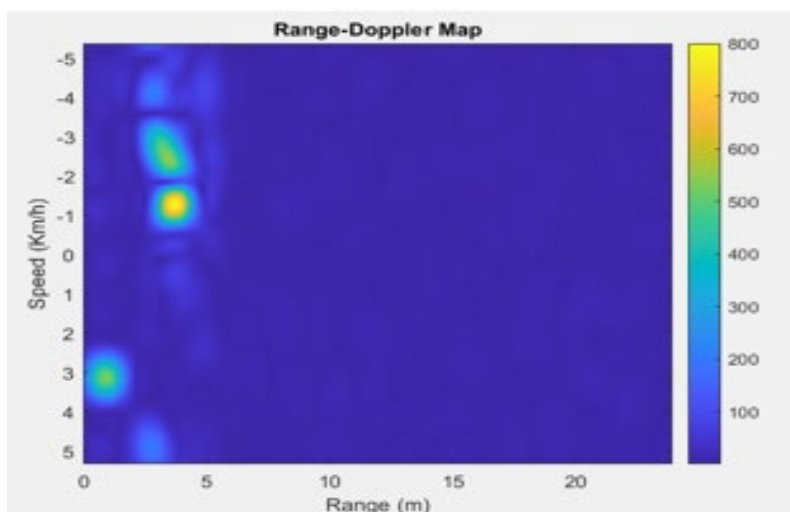
*Ministero dell'Istruzione,  
dell'Università e della Ricerca*



PON  
RICERCA  
E INNOVAZIONE  
2014 - 2020



**a**



**b**

**Figure 4.6.** R-D Maps of Two Sea States: (a) High Waves with Strong Water Flow, and (b) Moderate Energy Waves with Less Intense Flow.

In Figure 4.6 (a), the Range-Doppler map reveals several significant reflections occurring between 0 and 10 meters in range, with speeds concentrated around -3 km/h to -1 km/h. The highest intensity, indicated by the yellow regions on the color scale, occurs at approximately 5 meters in range and around -2 km/h in speed. This pattern suggests that the waves are relatively close to the radar and moving towards it at moderate speeds, reflecting a high-energy water flow in this region. The concentration of energy at these specific ranges and velocities indicates that the sea state is active, with substantial wave motion contributing to the overall dynamics. In Fig 4.6 (b), the

Range-Doppler map also shows wave activity primarily within the 0 to 10 meters range, but with a slight shift in the speed distribution. The most prominent reflection appears at around 5 meters in range and close to -2 km/h, like Fig 4.6 (a), but with slightly less intensity. Additionally, there is another notable reflection at a range of around 3 meters and a speed of approximately -3 km/h. The overall energy distribution in this map is slightly less concentrated compared to Fig 4.6 (a), suggesting a calmer water flow with less energetic wave activity.

## 4.7 Conclusion

The analysis of I/Q signal processing and power spectrum has proven to be highly effective for wave monitoring and characterization. I/Q signal processing enables the precise tracking of wave dynamics by capturing amplitude and phase information, which reflects the real-time behavior of waves. This method allows for detailed observation of variations in wave motion, including changes in height, direction, and energy.

The power spectrum complements I/Q analysis by offering a frequency-domain perspective of wave distribution. By identifying dominant frequencies and their associated energy levels, the power spectrum reveals key patterns in wave behavior. Low-frequency components typically indicate calm wave motion, while higher frequencies highlight strong conditions.

Together, these techniques create a comprehensive framework for wave monitoring. The combination of I/Q signal processing and power spectrum analysis enables both time-domain insights and broader frequency-domain understanding, improving the accuracy and reliability of wave monitoring systems.

# Chapter 5



UNIONE EUROPEA  
Fondo Sociale Europeo



*Ministero dell'Istruzione,  
dell'Università e della Ricerca*



PON  
RICERCA  
E INNOVAZIONE  
2014 - 2020

# Chapter 5: Analysis of Water Flow

## 5.1 Introduction

Tracking sea waves involves measuring their height, frequency, and direction over time, offering information's into sea movement and weather patterns. Similarly, monitoring river flow involves observing water velocity, depth, and turbulence, providing information about sediment transport, water quality, and flow behavior. Studying both systems helps us understand the physical processes driving water movement in different environments.

By combining the study of sea waves and river flows, this chapter aims to highlight the importance of tracking water flow in both environments. Through the experiments described, we seek to explore the unique characteristics of each system and how they complement each other in the broader context of water flow tracking.

## 5.2 Experiments

This section provides a general overview of the methods and tools used to track water flow, including sensors, radar systems, and simulation tools. It is divided into subsections describing the methodologies for each experiment:

### 5.2.1 Sea Waves Experiment

During my PhD research, I conducted a measurement experiment along the coastline of Genoa, Italy. The experimental setup involved deploying an FMCW radar system on the beach, approximately 1.5 meters from the water's edge, directly facing the sea. This positioning was chosen to maximize the radar's ability to capture signals from the waves. The radar system, previously described, was utilized to collect detailed data on sea wave dynamics, including parameters such as wave velocity, frequency, and direction. The acquired data were subsequently processed and analyzed using MATLAB software to extract and interpret key wave characteristics.

We set up the measurement environment using a radar front-end module and a real time data acquisition module in order to test the effectiveness of the proposed sea wave schema based on Doppler spectrum.

In Figure 5.1, illustrates the environment in which the experiment took place.





**Figure 5.1.** The environment of experiment.

Fig. 5.2 shows the Doppler spectrum and Range-Doppler map results from an experiment on sea waves.

The range-Doppler (R-D) map of the sea is a powerful tool aiding in the understanding and management of marine environments using radar sensors. The R-D map in Fig. 5.2 clearly indicates the presence of water flow, as evidenced by the high-intensity reflections observed at specific ranges and velocities. The accompanying camera image visually confirms the water flow conditions, validating the radar measurements.

From the R-D map, we can observe wave dynamics with significant detail. Specifically, the flow velocity is measured between -2 km/h and -4 km/h, with the negative sign indicating movement towards the radar system. The high-intensity reflection patterns are concentrated over a 4-meter range, suggesting localized but active wave motion.

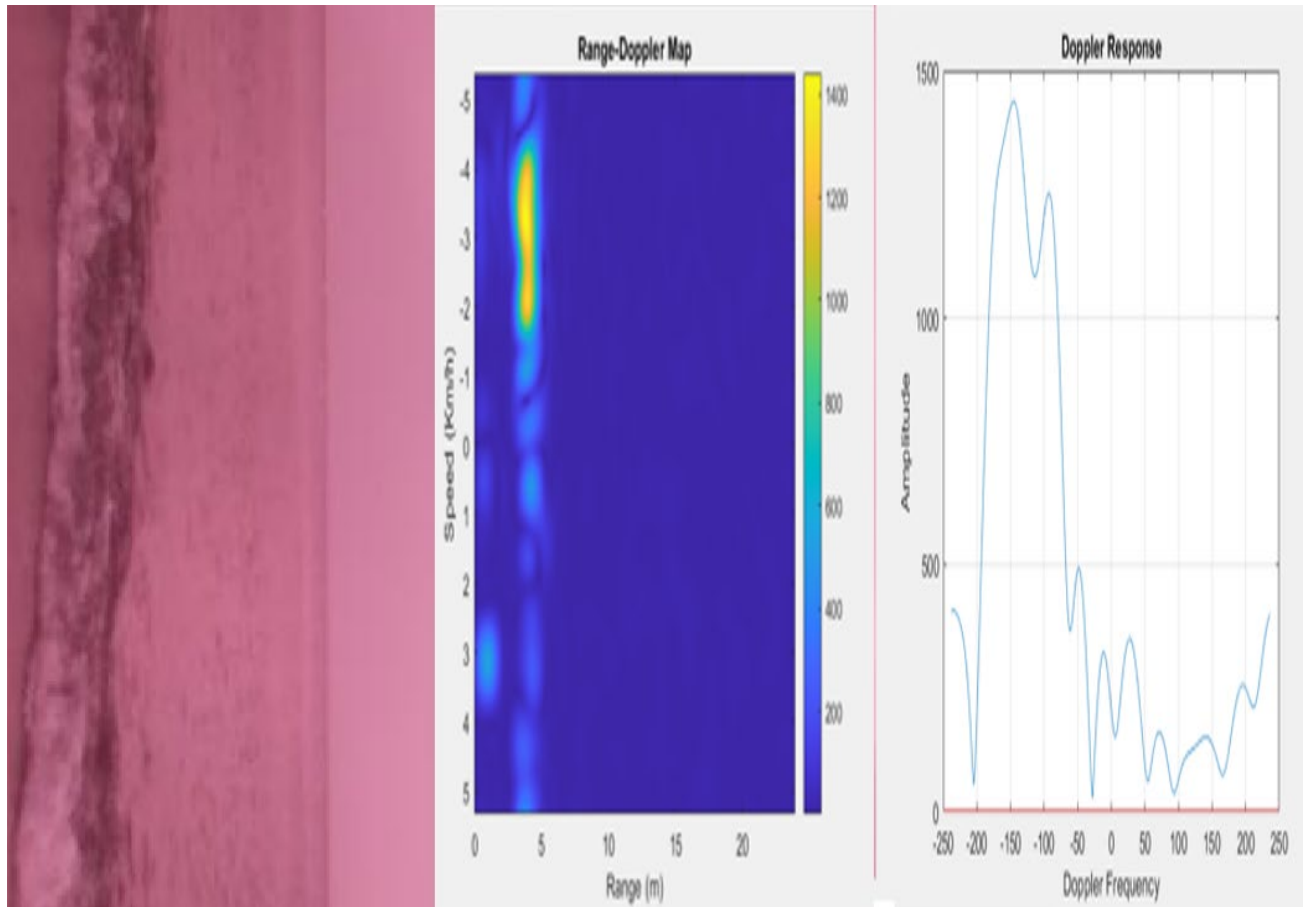


**Figure 5.2.** Camera Image, R-D map and Doppler spectrum at 4 m range for sea wave.

Further analysis of the Doppler spectrum provides additional valuable data. The spectrum exhibits multiple peaks at varying Doppler frequencies, indicating the presence of complex wave patterns and oscillations. For example, the dominant peaks in the Doppler spectrum range between -200 Hz and +150 Hz, which correspond to different wave components and their respective energy levels.

Range-Doppler Maps offer a powerful means of tracking sea waves, especially when they approach rapidly within a short timeframe. By analyzing the changes in range and velocity of

detected targets over time, these maps provide real-time insights into the behavior of approaching waves.

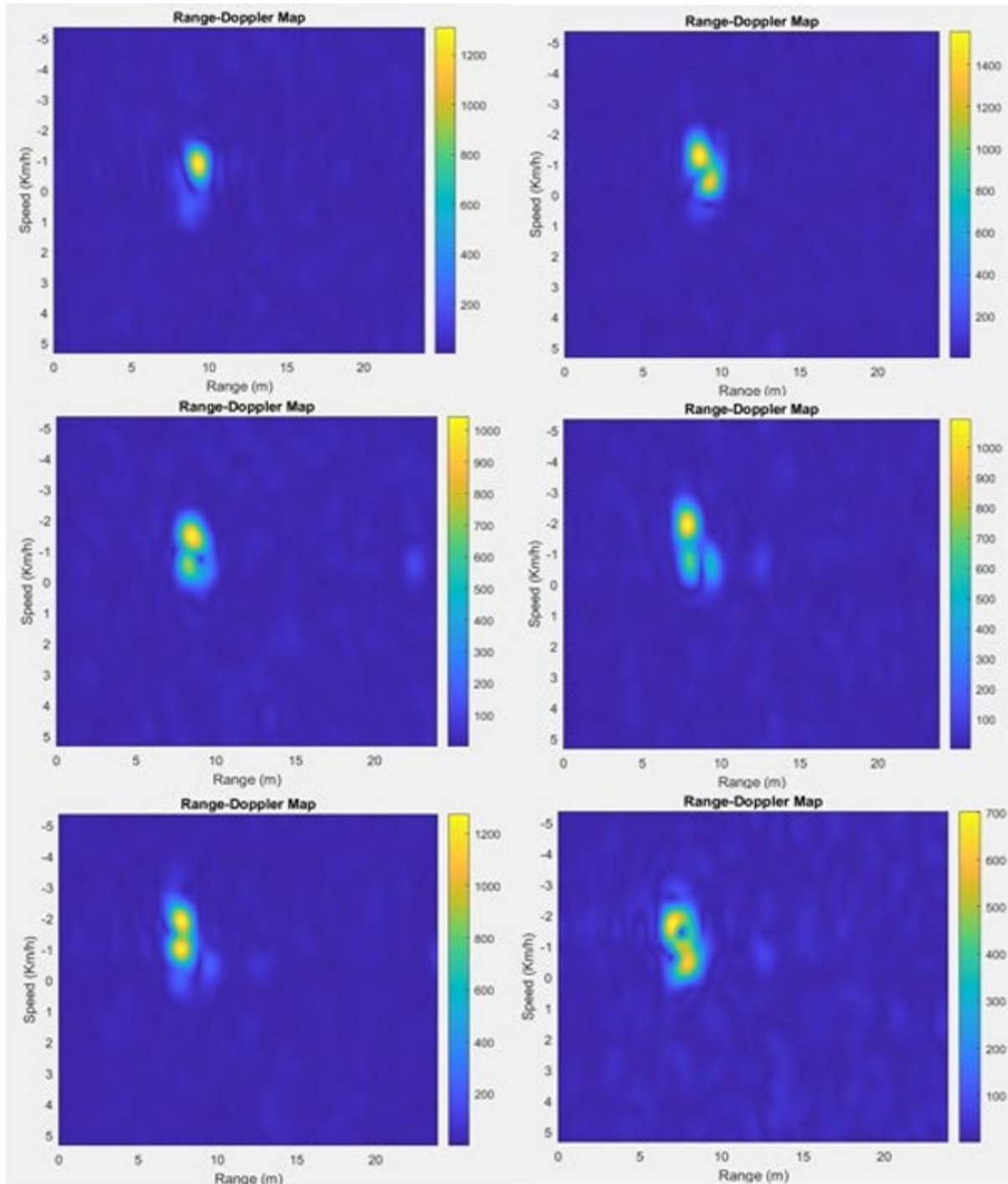


Figure 5.3. Tracking Sea wave.

When a sea wave approaches rapidly, its proximity to the radar system causes a noticeable shift in the reflected signal's range and velocity. This shift is captured and visualized on the Range-Doppler Map (see Fig. 5.3), where the wave's position and speed are represented as distinct features. In the map, the wave's approach is evident as a concentrated area of high signal intensity, indicating the wave's proximity to the radar source. Simultaneously, the wave's velocity is tracked through the Doppler frequency shift, represented horizontally on the map. A significant change in velocity, indicated by a distinct shift in the Doppler frequency spectrum, signals the wave's approach or departure.

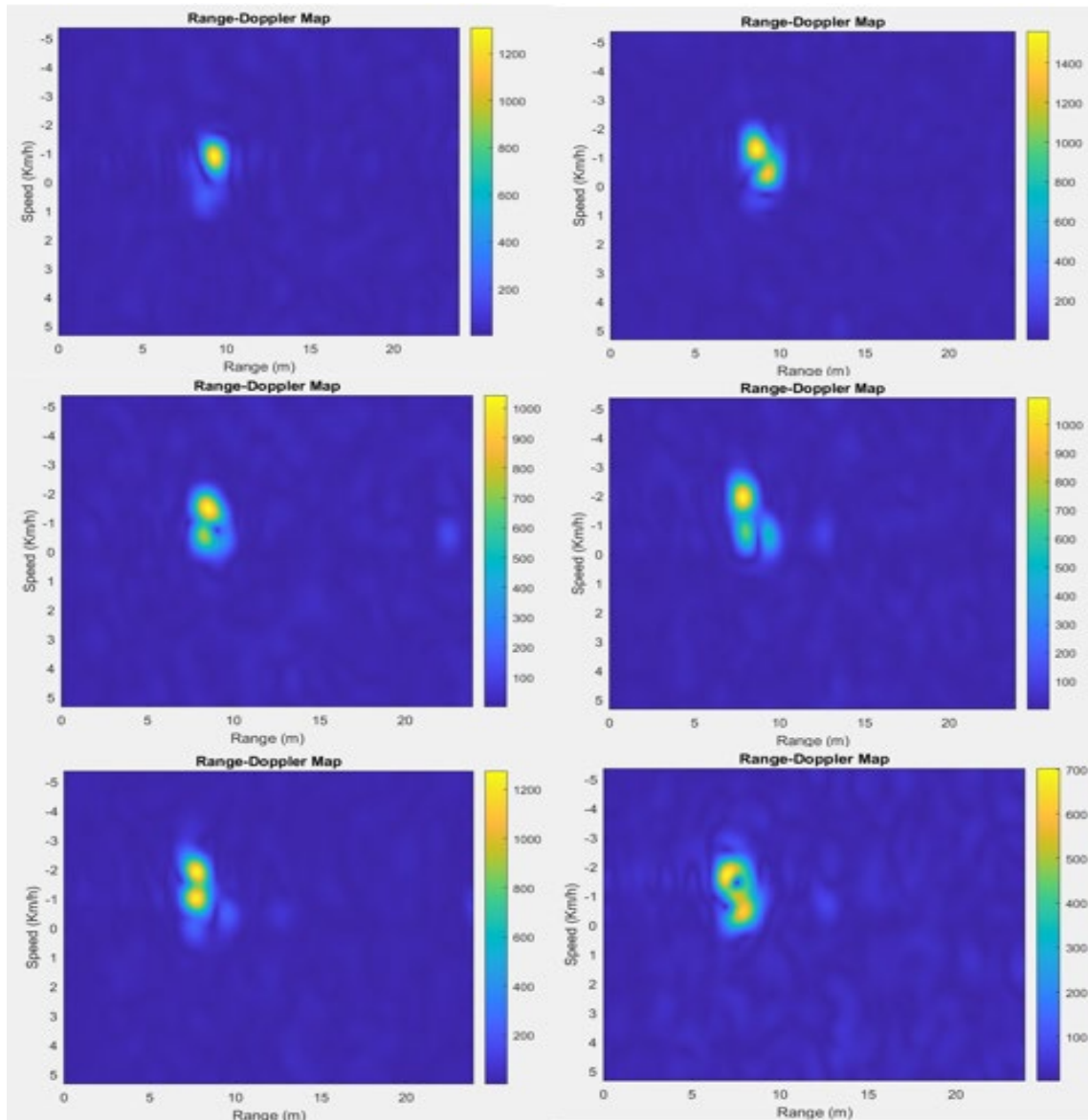
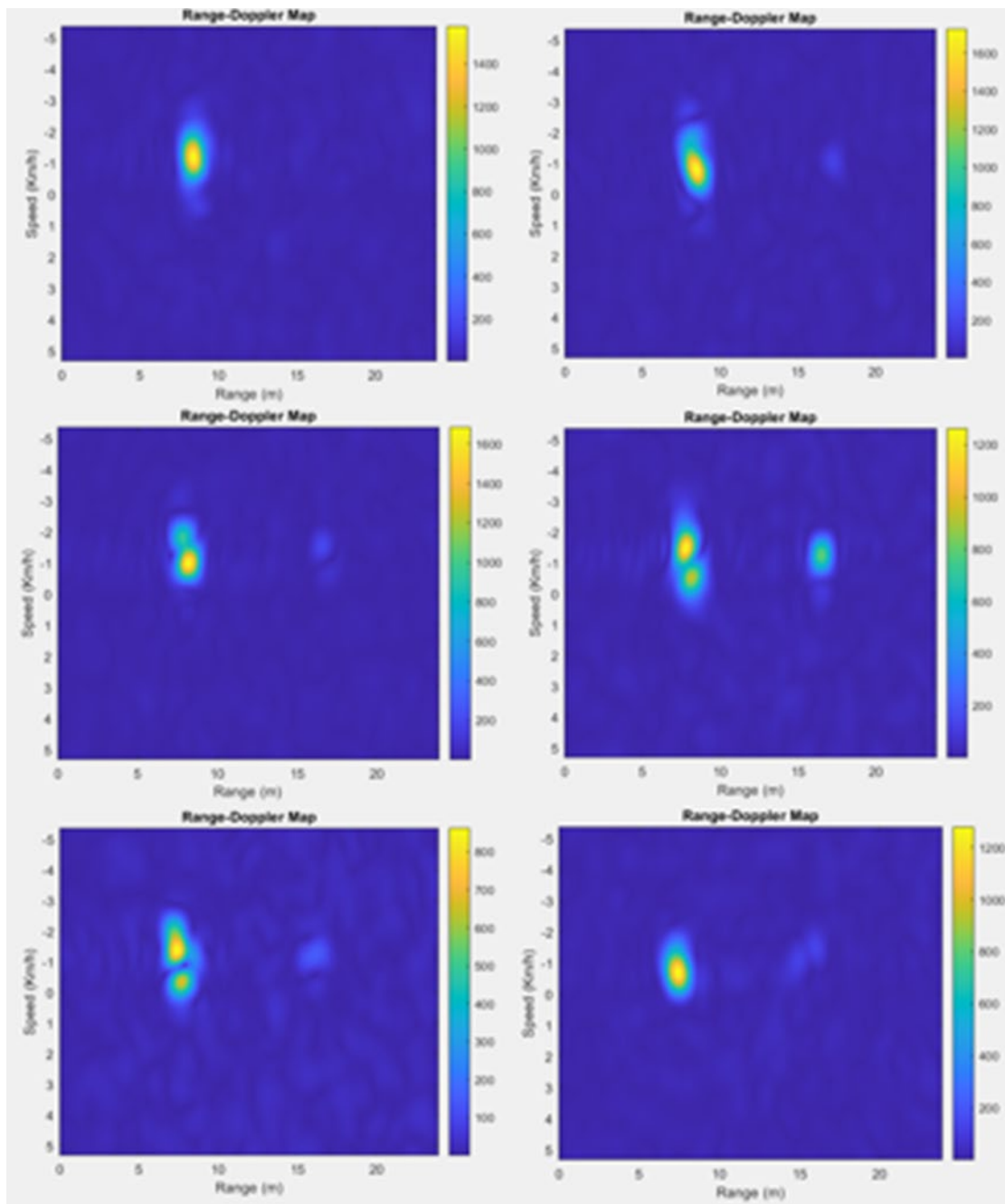


Figure 5.4. Tracking calm Sea wave.

In the initial experiment using only the radar, Fig. 5.4 captures the velocity changes observed in waves as they approach the beach. The figure highlights significant shifts in velocity as the waves move closer to the shore, with these variations being particularly noticeable over different distances during a 1 second data collection period. These fluctuations offer valuable insights into the waves' dynamic behavior as they travel toward the shoreline. Fig.5.4 also presents a Range-Doppler Map generated over a 1 second duration, with data captured at a rate of 6 frames per second. This figure visually depicts the continuous movement of the waves towards the radar, providing a clear representation of their spatial dynamics and the progression of their approach. As a sea wave approaches the radar, its movement causes distinct changes in the reflected signal's range and velocity. These changes are visualized on the Range-Doppler Map, which highlights the wave's position and speed as clear features. The approaching wave is represented by areas of concentrated signal intensity on the map, indicating its proximity to the radar system. Simultaneously, shifts in the Doppler frequency reveal the wave's velocity as it moves closer or recedes from the radar, providing a comprehensive overview of its behavior. The first wave type, as seen in the initial Range-Doppler maps, begins at a range of 10 meters, with a velocity of -1.5 km/h, indicating a smooth, steady approach toward the radar. As the wave moves closer to the shore, its range decreases to 6 meters, and its speed increases slightly to -2.5 km/h, reflecting moderate motion. The radar returns remain concentrated and strong throughout, indicating a focused and coherent wavefront. As the wave approaches the beach and nears the end of the radar's field of view, its velocity slows to around 0 km/h, and the signal begins to weaken, suggesting a dissipation of the wave's energy as it reaches shallower waters.

In contrast, the second wave type Fig. 5.5, shown in the second set of Range-Doppler maps, starts at a range of 10 meters with its velocity fluctuating between - 3 km/h and -1.5 km/h. These shifts in velocity suggest that the wave is breaking apart, likely due to local wind interference or interactions with other waves. By the time the wave reaches 6 meters, its structure becomes even more fragmented, with velocity components ranging from -2,5 km/h to -0.5 km/h indicating a chaotic, turbulent state. The wave's movement and irregular velocity suggest it may be a Wind-Driven Wave or Breaking Wave, which tends to experience fragmentation as it nears the shore due to environmental factors such as wind . These two wave types offer valuable insights into sea-state dynamics: the first wave reflects stable and calm conditions, while the second demonstrates the turbulence and fragmentation caused by wind and other environmental factors as the waves approach the shore. Range-Doppler Maps play a crucial role in maritime safety, enabling vessels to anticipate incoming waves and adjust their course or speed to minimize risks. By facilitating the effective tracking and monitoring of approaching waves in real-time, these maps enhance safety and situational awareness in maritime environments.



**Figure 5.5.** Tracking turbulence Sea wave.

In our study, we focus on interpreting four distinct types of sea waves: rolling waves, which gently rise and fall; slipping waves, characterized by their smooth peaks sliding downwind; whitecaps, notable for their frothy, breaking tips; and choppy waves, which are rough and irregular. By analyzing the range Doppler map, we can understand the conditions of the sea based on the

observed wave patterns. This mapping aids in visualizing how these different wave types move and interact with the wind, providing us with a clearer picture of the sea's dynamic nature.

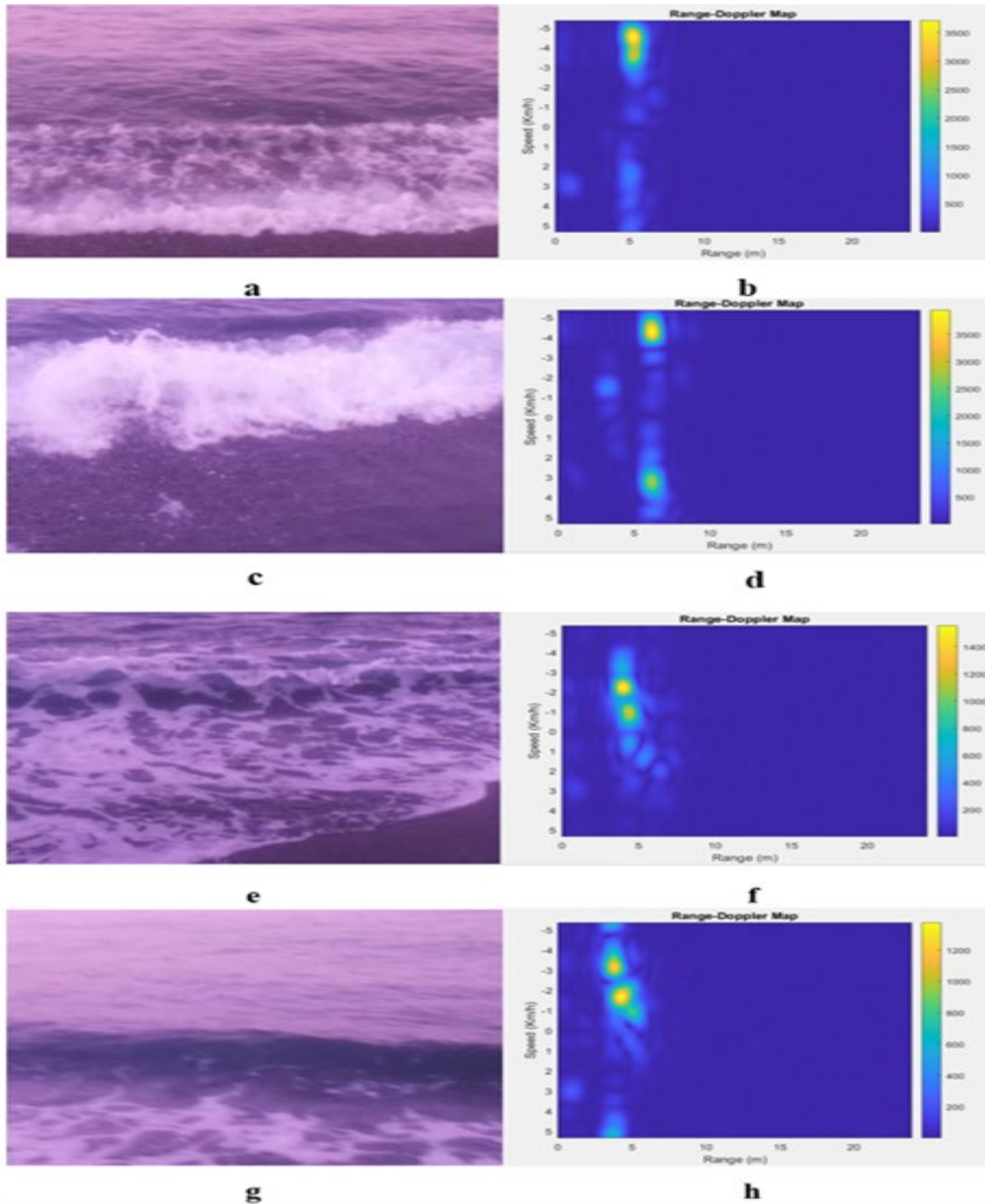
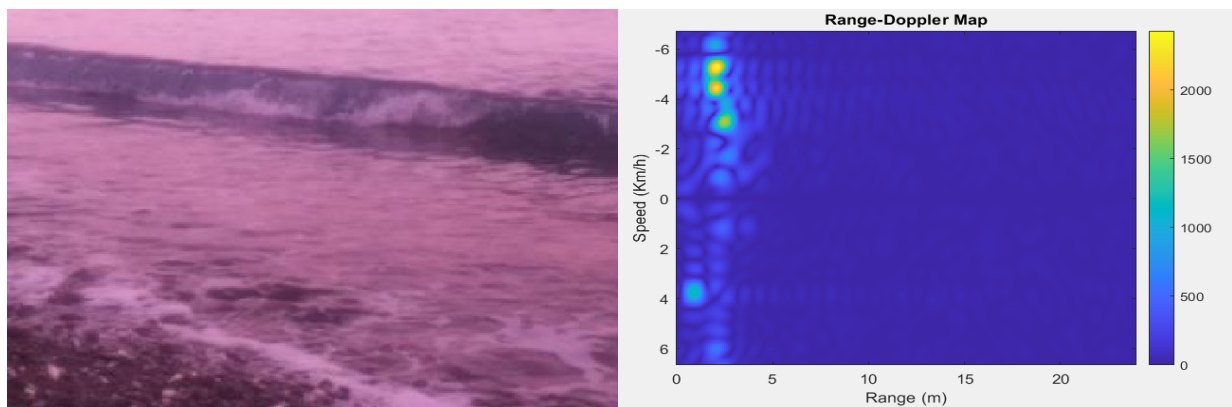
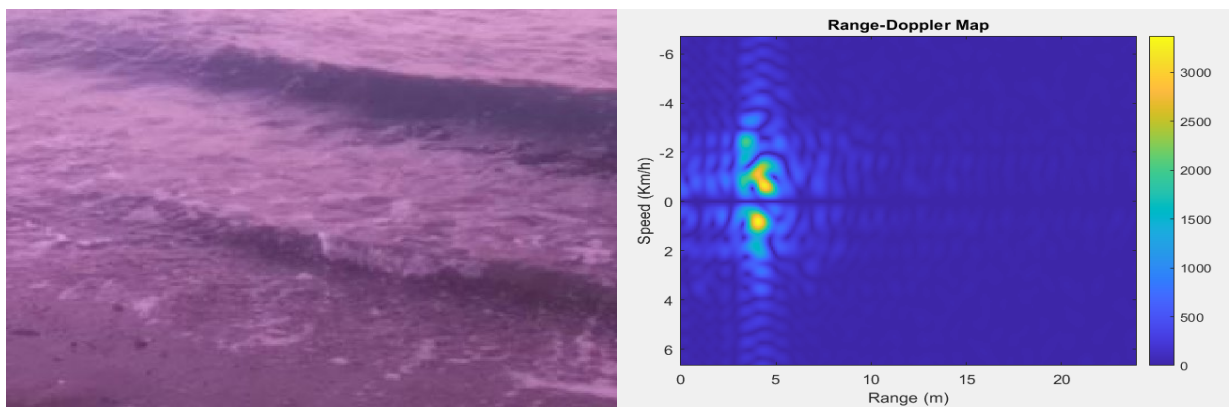


Figure 5.6. Camera image and Range Doppler map for sea states.

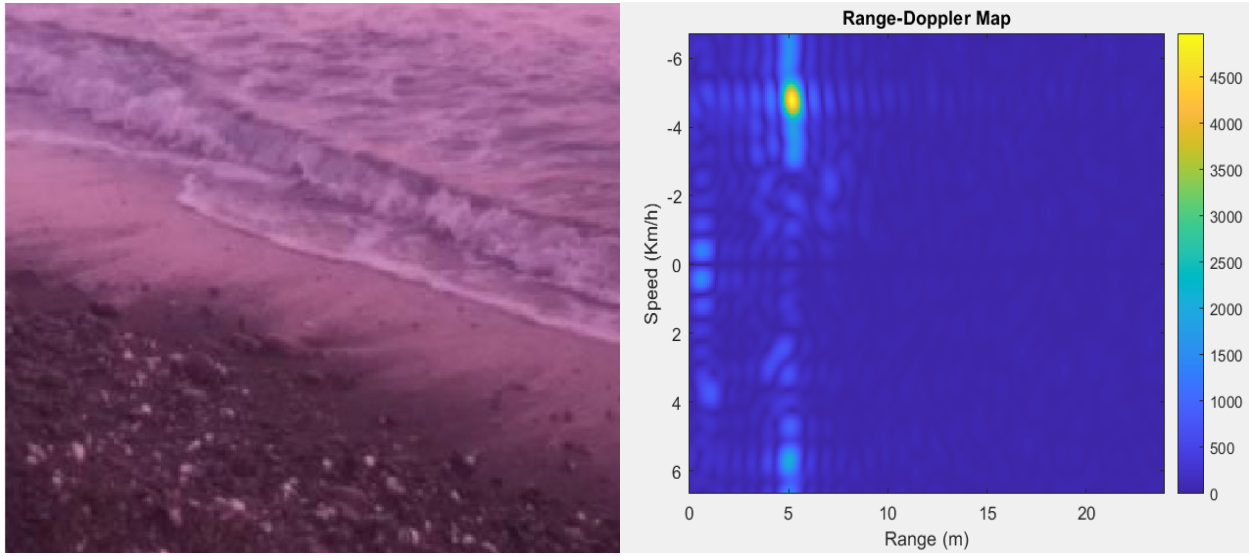
In turbulent sea conditions characterized by rolling waves (Fig. 5.6a), the dominance of large and fast-moving waves signifies a highly energetic environment. The extensive scattering depicted in the Range-Doppler Map corroborates this, confirming the rapid movement of waves. Conversely, slipping waves (Fig. 5.6c) depict a sea state where noticeable waves exhibit significant speed and energy, though not as intense as in turbulent conditions. The moderate scattering observed in the corresponding map indicates a considerable yet less intense wave movement. Transitioning to a calm sea state represented by whitecaps (Fig. 5.6e), minimal wave activity suggests a serene environment with low energy. The low scattering in the Range Doppler Map aligns with this observation, indicating slow wave movement due to minimal disturbance. Finally, in a moderate sea state characterized by choppy waves (Fig. 5.6g), the increasing pace of waves signals a rise in both energy and wave height. The heightened scattering in the corresponding map highlights the accelerated movement of waves compared to the calm state. These insights provided by Range-Doppler Maps enable a deeper understanding of sea dynamics, facilitating improved monitoring and prediction of oceanic conditions. Such knowledge is invaluable for diverse applications, including maritime navigation, weather forecasting, and environmental management.



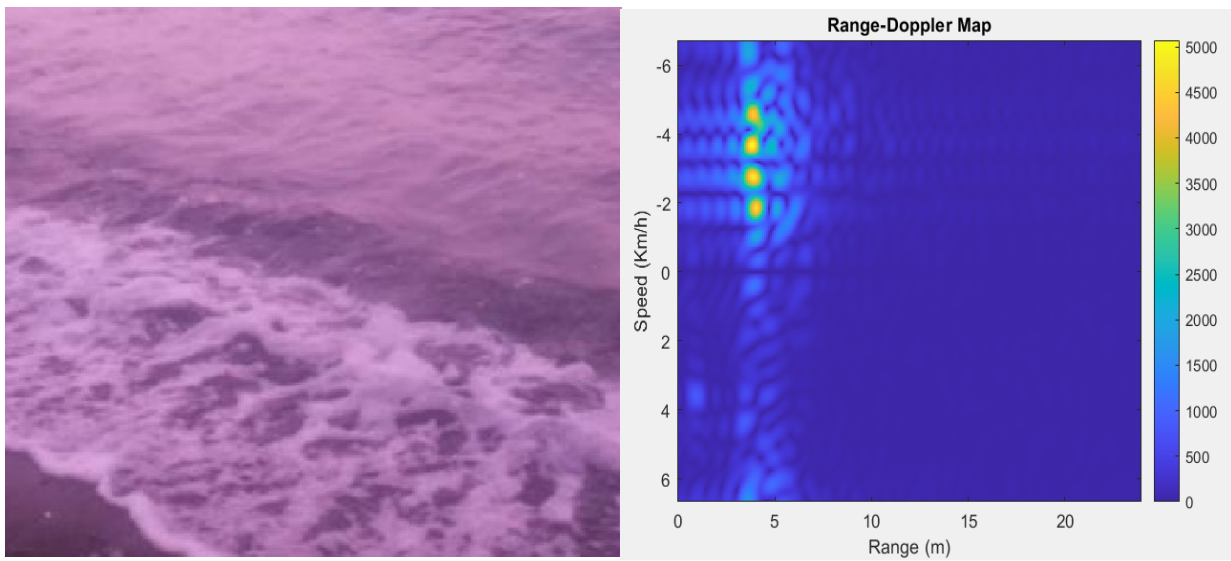
**a**



**b**



**c**



**d**

**Figure 5.7.** Camera image and Range Doppler map for sea states.

As a second example of different sea conditions, the combined interpretation of camera images and Range-Doppler Maps provides both qualitative and quantitative insights. In turbulent rolling

waves Fig 5.7 a, the camera shows large irregular crests with strong breaking, while the corresponding maps reveal intense scattering concentrated at 3 m in range and speeds reaching about  $-4$  to  $-5.2$  km/h, confirming the presence of highly energetic motion. In the case of slipping waves Fig. 5.7 b, the camera depicts visible but smoother undulations of reduced steepness. The Range-Doppler Maps indicate moderate scattering distributed around 4 m with speeds of about  $-2$  to  $-4$  km/h, reflecting active but less violent dynamics compared to turbulence. Short choppy waves Fig 5.7 c are shown in the camera as irregular patterns of increasing height, with the corresponding map presenting enhanced scattering at 5 m and speeds of about  $-3$  to  $-5$  km/h. Finally, under moderate sea conditions Fig 5.7d, the camera captures more organized but energetic waves, and the map displays broader scattering up 4 m and speeds reaching  $-4$  to  $-5.2$  km/h, indicating higher energy levels. Altogether, these examples demonstrate the ability of the system to characterize a wide spectrum of sea states, from calm to highly turbulent, by integrating visual and radar-based observations.

### 5.3 Conclusion

The experiments tracking sea waves provided valuable insights into wave dynamics and surface motion. By analyzing radar data, we were able to capture the characteristics of wave behavior under varying conditions, highlighting key features such as wave motion and variability. This approach demonstrates the effectiveness of radar technology for monitoring sea-state conditions, contributing to a more comprehensive understanding of ocean surface processes and supporting critical applications in environmental monitoring, maritime safety, and coastal engineering.

# Chapter 6



UNIONE EUROPEA  
Fondo Sociale Europeo



*Ministero dell'Istruzione,  
dell'Università e della Ricerca*



PON  
RICERCA  
E INNOVAZIONE  
2014 - 2020

# Chapter 6: Conclusion and Future work

## 6.1 Conclusion

This research has demonstrated the immense potential of Frequency Modulated Continuous Wave (FMCW) radar technology as a versatile, cost-effective, and robust tool for the real-time monitoring and analysis of water dynamics. By leveraging advanced signal processing methodologies, including the application of 2D Fast Fourier Transform (2D-FFT), Constant False Alarm Rate (CFAR) filtering, and time-domain analysis of In-Phase (I) and Quadrature (Q) components, this study captured key parameters with precision. These parameters, encompassing wave velocity, energy distribution, and surface dynamics, are critical for understanding and responding to hydrological phenomena.

The integration of CFAR filtering into the signal processing workflow proved particularly effective in enhancing target detection by dynamically adjusting thresholds to minimize noise and clutter, ensuring accurate representation of wave activity even in challenging environments. Similarly, the use of power spectral analysis enabled detailed information into energy distribution across wave frequencies, further enriching the characterization of sea states.

The findings underscore the advantages of radar-based non-contact sensing systems, particularly their ability to overcome the inherent limitations of traditional contact-based methods, such as mechanical or ultrasonic sensors, which require complex installations and are prone to high maintenance demands. The deployment of low-cost FMCW radar systems in coastal and near-shore environments, as well as in river settings, showcased their capability to deliver reliable, high-resolution data essential for various applications, including environmental monitoring.

The experimental assessments conducted in real-world coastal and river environments validated the radar system's effectiveness in providing reliable and detailed data on water dynamics. This research highlights the role of FMCW radar as a transformative technology for hydrological sensing, addressing practical challenges such as noise reduction and real-time signal processing.

Moreover, this research emphasizes the value of radar-based sensing in enabling proactive measures to safeguard vulnerable regions. Timely and accurate data on water flow, wave dynamics, and the potential impacts of debris flow can significantly contribute to disaster mitigation efforts.



The integration of CFAR techniques ensured robust performance in cluttered scenarios, making the system highly effective in delivering critical data in dynamic marine and river environments. The adaptability of FMCW radar, combined with its cost-efficiency and scalability, positions it as an essential tool for modern hydrological and environmental applications.

## 6.2 Future Work

Building upon the strong foundation established by this research, several promising directions for future exploration emerge. Enhancing CFAR algorithms through the integration of machine learning techniques could significantly improve their ability to adapt detection thresholds in highly variable and complex environments. Expanding the application of power spectral analysis to incorporate multi-modal sensing systems, such as combining radar with optical or acoustic sensors, could yield a more comprehensive understanding of wave dynamics and energy distribution. Further, deploying FMCW radar systems in diverse environments, including deep-sea regions and extreme weather conditions.

Another key avenue involves integrating radar data into advanced predictive models for long-term sea-state forecasting and wave energy resource assessment. This could enhance the utility of radar-based sensing in strategic planning and environmental management. Additionally, miniaturizing FMCW radar systems for integration into autonomous platforms, such as drones and unmanned surface vehicles, has the potential to revolutionize their deployment. This would enable efficient, real-time monitoring across remote and otherwise inaccessible areas, broadening the reach and impact of these systems.

These advancements collectively highlight the significant potential of FMCW radar technology to address pressing challenges in hydrology, coastal safety, and environmental sustainability, paving the way for innovative solutions to contemporary and future challenges.

# References

- [1] P. V. Brennan *et al.*, “Advanced radar imaging of geophysical flows,” in *Proc. 3rd IASME/WSEAS Int. Conf. Geology and Seismology*, Cambridge, U.K., 2009.
- [2] X.-Y. Xia *et al.*, “An empirical model of shape parameter of sea clutter based on X-band island-based radar database,” *IEEE Geosci. Remote Sens. Lett.*, 2023.
- [3] S. Adiningsih *et al.*, “An FFT-based method for wave decomposition from wave and tide monitoring using A01NYUB sensor,” in *Proc. IEEE Ocean Eng. Technol. Innov. Conf. (OETIC)*, 2022.
- [4] P. Yang, L. Dong, and W. Xu, “Detecting small infrared maritime targets overwhelmed in heavy waves by weighted multidirectional gradient measure,” *IEEE Geosci. Remote Sens. Lett.*, vol. 19, pp. 1–5, 2021.
- [5] A. H. Rathod *et al.*, “Estimating radar backscatter from water wave surface using X-band FMCW radar,” in *Proc. 2nd Int. Conf. Electron., Mater. Eng. & Nano-Technology (IEMENTech)*, 2018.
- [6] J. Li *et al.*, “First-order sea clutter suppression for high-frequency surface wave radar using orthogonal projection in spatial–temporal domain,” *IEEE Geosci. Remote Sens. Lett.*, vol. 19, pp. 1–5, 2021.
- [7] J.-P. Wasselin *et al.*, “FMCW radar system for detection and classification of small vessels in high sea state conditions,” in *Proc. 42nd Eur. Microwave Conf.*, 2012.
- [8] M.-E. Ma *et al.*, “Hydrological information measurement using an MM-wave FMCW radar,” in *Proc. Int. Conf. Microwave Millimeter Wave Technol. (ICMMT)*, 2020.
- [9] H. Li *et al.*, “Improving sea states monitoring of nautical radar using dispersion relation of nonlinear ocean waves,” in *Proc. IEEE Int. Geosci. Remote Sens. Symp. (IGARSS)*, vol. 3, 2009.
- [10] A. J. E. Smith *et al.*, “Maritime target and sea clutter measurements with a coherent Doppler polarimetric surveillance radar,” in *Proc. IEEE Radar Conf.*, 2002.
- [11] W. J. Plant *et al.*, “Measurement of river surface currents using rough surface scattering,” in *Proc. IEEE Antennas Propag. Soc. Int. Symp.*, vol. 1, 2005.
- [12] J. Xie and X. Xu, “Phase-feature-based detection of small targets in sea clutter,” *IEEE Geosci. Remote Sens. Lett.*, vol. 19, pp. 1–5, 2021.

- [13] B.-N. Kim *et al.*, “Real-time wave height measurements using a cable type wave monitoring system in shallow waters,” in *Proc. IEEE/OES 11th Current, Waves and Turbulence Measurement (CWTM)*, 2015.
- [14] M. A. Mutschler *et al.*, “River surface analysis and characterization using FMCW radar,” *IEEE J. Sel. Topics Appl. Earth Observ. Remote Sens.*, vol. 15, pp. 2493–2502, 2022.
- [15] L. Linghu *et al.*, “Sea clutter feature prediction and parameters inversion using deep learning model,” *IEEE Trans. Ind. Informatics*, 2022.
- [16] N. Braun *et al.*, “Sea-surface current features observed by Doppler radar,” *IEEE Trans. Geosci. Remote Sens.*, vol. 46, no. 4, pp. 1125–1133, Apr. 2008.
- [17] J. Cui *et al.*, “Wave height measurement using a short-range FMCW radar for unmanned surface craft,” in *Proc. OCEANS-MTS/IEEE Washington*, 2015.
- [18] G. B. Rossi *et al.*, “Measurement of sea waves,” *Sensors*, vol. 22, no. 1, p. 78, 2022.
- [19] G. B. Rossi *et al.*, “Investigation on spectrum estimation methods for bimodal sea state conditions,” *Sensors*, vol. 21, no. 9, p. 2995, 2021.
- [20] K. M. Carsell, N. D. Pingel, and D. T. Ford, “Quantifying the benefit of a flood warning system,” *Nat. Hazards Rev.*, vol. 5, no. 3, pp. 131–140, Aug. 2004.
- [21] A. Williams, “Current measurement technology development progress in the 90s—A review,” in *Proc. MTS/IEEE Conf. Coastal Ocean—Prospects for the 21st Century*, 1996, pp. 105–109.
- [22] T. M. Hammond and M. B. Collins, “Flume studies of the response of various current meter rotor/propellers to combinations of unidirectional and oscillatory flow,” *Deutsche Hydrografische Zeitschrift*, vol. 32, no. 2, pp. 39–58, 1979.
- [23] M. Tezuka, M. Mori, T. Suzuki, and T. Kanamine, “Ultrasonic pulse Doppler flow meter application for hydraulic power plants,” *Flow Meas. Instrum.*, vol. 19, no. 3–4, pp. 155–162, Jun. 2008.
- [24] M. Haide and W. Schroer, “Flow measurement in open channels by using an ultrasonic phased array sensor,” in *Proc. IEEE Sensors Conf.*, 2013, pp. 1–4.
- [25] T. Moramarco *et al.*, “River bathymetry estimate and discharge assessment from remote sensing,” *Water Resour. Res.*, vol. 55, no. 8, pp. 6692–6711, Aug. 2019.
- [26] Z. Ma *et al.*, “UHF surface currents radar hardware system design,” *IEEE Microw. Wireless Compon. Lett.*, vol. 15, no. 12, pp. 904–906, Dec. 2005.

- [27] D. E. Barrick, C. C. Teague, and P. M. Lilleboe, “Systems and methods for monitoring river flow parameters using a VHF/UHF radar station,” *U.S. Patent 7,688,251*, Mar. 30, 2010.
- [28] D. Barrick *et al.*, “Profiling river surface velocities and volume flow estimation with bistatic UHF riversonde radar,” in *Proc. IEEE/OES 7th Workshop Current Measurement Technology*, 2003, pp. 55–59.
- [29] Y. Lin, S. Chiu, and C. Chang, “A 24 GHz hydrology radar system capable of wide-range surface velocity detection for water resource management applications,” *Microw. Opt. Technol. Lett.*, vol. 62, no. 11, pp. 3463–3475, Nov. 2020.
- [30] C. Erhart *et al.*, “Surface velocity estimation of fluids using millimeter-wave radar,” in *Proc. Eur. Microwave Conf.*, 2015, pp. 566–569.
- [31] G. Wang *et al.*, “Highly accurate noncontact water level monitoring using continuous-wave Doppler radar,” in *Proc. IEEE Topical Conf. Wireless Sensors Sensor Netw.*, 2013, pp. 19–21.
- [32] R. Cheng and J. Gartner, “Complete velocity distribution in river cross sections measured by acoustic instruments,” in *Proc. IEEE/OES 7th Workshop Current Measurement Technology*, 2003, pp. 21–26.
- [33] V. T. Chow, D. R. Maidment, and L. W. Mays, *Applied Hydrology*. New York, NY, USA: McGraw-Hill, 1988.
- [34] T. Moramarco, C. Saltalippi, and V. P. Singh, “Estimation of mean velocity in natural channels based on Chiu’s velocity distribution equation,” *J. Hydrologic Eng.*, vol. 9, no. 1, pp. 42–50, Jan. 2004.
- [35] F. Alimenti *et al.*, “Noncontact measurement of river surface velocity and discharge estimation with a low-cost Doppler radar sensor,” *IEEE Trans. Geosci. Remote Sens.*, vol. 58, no. 7, pp. 5195–5207, Jul. 2020.
- [36] M. Scherhauf, C. Hesch, and J.-M. Sevar, “Fluid surface velocity estimation using a 77 GHz radar module,” in *Proc. IEEE Topical Conf. Wireless Sensors Sensor Netw.*, 2019, pp. 1–4.
- [37] W. Plant, W. Keller, and K. Hayes, “Measurement of river surface currents with coherent microwave systems,” *IEEE Trans. Geosci. Remote Sens.*, vol. 43, no. 6, pp. 1242–1257, Jun. 2005.
- [38] W. J. Plant, “A model for microwave Doppler sea return at high incidence angles: Bragg scattering from bound, tilted waves,” *J. Geophys. Res. Oceans*, vol. 102, no. C9, pp. 21131–21146, Sep. 1997.
- [39] P. H. Lee *et al.*, “Experiments on Bragg and non-Bragg scattering using single-frequency and chirped radars,” *Radio Sci.*, vol. 32, no. 5, pp. 1725–1744, Sep. 1997.

- [40] P. H. Y. Lee *et al.*, “X-band microwave backscattering from ocean waves,” *J. Geophys. Res. Oceans*, vol. 100, no. C2, pp. 2591–2611, Feb. 1995.
- [41] J. Fulton and J. Ostrowski, “Measuring real-time streamflow using emerging technologies: Radar, hydroacoustics, and the probability concept,” *J. Hydrol.*, vol. 357, nos. 1–2, pp. 1–10, Jul. 2008.
- [42] R. Herschy, *Streamflow Measurement*. London, U.K.: Elsevier, 1985.
- [43] T. Moramarco *et al.*, “River bathymetry estimate and discharge assessment from remote sensing,” *Water Resour. Res.*, vol. 55, no. 8, pp. 6692–6711, Aug. 2019.
- [44] A. I. Baskakov, *Spaceborne Precision Oceanographic Radio Altimeter*. Moscow, Russia: Moscow Power Engineering Institute Publ., 1994.
- [45] A. Bentamy, P. Queffeuilou, Y. Quilfen, and K. Katsaros, “Ocean surface wind fields estimated from satellite active and passive microwave instruments,” *IEEE Trans. Geosci. Remote Sens.*, vol. 37, no. 5, pp. 2469–2486, Sep. 1999.
- [46] “DEMO DISTANCE2GO – Infineon Technologies.” [Online]. Available: <https://www.infineon.com/cms/en/product/evaluation-boards/demo-distance2go>
- [47] G. L. Charvat, *Small and Short-Range Radar Systems*. Boca Raton, FL, USA: CRC Press, 2014.
- [48] M. Ash, M. Ritchie, and K. Chetty, “On the application of digital moving target indication techniques to short-range FMCW radar data,” *IEEE Sensors J.*, vol. 18, no. 10, pp. 4167–4175, May 2018.
- [49] G. L. Charvat, *Small and Short-Range Radar Systems*. Boca Raton, FL, USA: CRC Press, 2014.
- [50] M. Ash, M. Ritchie, and K. Chetty, “On the application of digital moving target indication techniques to short-range FMCW radar data,” *IEEE Sensors J.*, vol. 18, no. 10, pp. 4167–4175, May 2018.
- [51] G. L. Charvat, *Small and Short-Range Radar Systems*. Boca Raton, FL, USA: CRC Press, 2014.
- [52] M. A. Richards, *Fundamentals of Radar Signal Processing*, 2nd ed. New York, NY, USA: McGraw-Hill, 2014.
- [53] M. A. Richards, *Fundamentals of Radar Signal Processing*, 2nd ed. New York, NY, USA: McGraw-Hill, 2014.

- [54] A. Jalil, H. Yousaf, and M. I. Baig, “Analysis of CFAR techniques,” in *Proc. 13th Int. Bhurban Conf. Appl. Sci. & Technol.*, 2016, pp. 654–659.
- [55] W. Wang *et al.*, “Modified reference window for two-dimensional CFAR in radar target detection,” *J. Eng.*, vol. 2019, no. 17, pp. 4516–4520, 2019, doi: 10.1049/joe.2019.0687.
- [56] M. I. Skolnik, *Introduction to Radar Systems*. New York, NY, USA: McGraw-Hill Education, 2001.
- [57] M. A. Richards, *Fundamentals of Radar Signal Processing*. New York, NY, USA: McGraw-Hill, 2014.
- [58] N. Levanon and E. Mozeson, *Radar Signals*. Hoboken, NJ, USA: Wiley-Interscience, 2004.
- [59] J. Wang *et al.*, “Moving object recognition under simulated prosthetic vision using background-subtraction-based image processing strategies,” *Inf. Sci.*, vol. 277, pp. 512–524, Sep. 2014, doi: 10.1016/j.ins.2014.02.136.
- [60] A. V. Oppenheim and R. W. Schaffer, *Discrete-Time Signal Processing*, 3rd ed. Upper Saddle River, NJ, USA: Pearson, 2010.